Università degli Studi di Ferrara

DOTTORATO DI RICERCA IN FISICA

CICLO XXV

COORDINATORE Prof. GUIDI Vincenzo

Gravitational waves from the early Universe and their detection

Settore Scientifico Disciplinare FIS/05

Dottorando
Dott. EJLLI Damian

DAMIAN EJLLI
(firma)

Tutore
Prof. DOLGOV Alexander

(firma)

Co-Tutore
Prof. SEMIKOZ Dmitri

(firma)

Anni 2010/2012

To my family

Contents

Acknowledgements

Deep appreciations go to all people which made this thesis possible. In first place I want to give spacial thanks to Alexander D. Dolgov who helped and followed me in the realization of this thesis. Warm thanks goes to Dmitri Semikoz who followed me during my stage at APC and helped me for various issues regarding my work and this thesis. Special thanks goes to both referees George Raffelt and Fabio Finelli on being very available and very kind on the examination of my thesis work. I also want to thank all people involved in the IDAPP project especially Alessandra Tonazzo and Isabella Masina for helping me with all formalities and for their support on the realization of this program.

Introduction

Though the theory of gravitational waves was developed formally by Einstein in 1916 [1], the idea of a gravitational field traveling through space dates back to Maxwell and Poincaré [2, 3]. In his memorable book " Sur le Principe de la Gravitation Univeselle" of 1776, Pierre Laplace had considered the problem of an orbital damping force arising from a finite speed of propagation of the gravitational interaction. He was seeking for an explanation for the observed decrease of the Moon's orbital period with respect to ancient eclipse observations. The energy loss of a system due to emission of gravitational radiation was first suggested in 1908 by Poincaré [4]. His suggestion was that planetary orbits must slowly lose energy to wave emission in the gravitational field and pointed out that such an effect is too small to explain the perihelion shift of the Mercury planet.

The theory of gravitational waves has a longer history of disputes, false dawns and setbacks. Many theorists doubted, at one time or another, whether they existed at all. Albert Einstein himself, who founded the theory of gravitational waves in 1916 , numbered himself amongst the doubters on at least two occasions. In a letter to his friend Max Born, probably written sometime during 1936, Albert Einstein reported

Together with a young collaborator, I arrived at the interesting result that gravitational waves do not exist, though they had been assumed a certainty to the first approximation. This shows that the non-linear general relativistic field equations can tell us more or, rather, limit us more than we have believed up to now (Born 1971, p. 125)

The letter which Einstein sent to Born was based on his work with his young collaborator Nathan Rosen under the title " Do Gravitational Waves Exist ?". In that paper they apparently showed that according to their calculations, gravitational radiation does not exist but it is just an artifact of Einstein's theory and nothing else. Einstein convinced also Leopold Infield who was a new at Princeton, that according to Einstein's recent results gravitational waves do not exist. Once an idea has been putted forward on the table and accepted by the community, there is nothing more difficult than saying that it should be erased because is wrong! In fact not everyone after Einstein-Rosen paper was easily convinced on that. Shortly after their paper was sent to the *Physical Review* for publication it was returned to him with a critical referees report, accompanied by the editors mild request that he " would be glad to have your reaction to the various comments and criticisms the referee has made." (John T. Tate to Einstein July 23, 1936). Einstein

reaction was immediate and he wrote to the editor

Dear Sir,
We (Mr. Rosen and I) had sent you our manuscript for publication and had not authorized you to show it to specialists before it is printed. I see no reason to address the - in any case erroneous - comments of your anonymous expert. On the basis of this incident I prefer to publish the paper elsewhere.
respectfully,
P.S. Mr. Rosen, who has left for the Soviet Union, has authorized me to represent him in this matter.

Soon after, Tate replied to Einstein saying that he regretted Einstein's decision to withdraw the paper and that he would not set aside the journal's review procedure. However, despite Tate's letter Einstein from that incident never sent papers to publish to the *Physical Review*. Einstein-Rosen paper was subsequently accepted for publication by the Journal of the Franklin Institute of Philadelphia.

Einstein always had been not sure on the reality of gravitational waves which he derived 1916 where for the first time the famous "quadrupole formula" was found. Together with Rosen he was looking for exact solutions to the field equations of general relativity which described plane wave gravitational waves. What they found was that to do so was not possible without introducing singularities into the components of the metric describing the wave and as a result they showed that no regular periodic wave-like solutions were possible. However, in July of 1936, the relativist Howard Percy Robertson who was already known for his studies on the metric of a homogeneous and isotropic space which latter was coined the Robertson-Walker metric, discussing with Infeld (whom Einstein convinced on the non existence of gravitational radiation), he told to him that hid did not believe to Einstein's results. Once, Robertson showed to Infeld the errors contained in the Einstein-Rosen paper, Infeld was again convinced this time by Robertson and he rapidly communicated to Einstein the errors found in his paper. Einstein quickly contacted the Franklin Journal and made changes in the proof of the paper. The new title of the paper was "On Gravitational waves" [5]. The errors contained in the Einstein-Rosen paper were the same which the referee of the *Physical Review* pointed out! This little piece of story regarding the nature of gravitational waves learn us an important lesson, namely that the referee opinion and critics are always very important.

The just mentioned episode on the non existence of the gravitational radiation is one of many other episodes in the history of gravitational waves. In his 1922 famous paper [6], Sir Arthur Stanley Eddington one the most leading astrophysicist of that time remarked that gravitational waves do propagate with "the speed of thought". Eddingtons outlook on gravitational waves expressed in his paper has earned him a reputation as the first skeptic of gravitational waves. However, this does accurately reflect his skeptical attitude towards the analogy with electromagnetic waves, although he was emphatically not one of those who concluded that gravitational waves did not exist. On the infi-

nite speed of gravitational radiation, Eddington was arguing only that certain classes of gravitational waves the "longitudinal-longitudinal" and "transverse-longitudinal" were unphysical. He also showed that the transverse-transverse waves (today are called TT waves) could carry energy and corrected an erroneous factor two in the Einstein's previous quadrupole formula.

Starting from 1938, Einstein with his task force composed by Leopold Infeld and Banesh Hoffman started developing the post-Newtonian approach to the general problem of motion in general relativity. This method consist on expanding the equations of general relativity in powers of the gravitational field strength and in powers of v/c where $v \ll c$ is the source velocity. This method of attacking the general problem of motion in general relativity today is know as the EIH method and so far is on of the most influential. Inspired by the EIH method, in 1946 the Chinese student of the California Institute of Technology (Caltech) Ning Hu addressed the EIH method to the gravitational radiation to binary systems. His results were rather surprising since he found disagreement with the quadrupole formula for the case of two equal masses orbiting around each-other. However, Hu shortly after corrected his results already published where he found that the binary system gain energy instead of loosing energy as e result of gravitational wave emission. In the same period Infeld and his student Scheidegger found that the system does not present damping effects at all!

At the Bern conference of 1955, Rosen re-emerged again his skepticism on gravitational radiation but this time focusing on the energy that it carries. In fact during the conference he emphasized that gravitational waves maybe do not carry energy, conclusion which Infeld and Scheidegger arrived few years ago. Rosen arguments were based on the fact that the energy is non-localizable in general relativity where the energy conservation is expressed as the covariant derivative of the energy momentum tensor. He showed that both Einstein and Landau-Lifshitz pseudo tensors of gravitational wave which are not invariant quantities under coordinate transformations, do not carry energy in cylindric coordinates according to his paper with Einstein of 1937.

Despite of too many years of speculations on the nature of gravitational waves, we can safely say that today the gravitational wave science has become a reality. How all this happened? How it is possible that a field of research such as gravitational waves which has been debated for too many years, nowadays has become one of the most founded in the history of science with several ambitious projects being built around the globe for their detection? All these changes have not been instantaneously but it took too many years of intensive studies and contemporarily a lot of efforts on the construction of the first gravitational wave detectors. If gravitational waves really do not exist or do not carry energy was one of the most important problems related to the field. However, another realistic problem was that there were no available sources in order to test even what was then known. The only theoretical argument which could be compared with experimental results was only the quadrupole formula which Einstein found in 1916. In order to apply this relation to physical systems one must have a physical source of

gravitational waves and moreover the predicted signal at Earth was too small that people even wondered if it was possible to detect it.

Apart from some false claims made by Weber in 1960 that he had detected gravitational waves, an important point in the history of gravitational waves was the discovery of the first binary system of pulsars PSR B1913+16 by Hulse and Taylor in 1975 [7]. The discovery crystalized the excitement in the field providing the first test bed for strong fields effects of general relativity, although there were explicit doubts at first that the system would exhibit measurable orbital damping effects [8]. However, doubts went away in 1980 when after several years of observations Taylor and McCulloch announced the orbital decay in the period of the binary system PSR B1913+16 in good agreement with the prediction of the quadrupole formula with an accuracy of 20% [9]. Since then and mostly due to works of Thorne [10] and Damour [11] gravitational radiation has been an object of intensive studies. The general consensus today see gravitational waves as fluctuations in the curvature of space-time, which propagate as waves, traveling outward from the source.

Roughly speaking there are two groups of possible sources of gravitational radiation which may be registered by gravitational wave detectors either on the Earth or by space missions. The first group includes energetic phenomena in the contemporary universe, such as emission of gravitational waves by black hole or compact star binaries, supernova explosions, and possibly some other catastrophic phenomena. The second group contains gravitational radiation coming from the early Universe, which creates today an isotropic background usually with rather low frequency. Such gravitational radiation could be produced at inflation, phase transitions in the primeval plasma, by the decay or interaction of topological defects, e.g. cosmic strings, etc.

The graviton (gravitational wave) production in the Friedmann-Robertson-Walker metric was first considered by Grishchuk [12], who noticed that the graviton wave equation is not conformal invariant and thus such quanta can be produced by conformal flat external gravitational field. Generation of gravitational waves at the De Sitter (inflationary) stage was studied by Starobinsky [13]. The stochastic homogeneous background of the low frequency gravitational waves is now one of the very important predictions of inflationary cosmology, which may present test bed for inflationary models.

The structure of this thesis is as follows: In chapter 1 we discuss the basic theory of gravitational waves. We start from the Einstein field equation and after expand them around the Minkowski metric arriving at the end at the quadrupole formula. After that we define the plane gravitational waves and expand a general gravitational wave in the TT gauge. The last part of chapter 1 concern the energy of gravitational waves and their energy-momentum tensor. In chapter 2 we introduce some basic quantities and definitions regarding gravitational wave detectors. We start by defining the detector signal and sensitivity and how this quantities are related to the gravitational wave detector signal. Next we discuss the main noise sources concerning both interferometer and resonant bars. We discuss the many difficulties which people have to face in order to

reduce the detector noise and how to distinguish it from the gravitational wave signal. We then conclude with an overview on the status of the present and future gravitational interferometers such as Virgo, LIGO etc. In chapter 3 we begin with the definition of several quantities of a stochastic background of gravitational waves such as its energy density, density parameter, amplitude etc. Next we proceed to discussion on the phenomenological bounds on the density parameter of gravitational waves. We conclude with an overview (not complete) on the most important models of gravitational wave generation in the early Universe. In chapter 4 and chapter 5 we review the gravitational wave production by light primordial black holes and their detection. This mechanism of gravitational wave production will introduce an additional expansion regime in the early Universe where a large amount of gravitational waves is produced. In connection with that we study the mechanism of graviton to photon transition in the post recombination epoch which presents an alternative way on looking for gravitational waves [14, 15].

Chapter 1

General theory of gravitational waves

Special relativity has been one of the most important achievement in the last century, removing from the mainstream of theoretical physics the concept of absolute time. In his seminal paper of 1905, Einstein showed for the first time that the laws of physics should be changed and the old Galileo transformation should be replaced with the Lorentz transformation. Despite the success of the theory of special relativity, it lacks an important key ingredient in order to explain the macroscopic physics, the gravity.

General relativity is the theory which unify the theory Special relativity with gravity, where gravity manifest itself as curvature of the space-time. On of the most important achievements of this theory is that it admits wave-like solutions of the field equations where waves do propagate outward from the source with the velocity of light. In this chapter we present a simplified derivation of the field equations in vacuum and most important properties of gravitational radiation. In deriving our results we closely follow those in [16, 17, 18]. In this thesis we work in the natural units $c = \hbar = k_B = 1$.

1.1 Weak field approximation

The weak field approximation is a powerful method used to solve the Einstein field equations in regions where the gravitational field is weak and the space-time perturbations are small. The Einstein field equations are given by

$$R_{\mu\nu} - \frac{1}{2} g_{\mu\nu} R = 8\pi G T_{\mu\nu}, \tag{1.1}$$

where $g_{\mu\nu}$ is the metric tensor, $T_{\mu\nu}$ is the energy-momentum tensor, $R_{\mu\nu}$ is the Ricci tensor and R is the Ricci scalar. The Ricci tensor is defined in terms of Riemann tensor as $R_{\mu\nu} = R^{\alpha}_{\mu\alpha\nu}$ where the Riemann tensor is given by

$$R^{\alpha}_{\beta\mu\nu} = \partial_\mu \Gamma^{\alpha}_{\beta\nu} - \partial_\nu \Gamma^{\alpha}_{\beta\mu} + \Gamma^{\alpha}_{\mu\rho}\Gamma^{\rho}_{\beta\nu} - \Gamma^{\alpha}_{\nu\rho}\Gamma^{\rho}_{\beta\nu}, \tag{1.2}$$

with $\Gamma^{\alpha}_{\sigma\rho}$ being the Christoffel symbols which are expressed in terms of the metric tensor as follows

$$\Gamma^{\alpha}_{\sigma\rho} = \frac{1}{2} g^{\alpha\beta}(\partial_\sigma g_{\beta\rho} + \partial_\rho g_{\beta\sigma} - \partial_\beta g_{\sigma\rho}). \tag{1.3}$$

The similarities of Einstein's theory of gravitation with the Maxwell theory of electromagnetism are enough such we should not be surprised that, like the electromagnetic field which has wave properties even the gravitational field itself has such property. As a first step to understand the radiative properties of the gravitational field, we start by expanding Einstein's equations around the flat space-time metric. Let us suppose that the metric under investigation is very close to the Minkowski metric $\eta_{\mu\nu} = \text{diag}(-1, 1, 1, 1)$ and write the general metric tensor as

$$g_{\mu\nu} = \eta_{\mu\nu} + h_{\mu\nu}, \qquad |h_{\mu\nu}| \ll 1. \tag{1.4}$$

To linear order in $h_{\mu\nu}$, the Riemann tensor becomes

$$R_{\alpha\mu\beta\nu} = \frac{1}{2}(\partial_\mu\partial_\beta h_{\alpha\nu} + \partial_\alpha\partial_\nu h_{\mu\beta} - \partial_\alpha\partial_\beta h_{\mu\nu} - \partial_\mu\partial_\nu h_{\alpha\beta}) \tag{1.5}$$

and the Ricci tensor is given by $R_{\mu\nu} = g^{\alpha\beta}R_{\alpha\mu\beta\nu}$

$$R_{\mu\nu} = \frac{1}{2}(\partial_\mu\partial^\alpha h_{\alpha\nu} + \partial^\beta\partial_\nu h_{\mu\beta} - \Box h_{\mu\nu} - \partial_\mu\partial_\nu h). \tag{1.6}$$

The Ricci scalar is $R = g^{\mu\nu}R_{\mu\nu}$

$$R = \partial^\alpha\partial^\beta h_{\alpha\beta} - \Box h \tag{1.7}$$

Inserting Equation 1.6 and Equation 1.7 into the Einstein field equations, Equation 1.1 we get the linearized Einstein field equations

$$\Box h_{\mu\nu} + \partial_\mu\partial_\nu h - \partial_\mu\partial^\alpha h_{\alpha\nu} - \partial_\nu\partial^\beta h_{\mu\beta} + \eta_{\mu\nu}\partial^\alpha\partial^\beta h_{\alpha\beta} - \eta_{\mu\nu}\Box h = -16\pi G T_{\mu\nu}. \tag{1.8}$$

Having chosen a particular reference system given by Equation 1.4 breaks down the invariance under general coordinate transformation in general relativity. This allows us to get rid of spurious degrees of freedom of the theory and understand the physical content of the chosen reference system. In order to see this, let us make an infinitesimal coordinate transformation of the kind

$$x^\mu \to x'^\mu = x^\mu + \xi^\mu(x). \tag{1.9}$$

Then

$$\frac{\partial x'^\mu}{\partial x^\nu} = \delta^\mu_\nu + \partial_\nu\xi^\mu, \tag{1.10}$$

and applying the transformation of the metric tensor under general coordinate transformation

$$g_{\mu\nu}(x) \to g'_{\mu\nu}(x') = \frac{\partial x^\alpha}{\partial x'^\mu}\frac{\partial x^\beta}{\partial x'^\nu}\, g_{\alpha\beta}(x) \tag{1.11}$$

we get the general transformation of the gravitational field tensor $h_{\mu\nu}$

$$h_{\mu\nu}(x) \rightarrow h'_{\mu\nu}(x) = h_{\mu\nu}(x) - (\partial_\mu \xi_\nu + \partial_\nu \xi_\mu). \tag{1.12}$$

In complete analogy with the electromagnetic counterpart the transformations given by Equation 1.12 are called gauge transformation for the fields $h_{\mu\nu}$. We may notice that the only requirement is that $|\partial_\mu \xi_\nu| \simeq |h_{\mu\nu}|$ and is not necessary to require that $|\xi_\mu|$ are themselves small. The second order corrections to the right hand side of equation Equation 1.12, $O(h\partial\xi)$ and $O(\partial\xi\partial\xi)$ have been neglected. Moreover, we can easily see that requiring $|\partial_\mu \xi_\nu| \ll 1$ implies that the transformed gravitational tensor is small, $|h'_{\mu\nu}| \ll 1$ and both the Ricci tensor Equation 1.6 and the Ricci scalar Equation 1.7 are gauge invariant quantities under general transformations given by Equation 1.12.

As in electrodynamics we can impose further conditions in order to fix gauge transformations. It is convenient at this stage to define the new variables $\bar{h}_{\mu\nu}$ as

$$\bar{h}_{\mu\nu} = h_{\mu\nu} - \frac{1}{2}\eta_{\mu\nu} h, \tag{1.13}$$

where indices are raised and lowed by the flat space-time metric $\eta_{\mu\nu}$ and $h = \eta^{\mu\nu} h_{\mu\nu}$. We can observe that $\bar{h} = \eta^{\mu\nu}\bar{h}_{\mu\nu} = h - 2h = -h$ and

$$h_{\mu\nu} = \bar{h}_{\mu\nu} - \frac{1}{2}\eta_{\mu\nu}\bar{h}. \tag{1.14}$$

Inserting Equation 1.14 into Equation 1.8, the linearized Einstein field equations in terms of variables $\bar{h}_{\mu\nu}$ read

$$\Box\bar{h}_{\mu\nu} + \eta_{\mu\nu}\partial^\alpha\partial^\beta\bar{h}_{\alpha\beta} - \partial^\alpha\partial_\mu\bar{h}_{\nu\alpha} - \partial^\alpha\partial_\nu\bar{h}_{\mu\alpha} = -16\pi G T_{\mu\nu}. \tag{1.15}$$

Equation 1.15 will reduce to a wave equation if we use the gauge freedom Equation 1.12 to chose the Lorentz or Hilbert or harmonic gauge, namely

$$\partial^\nu\bar{h}_{\mu\nu} = 0. \tag{1.16}$$

Equation 1.16 gives four conditions that reduces the 10 independent component of $h_{\mu\nu}$ to 10-4=6 independent components. Using the general coordinate transformation given by Equation 1.9, the field variables $\bar{h}_{\mu\nu}$ would transform as

$$\bar{h}_{\mu\nu} \rightarrow \bar{h}'_{\mu\nu} = \bar{h}_{\mu\nu} - \partial_\mu\xi_\nu - \partial_\nu\xi_\mu + \eta_{\mu\nu}\partial_\alpha\xi^\alpha, \tag{1.17}$$

and then using Equation 1.16 we get

$$\partial^\nu\bar{h}_{\mu\nu} \rightarrow (\partial^\nu\bar{h}_{\mu\nu})' = \partial^\nu\bar{h}_{\mu\nu} - \Box\xi_\mu. \tag{1.18}$$

It follows that coordinate transformation, Equation 1.9, will transform Equation 1.18 in the Lorentz gauge for the variables $\bar{h}'_{\mu\nu}$ if we choose the additional condition

$$(\partial^\nu\bar{h}_{\mu\nu})' = \Box\xi_\mu. \tag{1.19}$$

So if for example the initial field configuration is such that $\partial^\nu \bar{h}_{\mu\nu} = f_\mu(x)$, Equation 1.19 will reduce on finding the solutions of equation

$$\Box \xi_\mu = f_\mu(x). \tag{1.20}$$

Using the Lorentz gauge given by Equation 1.16, the linearized Einstein field equations, Equation 1.15, for the variables $\bar{h}_{\mu\nu}$ become

$$\Box \bar{h}_{\mu\nu} = -16\pi G T_{\mu\nu}. \tag{1.21}$$

The linearized equations Equation 1.21 are the most important equations derived from Einstein field equations since they allow us to calculate the gravitational radiation in different situation in both vacuum and inside a given source. Here the bodies acts as source of GWs when they move in flat space-time and the curvature caused by them is neglected where in general the Newtonian dynamics is appropriate to determine their motion.

1.2 Vacuum solutions and the TT gauge

In this section we look for vacuum solutions of Equation 1.21 in regions where the energy-momentum tensor is $T_{\mu\nu} = 0$. The equation of motion given by Equation 1.21 outside the source, reduce to

$$\Box \bar{h}_{\mu\nu} = 0. \tag{1.22}$$

As we saw in section 1.1 coordinate transformation Equation 1.9 do not fix the Lorentz gauge Equation 1.16 uniquely since under Equation 1.9, $\partial^\nu \bar{h}_{\mu\nu}$ transforms as in Equation 1.18. As a consequence the Lorentz gauge Equation 1.16 remains invariant under Equation 1.9, if the ξ_μ satisfy the wave equation

$$\Box \xi_\mu = 0. \tag{1.23}$$

Solutions of Equation 1.23, namely the four functions $\xi_\mu(x)$, can be used to further reduce the number of six independent components of $\bar{h}'_{\mu\nu}$ in Equation 1.17 to just only two independent components which are physically significant. We can choose for example the functions ξ^0 and ξ^i in such a way that the trace $\bar{h} = 0$ and $h_{0i} = 0$ and applying the Lorentz gauge Equation 1.16 we get the following conditions on the fields $h_{\mu\nu}$

$$\partial^j h_{ij} = 0, \qquad h^i_i = 0, \qquad h_{0\mu} = 0. \tag{1.24}$$

Equation 1.24 defines the so called transverse traceless gauge or TT gauge which is valid only *outside* the source.

Let us now turn on possible solutions of Equation 1.22. We consider first plane wave solutions because they are very important in many physical situations and because the retarded wave solutions of Equation 1.21 approache to plane wave solutions as far as

the distance from the source goes to infinity, $r \to \infty$. In the TT gauge the plane wave solutions are of the form

$$h_{ij}^{TT}(x) = \Re\{e_{ij}(\mathbf{k})e^{ikx}\}, \tag{1.25}$$

where $e_{ij}(\mathbf{k})$ is called the polarization tensor and $\Re\{..\}$ means* that we should consider only the real part of Equation 1.25. If we consider a single plane wave propagating in the direction $\hat{\mathbf{n}} = \mathbf{k}/|\mathbf{k}|$ and take into account that we are in the TT gauge we have that the trace of $h_{\mu\nu}$ is zero and the wave is transverse, $n^i h_{ij} = 0$. In this case if we chose the propagation direction along the z axis, the general form of the spatial components of $h_{\mu\nu}$ in the TT gauge is

$$h_{ij}^{TT}(z,t) = \begin{pmatrix} h_+ & h_\times & 0 \\ h_\times & -h_+ & 0 \\ 0 & 0 & 0 \end{pmatrix} \cdot \cos[\omega(t - z/c)], \tag{1.26}$$

where ω is the gravitational frequency, t is the time and $h_+, h_\times$ are the amplitudes associated with the plane wave. A general GW can be expanded into plane waves of GWs (Fourier components) in complete analogy with other wave phenomena. In this case the general form of the wave is given by

$$h_{ij}^{TT}(x) = \int \frac{d^3k}{(2\pi)^3} \left(e_{ij}(\mathbf{k})e^{ikx} + e_{ij}^*(\mathbf{k})e^{-ikx} \right), \tag{1.27}$$

where e_{ij}^* is the complex conjugate tensor of e_{ij} and $\mathbf{k}$ is the wave wave-vector. The TT gauge conditions for the expansion, Equation 1.27, give $e_i^i(\mathbf{k}) = 0$ and $k^i e_{ij}(\mathbf{k}) = 0$. Another important wave decomposition is through energy Fourier components, namely

$$h_{ij}^{TT}(\mathbf{x},t) = \frac{1}{2\pi} \int_0^\infty d\omega \left(\tilde{h}_{ij}(\mathbf{x},\omega)e^{-i\omega t} + \tilde{h}_{ij}^*(\mathbf{x},\omega)e^{i\omega t} \right), \tag{1.28}$$

where $\tilde{h}_{ij}(\mathbf{x},\omega)$ are the Fourier components of h_{ij}^{TT}. These kind of decomposition is important especially when we are interested in the GW at the detector position, where the spatial dependence on $\mathbf{x}$ can be completely neglected.

As we have seen for a GW propagating along the z axis, the only non zero components are $h_{xx}^{TT} = -h_{yy}^{TT}$ and $h_{xy}^{TT} = h_{yx}^{TT}$. So it is very convenient to write a general GW as a superposition of plane GWs with given polarization states, h_+ and $h_\times$. Again in complete analogy with electromagnetic waves which have two polarization states $e_\lambda(\mathbf{k})$, the polarization tensor corresponding to the two polarization states of the GWs is given by

$$e_{ij}^\lambda(\mathbf{k}) = (\mathbf{e}_i^+\mathbf{e}_j^+ - \mathbf{e}_i^\times\mathbf{e}_j^\times)\delta_+^\lambda + (\mathbf{e}_i^+\mathbf{e}_j^\times + \mathbf{e}_i^\times\mathbf{e}_j^+)\delta_\times^\lambda, \tag{1.29}$$

where λ is a polarization index and $\mathbf{e}^+, \mathbf{e}^\times$ are two unit vectors perpendicular to each-other and to the direction of propagation. Choosing a frame when the propagation direction $\hat{\mathbf{n}}$ is along the z axis and $\mathbf{e}^+ = \hat{\mathbf{x}}, \mathbf{e}^\times = \hat{\mathbf{y}}$, the form of the polarization tensor in this

*From now we explicitly omit the symbol $\Re\{..\}$ from our equations, however always keeping in mind to consider the real part at the end of our derivations.

frame is

$$e_{ij}^{+} = \begin{pmatrix} 1 & 0 \\ 0 & -1 \end{pmatrix}, \qquad e_{ij}^{\times} = \begin{pmatrix} 0 & 1 \\ 1 & 0 \end{pmatrix}. \tag{1.30}$$

Still in the TT gauge a general gravitational wave can expanded in terms of polarization states and it energy Fourier components

$$h_{ij}^{TT}(\mathbf{x},t) = \sum_{\lambda=+,\times} \int \frac{d^4k}{(2\pi)^4} h_\lambda(\mathbf{k},\omega) e_{ij}^{\lambda}(\mathbf{k}) e^{-i\omega(t-\mathbf{k}\cdot\mathbf{x})}, \tag{1.31}$$

where $d^4k = d\omega\, d^3k/c$ and defined $h_\lambda(\mathbf{k},-\omega) = h_\lambda^*(\mathbf{k},\omega)$.

1.3 Energy-momentum of gravitational waves

In this section we want to discuss the energy and momentum carried by GWs and find an explicit expression for their energy-momentum tensor. To start with we first study how a test particle with a mass m reacts when it interacts with a GW? In general equation of motion of a test particle of mass m, under the influence of a gravitational field is given by

$$\frac{D^2\xi^\mu}{D\tau^2} = -R^\mu_{\nu\alpha\beta}\,\xi^\alpha \frac{dx^\nu}{d\tau}\frac{dx^\beta}{d\tau}, \tag{1.32}$$

where $\xi(\tau)$ is called the geodesic deviation and τ is the proper time which each geodesic is parametrized. The solution of Equation 1.32 is shown to be [16]

$$\ddot{\xi}^i(\tau) = \frac{1}{2}\ddot{h}_{ij}^{TT}\xi^j(\tau). \tag{1.33}$$

This equation implies that, in the proper detector frame, the effect of GWs on a test particle with mass m can be described in terms of a Newtonian force with strength

$$F_i = \frac{m}{2}\,\ddot{h}_{ij}^{TT}\xi^j(\tau), \tag{1.34}$$

where the detector response can be simply analyzed in Newtonian physics without any other reference to general relativity. Since the interaction of a GW with a test mass particle can be described in terms of a force Equation 1.34 acting on the particle it is interesting to see how the particle position changes with time when it interacts with a GW.

Let us assume to have a ring of test particles at rest at given coordinate system and located in the (x,y) plane. Consider then that the GW do propagates along the z axis, so the only non zero components of h_{ij}^{TT} are those for $i = 1,2$ or $j = 1,2$. According to Equation 1.34 a particle which is at rest at $z = 0$, will also remain at rest during its interaction with the GW and the motion will take place only in the (x,y) plane. In this case it can be easily shown that by writing the geodesic deviation of the particle as $\xi_i(t) = (x_0 + \delta x(t), y_0 + \delta y(t))$ where (x_0, y_0) are the coordinates of the equilibrium

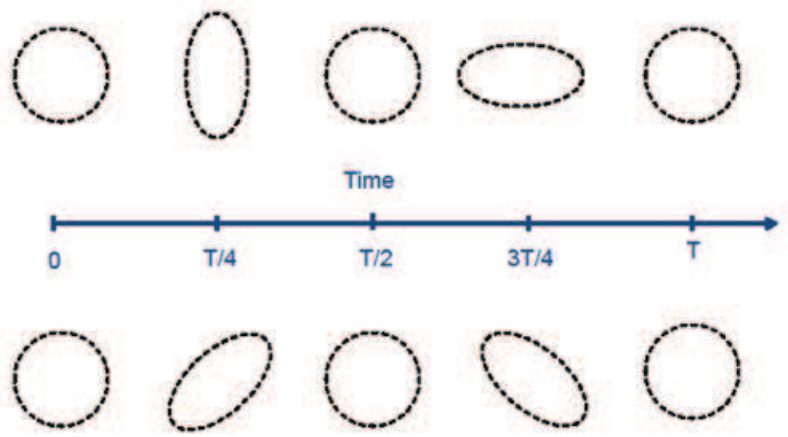

Figure 1.1: Time evolution of GW polarization states, h_+(top panel) and $h_\times$ (bottom panel) when they do interact with a ring of test mass particles.

position of the particle and $\delta x(t), \delta y(t)$ are the displacement induced by the GW, the time evolution of $\delta x(t)$ and $\delta y(t)$ for the $+$ polarization state are given by

$$\delta x(t) = \frac{h_+}{2} x_0 \cos \omega t, \qquad \delta y(t) = -\frac{h_+}{2} y_0 \cos \omega t, \tag{1.35}$$

and for the $\times$ polarization state

$$\delta x(t) = \frac{h_\times}{2} y_0 \cos \omega t, \qquad \delta y(t) = \frac{h_\times}{2} x_0 \cos \omega t. \tag{1.36}$$

The resulting deformation of a ring of test particles located in the (x, y) plane is shown in Figure 1.1.

With the argument considered above, GWs interacting with test masses make them move as a result of a force applied on them which implies that GWs do indeed carry energy and momentum where the kinetic energy carried by GWs goes to the test particles. In order to quantify this energy is important to note that any form of energy contributes to the space-time curvature, so in principle we should expect that even GWs themselves contribute to the space-time curvature. In section 1.1 we derived equations of motions, Equation 1.21, for the field $h_{\mu\nu}$ in the approximation where the background metric was the Minkowski flat metric $\eta_{\mu\nu}$. It is clear that in this case we are completely neglecting the possibility that GWs contribute to the space-time curvature. To take into account it we must allow the background metric to have a dynamical structure where GWs can be viewed as perturbations over a generic curved space-time rather than a flat space-time. In this case we can write the total metric tensor $g_{\mu\nu}(x)$ as follows

$$g_{\mu\nu}(x) = g^B_{\mu\nu}(x) + h_{\mu\nu}(x), \qquad |h_{\mu\nu}(x)| \ll 1. \tag{1.37}$$

In general the separation given by Equation 1.37 do not tell us which part can be considered the background and which part is the GW. An analogy with this situation can be

made by considering water waves or gravity waves on the surface of the sea. We can not say with a precision which part belong to the wave (vertical movements) and which part belong to the unperturbed sea or background which is originated by the incoherent superpositions of different modes.

A natural way where we can remove the ambiguity in Equation 1.37 is only possible when there is a clear separation of scales. With this we mean that given a reference system, a background with curvature radius $\mathcal{R}_B$ and small perturbations with reduced wavelength $\lambda\!\!\!^{-} = 2\pi/\lambda$, we require that

$$\lambda\!\!\!^{-} \ll \mathcal{R}_B, \tag{1.38}$$

or equivalently

$$f \gg f_B, \tag{1.39}$$

where f is a characteristic peak frequency of a GW and f_B is the background peak frequency. The separation of the kind Equation 1.38, namely the short wave expansion [19, 20] includes most cases of GWs at far distance from the source where the background space-time is almost almost flat. In this context we separate the Ricci tensor as

$$R_{\mu\nu} = R^{(B)}_{\mu\nu} + R^{(1)}_{\mu\nu} + R^{(2)}_{\mu\nu} + ..., \tag{1.40}$$

where $R^{(B)}_{\mu\nu}$ is the background Ricci tensor and $R^{(1)}_{\mu\nu}, R^{(2)}_{\mu\nu}$ contains respectively first and second order terms in $h_{\mu\nu}$. The explicit expression for $R^{(1)}_{\mu\nu}$ is

$$R^{(1)}_{\mu\nu} = \frac{1}{2}(\nabla_\mu\nabla^\alpha h_{\alpha\nu} + \nabla^\beta\nabla_\nu h_{\mu\beta} - \nabla_\alpha\nabla^\alpha h_{\mu\nu} - \nabla_\mu\nabla_\nu h), \tag{1.41}$$

where we made use of Equation 1.6 and have replaced $\partial_\mu \rightarrow \nabla_\mu$ with ∇_μ being the covariant derivative which is constructed with the metric tensor $g^{(B)}_{\mu\nu}$

$$\nabla_\alpha h_{\mu\nu} = \partial_\alpha h_{\mu\nu} - \Gamma^{\beta\,(B)}_{\mu\alpha} h_{\beta\nu} - \Gamma^{\beta\,(B)}_{\nu\alpha} h_{\beta\mu}. \tag{1.42}$$

Calculations for $R^{(2)}_{\mu\nu}$ are rather tedious and we here present only its final form

$$R^{(2)}_{\mu\nu} = \frac{1}{2} g^{\alpha\beta}_{(B)}\, g^{\rho\sigma}_{(B)} \left[\frac{1}{2}\nabla_\mu h_{\alpha\rho}\nabla_\nu h_{\beta\sigma} + (\nabla_\rho h_{\alpha\nu})(\nabla_\sigma h_{\beta\mu} - \nabla_\beta h_{\sigma\mu}) + h_{\rho\alpha}(\nabla_\nu\nabla_\mu h_{\sigma\beta} + \right.$$
$$\left. \nabla_\beta\nabla_\sigma h_{\mu\nu} - \nabla_\beta\nabla_\nu h_{\mu\sigma} - \nabla_\beta\nabla_\mu h_{\nu\sigma}) + (\frac{1}{2}\nabla_\alpha h_{\rho\sigma} - \nabla_\rho h_{\alpha\sigma})(\nabla_\nu h_{\mu\beta} + \nabla_\mu h_{\nu\beta} - \nabla_\beta h_{\mu\nu}) \right], \tag{1.43}$$

where indices are raised and lowered with the background metric tensor $g^{(B)}_{\mu\nu}$.

Our next step is to separate the Einstein's field equation Equation 1.1 in low and high frequency terms. Writing

$$R_{\mu\nu} = 8\pi G \left(T_{\mu\nu} - \frac{1}{2} g_{\mu\nu} T \right), \tag{1.44}$$

where $T = g^{\mu\nu}T_{\mu\nu}$ and inserting Equation 1.40 into Equation 1.44 we get the following scale separation

$$\begin{aligned} R^{(B)}_{\mu\nu} &= -R^{(2)}_{\mu\nu} + 8\pi G\left(T_{\mu\nu} - \frac{1}{2}g_{\mu\nu}T\right), \qquad \text{Low frequency} \\ R^{(1)}_{\mu\nu} &= -R^{(2)}_{\mu\nu} + 8\pi G\left(T_{\mu\nu} - \frac{1}{2}g_{\mu\nu}T\right). \qquad \text{High frequency} \end{aligned} \tag{1.45}$$

Here we are in the regime given by Equation 1.38 and $h \ll 1$ where h is the typical value of GW amplitude. In this case $R^{(B)}_{\mu\nu}$ contains by definition terms which are of low frequencies since $\partial_\alpha g^{(B)}_{\mu\nu} \lesssim 1/\mathcal{R}_B$ and $\partial_\alpha h_{\mu\nu} \lesssim h/\lambda\!\!\!^{-}$. Moreover, we may notice that $R^{(2)}_{\mu\nu}$ contains parts which are both low and high frequency. The low frequency equation indicates that GWs and matter contribute to the background curvature and the high frequency equation takes into account the propagation of GWs on the background space-time. To see more closely the meaning of Equation 1.45 let us specialize in vacuum, namely in regions where $T_{\mu\nu} = 0$. In this case we have

$$\begin{aligned} R^{(B)}_{\mu\nu} + R^{(2)}_{\mu\nu} + O(h^3) + ... &= 0, \qquad \text{Low frequency} \\ R^{(1)}_{\mu\nu} + R^{(2)}_{\mu\nu} + O(h^3) + ... &= 0. \qquad \text{High frequency} \end{aligned} \tag{1.46}$$

From Equation 1.43 we get the order of magnitude of $R^{(2)}_{\mu\nu} \sim (\partial h)^2$ which from Equation 1.46 implies $R^{(B)}_{\mu\nu} \sim (\partial h)^2$. The background Ricci tensor is constructed with the second derivatives of $g^{(B)}_{\mu\nu}$ and its order of magnitude estimate is

$$R^{(B)}_{\mu\nu} \sim \partial^2 g^{(B)}_{\mu\nu} \sim 1/\mathcal{R}^2_B. \tag{1.47}$$

On the other hand we have $(\partial h)^2 \sim (h/\lambda\!\!\!^{-})^2$, so we get the following condition

$$h \lesssim \frac{\lambda\!\!\!^{-}}{\mathcal{R}_B}. \tag{1.48}$$

Equation 1.48 gives a condition for the GW amplitude in order to contribute to the space-time curvature. If we consider a region where $T_{\mu\nu} \neq 0$, then the matter contribution to the curvature will dominate the GW contribution and we have $h \ll \lambda\!\!\!^{-}/\mathcal{R}_B$.

In the case of a flat space-time, the curvature $\mathcal{R}_B$ is infinite and Equation 1.48 breaks down for any value of $h \ll 1$. Summarizing, we conclude that the concept of GW has meaning if and only if condition Equation 1.48 is satisfied. In fact as we saw above, we can talk about GW only where is a clear separation of scales as given in Equation 1.38 but if $h \sim 1$ according to Equation 1.48 $\lambda\!\!\!^{-} \sim \mathcal{R}_B$ and Equation 1.38 is not satisfied anymore. So the concept of GW is valid only when its amplitude is small compared to unity.

After having discussed how GWs contribute to the space-time curvature and have seen the validity of GW concept let us now turn on evaluation of the effective energy-momentum tensor of GWs. After straightforward manipulations, the low frequency part

of Einstein field equations, Equation 1.45 can be written in the form

$$R_{\mu\nu}^{(B)} - \frac{1}{2} g_{\mu\nu}^{(B)} R^{(B)} = 8\pi G \langle T_{\mu\nu} + t_{\mu\nu} \rangle, \tag{1.49}$$

where we define the quantity $t_{\mu\nu}$ as

$$t_{\mu\nu} = -\frac{1}{8\pi G} \langle R_{\mu\nu}^{(2)} - \frac{1}{2} g_{\mu\nu}^{(B)} R^{(2)} \rangle, \tag{1.50}$$

$\langle ... \rangle$ denotes a spatial average over many reduced wavelengths $\lambda\!\!\!^{-}$ or a temporal average over several periods $1/f$. The spatial average basically is done by introducing a length scale l where $\lambda\!\!\!^{-} \ll l \ll \mathcal{R}_B$ and averaging over a volume of side l [19, 20]. If we consider a region where $\langle T_{\mu\nu} \rangle = 0$ only $t_{\mu\nu}$ contributes to the background metric $g_{\mu\nu}^{(B)}$, so it represents the contribution of the gravitational field itself to the background curvature and we define $t_{\mu\nu}$ as the effective energy-momentum tensor of GWs.

Let us now compute the energy-momentum tensor of gravitational waves at far distance from a given source where the space-time is almost flat. The starting point is Equation 1.50 where we make use of the fact that the space-time is asymptotically flat and we can replace, $\nabla \rightarrow \partial$ in Equation 1.43. Moreover we use the Lorentz gauge, Equation 1.16 in order to take into account of only physical degrees of freedom and get rid to spurious degrees of freedom. In this case Equation 1.43 reads,

$$\langle R_{\mu\nu}^{(2)} \rangle = -\frac{1}{4} \langle \partial_\mu h_{\alpha\beta} \, \partial_\nu h^{\alpha\beta}, \rangle \tag{1.51}$$

where it can be easily shown that $\langle R^{(2)} \rangle = 0$. Inserting Equation 1.51 into Equation 1.50 we get an important expression for the energy-momentum tensor of GWs for asymptotically flat space-time

$$t_{\mu\nu} = \frac{1}{32\pi G} \langle \partial_\mu h_{\alpha\beta} \, \partial_\nu h^{\alpha\beta} \rangle. \tag{1.52}$$

An important property of Equation 1.52 is that it is gauge invariant under coordinate transformations Equation 1.9 and we can replace $h_{\alpha\beta} \rightarrow h_{\alpha\beta}^{TT}$ in Equation 1.52 since it takes into account only physical degrees of freedom.

1.3.1 Energy density and flux of GWs

In the previous section, we derived an important expression for the energy-momentum tensor of GWs, $t_{\mu\nu}$. In this section we want to evaluate expression for the energy density and flux of GWs. In the Lorentz gauge $\partial^j h_{ij} = 0$, expression for the energy density of GWs, $\rho_{\rm gw}$ is given by t_{00}

$$\rho_{\rm gw} \equiv t_{00} = \frac{1}{32\pi G} \langle \dot{h}_{ij}^{TT} \, \dot{h}_{ij}^{TT} \rangle, \tag{1.53}$$

where we used $\partial_t = \partial_0$ and $h_{ij} = h^{ij}$. Writing $h_{ij}^{TT} = \sum_\lambda h_\lambda e_{ij}^\lambda(\mathbf{k})$ and using the property of the polarization tensor $e_{ij}^\lambda e_{ij}^{\lambda'} = 2\delta_{\lambda\lambda'}$ we get the following expression for the energy density

$$\rho_{\rm gw} = \frac{1}{16\pi G} \langle \dot{h}_+^2 + \dot{h}_\times^2 \rangle. \tag{1.54}$$

Let us now calculate the energy flux of GWs. In order to do this we intuitively should expect that the total energy-momentum tensor of matter plus GWs is a conserved quantity. In fact, this can be easily seen by applying the covariant derivative on the left hand side of Equation 1.49, where we get the following conserved quantity

$$\nabla^{\mu}(T_{\mu\nu} + t_{\mu\nu}) = 0. \tag{1.55}$$

Equation 1.55 implies that instead of conservation of each quantity separately, what is conserved is the sum of energy-momentum of matter plus radiation as we expected! So there is a exchange in energy and momentum between matter and GWs.

If we limit our considerations far away from the source where $T_{\mu\nu} \to 0$ and $\nabla^{\mu} \to \partial^{\mu}$ we get $\partial^{\mu} t_{\mu\nu} = 0$. Integrating over a volume V bounded by a surface S we get the following relation

$$\int_V d^3x \left(\partial_0 t^{00} + \partial_i t^{i0}\right) = 0. \tag{1.56}$$

Equation 1.56 implies

$$\frac{dE}{dt} = -\int_V d^3x\, \partial_i t^{i0} = -\int_S dA\, n_i t^{i0}, \tag{1.57}$$

where $E_V = \int_V d^3x\, t^{00}$ and we made use of Gauss theorem with n^i is a vector normal to the surface S. In general if S is a surface with a spherical symmetry, every direction will be the same and we can write $n_i t^{i0} = \hat{r} t^{r0} = t^{r0}$. At large distances from the source, $h_{ij}(r,t)$ is almost a plane wave and $\partial_r h_{ij} = \partial^0 h_{ij} + O(1/r^2)$ which implies $t^{r0} = t^{00}$. In this case we have

$$\frac{dE}{dt} = -\int_S dA\, t^{00}, \tag{1.58}$$

where the minus sign in front of Equation 1.58 means that energy is being subtracted to the source and that the energy flux carried by GWs is positive. Thus we obtain an important expression for the energy flux carried by GWs

$$F_{\rm gw} = \frac{dE}{dA\, dt} = \frac{1}{16\pi G}\langle \dot{h}_+^2 + \dot{h}_\times^2 \rangle. \tag{1.59}$$

Thus the energy flux of gravitational waves at far distance from the source is simply proportional to the square of time derivative of the GW polarization state, averaged over several wavelengths. The flux in units of a given frequency is given by

$$F_{\rm gw}(f) = \frac{dE}{dA\, df} = \frac{\pi}{2G} f^2 (|h_+^2(f)| + |h_\times^2(f)|), \tag{1.60}$$

where $h_\lambda(f)$ are the Fourier components of h_{ij}. The total energy per unit area contained in the GW is calculated by integrating Equation 1.60 over the physical frequencies $f > 0$.

1.4 Generation of gravitational waves

As we saw in section 1.1 the weak field Einstein's equation are given by Equation 1.21 in the Lorentz gauge, $\partial^\mu \bar{h}_{\mu\nu} = 0$. One possible solution of Equation 1.21 is given trough the Green function

$$\bar{h}_{\mu\nu}(x) = -16\pi G \int d^4x' G(x-x') T_{\mu\nu}(x'), \tag{1.61}$$

where $G(x-x')$ is the Green function which satisfies equation

$$\Box_x G(x-x') = \delta^4(x-x'). \tag{1.62}$$

Just as in the case of electromagnetic theory the appropriate choice of the Green function for radiative processes is the retarded Green function

$$G(x-x') = -\frac{1}{4\pi|\mathbf{x}-\mathbf{x}'|}\delta(x^0_{\text{ret}} - x'^0), \tag{1.63}$$

where $t_{\text{ret}} = t - |\mathbf{x}-\mathbf{x}'|$. Inserting Equation 1.63 into Equation 1.61 we get the following equation for the retarded potential

$$\bar{h}_{\mu\nu}(\mathbf{x},t) = 4G \int d^3x' \, \frac{1}{|\mathbf{x}-\mathbf{x}'|} \, T_{\mu\nu}(\mathbf{x}', t - |\mathbf{x}-\mathbf{x}'|). \tag{1.64}$$

The dependence of the energy-momentum tensor through the combination $t - |\mathbf{x}-\mathbf{x}'|$ emphasize the fact that gravitational effects propagate with the speed of light. Equation 1.64 automatically satisfies the Lorentz gauge, Equation 1.16 because of the conservation of the energy-momentum tensor in flat space-time, $\partial_\mu T^{\mu\nu} = 0$. However, outside the source we can choose a reference system where we can put the potential $\bar{h}_{\mu\nu}$ in the TT gauge, Equation 1.24. This can be achieved by introducing the projector operator $\Lambda_{ij,kl}(\hat{\mathbf{n}})$ which projects a general solution of Equation 1.21 into the TT gauge

$$\Lambda_{ij,kl}(\hat{\mathbf{n}}) = \delta_{ik}\delta_{jl} - \frac{1}{2}\delta_{ij}\delta_{kl} + \frac{1}{2}n_k n_l \delta_{ij} + \frac{1}{2}n_i n_j \delta_{kl} + \frac{1}{2}n_i n_j n_k n_l - n_j n_l \delta_{ik} - n_i n_k \delta_{jl}, \tag{1.65}$$

where $\hat{\mathbf{n}} = \hat{\mathbf{x}} = \hat{\mathbf{k}} = \mathbf{k}/|\mathbf{k}| = \mathbf{k}/\omega$. Therefore in the TT gauge Equation 1.64 reads

$$h^{TT}_{ij}(\mathbf{x},t) = 4G\Lambda_{ij,kl}(\hat{\mathbf{n}}) \int d^3x' \, \frac{1}{|\mathbf{x}-\mathbf{x}'|} \, T_{kl}(\mathbf{x}', t - |\mathbf{x}-\mathbf{x}'|). \tag{1.66}$$

Let us suppose to observe the source radiation in the wave zone $r = |\mathbf{x}|$, namely at a distance larger than its physical dimension d, $r \gg d$. In this case we can expand $|\mathbf{x}-\mathbf{x}'|$ as follows

$$|\mathbf{x}-\mathbf{x}'| \simeq r - \mathbf{x}'\cdot\hat{\mathbf{n}}, \tag{1.67}$$

where $|\mathbf{x}| = r$. If we are interested in the wave at spatial infinity $r \to \infty$ we may approximate $|\mathbf{x}-\mathbf{x}'| \simeq r$, thus Equation 1.66 becomes

$$h^{TT}_{ij}(\mathbf{x},t) = \frac{4G}{r}\Lambda_{ij,kl}(\hat{\mathbf{n}}) \int d^3x' \, T_{kl}(\mathbf{x}', t - r + \mathbf{x}'\cdot\hat{\mathbf{n}}). \tag{1.68}$$

If we write T_{kl} in Fourier components such as

$$T_{kl}(\mathbf{x},t) = \frac{1}{(2\pi)^4}\int d\omega\, d^3k\, T_{kl}(\mathbf{k},\omega)\, e^{-i(\omega t-\mathbf{k}\cdot\mathbf{x})} \tag{1.69}$$

and inserting it into Equation 1.66 after some straightforward calculations we get

$$h_{ij}^{TT}(\mathbf{x},t) = \frac{4G}{r}\Lambda_{ij,kl}(\hat{\mathbf{n}})\int_{-\infty}^{\infty}\frac{d\omega}{2\pi}\,T_{kl}(\mathbf{k},\omega)e^{-i\omega(t-r)}. \tag{1.70}$$

Using the fact that the energy emitted by a source per unit solid angle Ω is given by

$$\frac{dE}{d\Omega} = \frac{r^2}{32\pi G}\int_{-\infty}^{\infty} dt\,\dot{h}_{ij}^{TT}\dot{h}_{ij}^{TT}, \tag{1.71}$$

where we used Equation 1.53 and using the expansion Equation 1.70 we get

$$\frac{dE}{d\Omega} = \frac{G}{2\pi^2}\Lambda_{ij,kl}(\hat{\mathbf{n}})\int_0^{\infty} d\omega\,\omega^2\, T_{ij}(\mathbf{k},\omega)\, T_{kl}^{*}(\mathbf{k},\omega). \tag{1.72}$$

Equation 1.72 gives the energy emitted per solid angle in terms of the Fourier components of the energy momentum tensor. The problem is thus solved once we have calculated the Fourier transform of Equation 1.69.

1.5 Low velocity expansion and the quadrupole radiation

Hitherto the derived results of the previous section were general in the sense that the only approximation used there was that we considered the observation distance of the wave front at spatial infinity where the wave can be considered as a plane wave. In this section we make a further approximation and assume that the source size d is smaller than the wavelength $\lambda\!\!\!^{-} = 1/\omega$

$$\omega\, d \ll 1 \Longleftrightarrow \lambda\!\!\!^{-} \gg d. \tag{1.73}$$

Since the typical velocity of motion inside the source is $v \sim \omega d$, the above conditions is valid as far as the source velocity is non relativistic $v \ll 1$. In this case we don't need to know the internal composition of the source but only some macroscopic parameters such its mass, velocity through space etc. In the non relativistic regime the Fourier components $T_{kl}(\mathbf{k},\omega)$ of the energy momentum tensor are maximal around some particular frequency ω_s and satisfy $\omega_s d \ll 1$. Taking also into account that the integration region is limited by $|\mathbf{x}'| \ll d$ we have that in general $\omega\,\mathbf{x}'\cdot\hat{\mathbf{n}} \ll 1$ and thus we can expand the energy momentum tensor in Equation 1.68 at the point $(\mathbf{x}', t-r)$ as

$$T_{kl}(\mathbf{x}', t-r+\mathbf{x}'\cdot\hat{\mathbf{n}}) \simeq T_{kl}(\mathbf{x}', t-r) + n^i\, x'^i\, \partial_t\, T_{kl} + \frac{1}{2}n^i\, n^j\, x'^i\, x'^j\, \partial_t^2\, T_{kl} + \ldots \tag{1.74}$$

At this stage is very convenient to define the multipoles of the energy-momentum tensor T_{ij} as follows

$$S^{ij}(t) = \int d^3x T^{ij}(\mathbf{x},t), \tag{1.75}$$

$$S^{ij,k}(t) = \int d^3x\, x^k\, T^{ij}(\mathbf{x},t), \tag{1.76}$$

$$S^{ij,kl}(t) = \int d^3x\, x^k\, x^l\, T^{ij}(\mathbf{x},t), \tag{1.77}$$

where the indexes k,l after the comma in the above equations reflect the fact that they belong to the k-th and j-th direction x^k and x^j. Using the above multipole expansion into Equation 1.74 and then inserting it into Equation 1.68 we get the following expansion for the retarded potential evaluated at the retarded time $t_{\rm ret} = t - r$

$$h_{ij}^{TT}(\mathbf{x},t) = \frac{4G}{r}\Lambda_{ij,kl}(\hat{\mathbf{n}})\left[S^{kl} + n_a\dot{S}^{kl,a} + \frac{1}{2}n_a n_b\ddot{S}^{kl,ab} + ...\right]. \tag{1.78}$$

Equation 1.78 in general can be casted in a more convenient way if we write the corresponding momenta respect to the energy density of the matter T_{00} and linear momentum T_{0i}. Let be M, M^i, M^{ij}, M^{ink} respectively the monopole, dipole, quadrupole and octupole momenta of the energy density defined as follows

$$M = \int d^3x T^{00}(\mathbf{x},t), \tag{1.79}$$

$$M^i = \int d^3x T^{00}(\mathbf{x},t)x^i, \tag{1.80}$$

$$M^{ij} = \int d^3x T^{00}(\mathbf{x},t)x^i x^j, \tag{1.81}$$

$$M^{ijk} = \int d^3x T^{00}(\mathbf{x},t)x^i x^j x^k, \tag{1.82}$$

and the linear momentum momenta defined as follows

$$P^i = \int d^3x T^{0i}(\mathbf{x},t), \tag{1.83}$$

$$P^{i,j} = \int d^3x T^{0i}(\mathbf{x},t)x^j, \tag{1.84}$$

$$P^{i,jk} = \int d^3x T^{0i}(\mathbf{x},t)x^j x^k. \tag{1.85}$$

Important relations between the energy density momenta and linear momentum momenta together with their time derivative can be obtained by considering that we are still working in the flat space-time background metric where the energy-momentum tensor satisfies the conservation law $\partial_\mu T^{\mu\nu} = 0$. One can easily get from the conservation of the energy-momentum tensor the following relations for the energy density momenta up

to the octupole

$$\dot{M} = 0, \tag{1.86}$$
$$\dot{M}^i = P^i, \tag{1.87}$$
$$\dot{M}^{ij} = P^{i,j} + P^{j,i}, \tag{1.88}$$
$$\dot{M}^{ijk} = P^{i,jk} + P^{j,ki} + P^{k,ij}, \tag{1.89}$$

and the following relations for the momenta of the linear momentum

$$\dot{P}^i = 0, \tag{1.90}$$
$$\dot{P}^{i,j} = S^{ij}, \tag{1.91}$$
$$\dot{P}^{i,jk} = S^{ij,k} + S^{i,kj}. \tag{1.92}$$

The above sets of relations between various momenta of the energy density and linear momentum allows us to express the various momenta of S^{ij} etc. in terms of the sets composed by $\{M, M^i, M^{ij}, ...\}$ and $\{P^i, P^{ij}, ...\}$. For example an important relation can be obtained by taking the time derivative of $\dot{M}^{ij}$ which gives

$$\ddot{M}^{ij} = \dot{P}^{i,j} + \dot{P}^{j,i}, \tag{1.93}$$

and using the fact that $\dot{P}^{i,j} = S^{ij}$ with S^{ij} symmetric respect to the indexes i, j we get

$$S^{ij} = \frac{1}{2}\ddot{M}^{ij}. \tag{1.94}$$

Using similar relations between various momenta we can also easily get the next leading momenta for S^{ij} which reads

$$\dot{S}^{i,jk} = \frac{1}{6}\dddot{M}^{ijk} + \frac{1}{3}\left(\ddot{P}^{i,jk} + \ddot{P}^{j,ik} - 2\ddot{P}^{k,ij}\right). \tag{1.95}$$

However at the moment we are interested only in the first moment of the set $\{S^{ij}, S^{i,jk}...\}$ because the other moments give smaller contributions to Equation 1.78 which in this case becomes

$$h_{ij}^{TT}(\mathbf{x}, t) = \frac{2G}{r}\Lambda_{ij,kl}(\hat{\mathbf{n}})\ddot{M}^{kl}(t - r). \tag{1.96}$$

At this point is more convenient to express the tensor $\ddot{M}^{kl}$ as follows

$$\ddot{M}^{kl} = \left(\ddot{M}^{kl} - \frac{1}{3}\delta^{kl}M^j_j\right) + \frac{1}{3}\delta^{kl}M^j_j, \tag{1.97}$$

where M^j_j is the trace of the tensor M^{kl} and the term with the brackets is traceless. Let us denote with Q_{ij} the traceless part

$$Q^{ij} = M^{ij} - \frac{1}{3}\delta^{ij}M^k_k = \int d^3x\,\rho(\mathbf{x}, t)(x^i x^j - \frac{1}{3}r^2\delta^{ij}), \tag{1.98}$$

where $\rho = T_{00}$. By noting that $\Lambda_{ij,kl}M^{kl} = \Lambda_{ij,kl}(\hat{\mathbf{n}})Q_{kl}$ we get the following relation for the retarded potential

$$h_{ij}^{TT}(\mathbf{x},t) = \frac{2G}{r}\Lambda_{ij,kl}(\hat{\mathbf{n}})\ddot{Q}_{kl}(t-r). \tag{1.99}$$

Equation 1.99 is of fundamental importance since it allows us to find the energy emitted by a moving source. Since it depends on the quadrupole tensor Q_{ij} which is derived from M_{ij} it is also referred as the quadrupole retarded potential. By noting that the power emitted per unit solid angle is $dP/d\Omega = r^2\rho_{\rm gw}$ where $\rho_{\rm gw}$ is given by Equation 1.53, we get following expression for the quadrupole emitted power per unit solid angle

$$\frac{dP}{d\Omega} = \frac{G}{8\pi}\Lambda_{ij,kl}(\hat{\mathbf{n}})\langle\dddot{Q}_{ij}\dddot{Q}_{kl}\rangle_{\rm ret} \tag{1.100}$$

The total power emitted by the source is obtained by integrating Equation 1.100 over the solid angle where the angular dependence is encoded on the projector operator $\Lambda_{ij,kl}$. Integration over the angles can be done by first noting that

$$\int d\Omega\, n_{i_1}...n_{i_{2l}} = \frac{1}{(2l+1)!!}(\delta_{i_1}\delta_{i_2}...\delta_{i_{2l-1}i_{2l}} + ...) \tag{1.101}$$

Using the above result, the integration over angles of the projection operator reads

$$\int d\Omega\,\Lambda_{ij,kl}(\hat{\mathbf{n}}) = \frac{2\pi}{15}(\delta_{il}\delta_{jk} + 11\delta_{ik}\delta_{jl} - 4\delta_{ij}\delta_{kl}) \tag{1.102}$$

Inserting Equation 1.102 into Equation 1.100 we get the following expression for the total power emitted by the source in the quadrupole approximation

$$P_{\rm quad} = \frac{G}{5}\langle\dddot{Q}_{ij}\dddot{Q}_{kl}\rangle_{\rm ret} \tag{1.103}$$

Equation 1.103 is a very important result in the theory of gravitational waves which was first derived by Einstein in 1916. It allows to compute the total power emitted by a given source by just knowing its spatial distribution which is encoded in the quadrupole tensor Q_{ij}. It is important to emphasize that there is no general consensus on the definition of the quadrupole tensor, Equation 1.98 in the literature where in several cases these definitions do not coincide with our notations such as in the Landau e Lifshitz Vol. 2. As a result in many cases the total power emitted by a source with a given quadrupole tensor may differ from one textbook to the other by a numerical factor of the order of unity.

In general the quadrupole formula is widely used in the context of two point masses in circular or elliptic orbit and in isolated systems such as neutron stars and black holes. The first case include calculation of the total power emitted by compact objects orbiting around each other such as binaries of neutron stars and black holes. In fact, the quadrupole formula was first applied to the binary system PSR B1913+16 by Hulse and Taylor in 1975 and found that the secular approach of the system is in good agreement with the experimental data and was one of the first indirect prove of the existence

of gravitational waves. On the other hand the quadrupole formula can be applied directly to isolated systems with known quadrupole tensor where the source must have non-spherical geometry in order to emit gravitational waves as stated in the Birkhoff's theorem.

Chapter 2

Gravitational waves astronomy

Gravitational waves detectors are divided in two classes: resonant mass detectors and beam detectors. The former class is based in the fact that gravitational waves can carry energy and it can be extracted from the wave. In fact, if two masses connected with a spring are stretched apart and after compressed by a gravitational wave, potential energy is transferred to the spring. If the wave peak frequency is close to the resonance frequency of the detecting system, the system response is magnified with possible energy enhancement. Based on this simple principle, Joseph Weber [21, 22] was the first person ever to built a laboratory detector to detected gravitational waves. He built two cylindrical aluminum bar detectors, the Weber bars and attempted to find correlated disturbances that might have been caused by a passing gravitational wave. After his claims on detection of gravitational waves, other bar detectors of better sensitivity were built which never verified his claims.

The basic idea of gravitational wave interferometer dates back to Gertsenshtein and Pustovoit [23]. It can be comparable with a right angle Michelson laser interferometer where gravitational waves interact with a beam of electromagnetic radiation and eventually induces a phase difference between the light returning from the arms of the detector. The phase difference increases with time that follow the passage of gravitational wave causing the redshifted light a longer round trip in the arm than the blue shifted light, see Figure 2.2

In this chapter we discuss the underlying working mechanisms of GW detectors, introduce some general concepts which characterize most of GW detectors, discuss main detector noise sources and overview the present status of GW detectors.

2.1 Detector signal and sensitivity

Independently of what kind of detector is being used for the detection of gravitational waves (resonant or interferometer), the output which the detector generates is in general

Figure 2.1: Joseph Weber working on the first resonant mass detector at the University of Maryland.

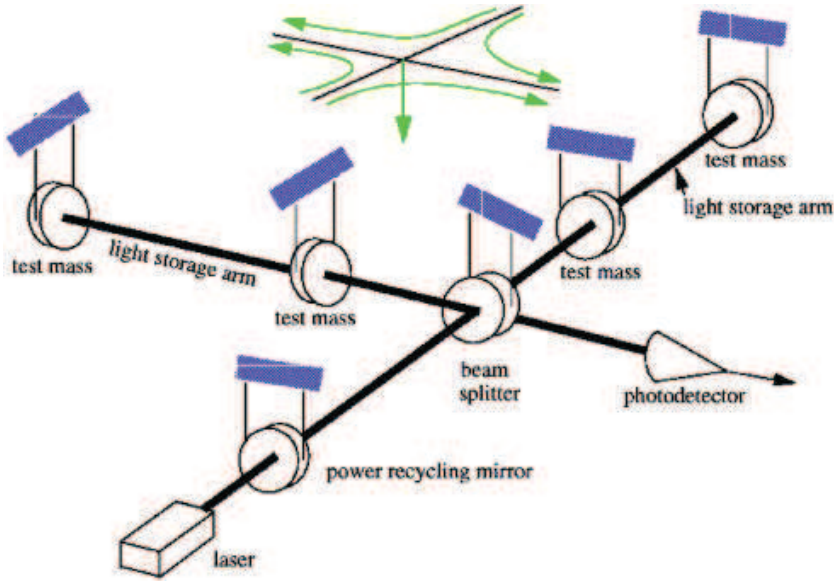

Figure 2.2: General design of a gravitational wave interferometer.

the sum of the true gravitational wave signal plus noise arising from the detector itself. Both the input and the output of the detector are scalar quantities while gravitational waves are tensor quantities, namely h_{ij}. So, in general the total output of the detector has the form

$$s(t) = h(t) + n(t), \tag{2.1}$$

where $n(t)$ is the noise , $h(t)$ is the total output in GW due to the detector and $s(t)$ is the total output of the detector. The GW output $h(t)$ is in general expressed as

$$h(t) = D^{ij}h_{ij}(t), \tag{2.2}$$

where the spatial dependence of h_{ij} has been omitted because we are considering the origin at the detector position, $\mathbf{x} = 0$ and the quantity D^{ij} is called detector tensor which depends on the detector geometry.

In general for a stationary noise, the different Fourier components of the noise $n(f)$ where f is the frequency are uncorrelated. Thus, in this case the ensemble average of the noise is

$$\langle n^*(f)n(f)\rangle = \delta(f - f')\frac{1}{2}S_n(f), \tag{2.3}$$

where $S_n(f)$ is a function of frequency f and has the physical dimensions of Hz^{-1}. For uncorrelated noise components, an important assumption which is usually made is that the ensemble average of the noise is zero $\langle n(t)\rangle = 0$. However, the mean square value of the noise is different from zero and is usually expressed through

$$\langle n^2(t)\rangle = \int_{-\infty}^{\infty} df\, df' \langle n^*(f)n(f)\rangle = \frac{1}{2}\int_{-\infty}^{\infty} df\, S_n(f) = \int_0^{\infty} df\, S_n(f), \tag{2.4}$$

where the function $S_n(f)$ is called the *noise spectral density* or the *noise power spectrum*. With the ensemble average of the noise equal to zero, we can equivalently characterize the noise of a detector as

$$h_f \equiv \sqrt{S_n(f)}, \tag{2.5}$$

where h_f is called *spectral strain sensitivity* or simply *strain sensitivity* and has the dimension of $\mathrm{Hz}^{-1/2}$.

As we saw in the previous chapter, a general gravitational wave in the TT-gauge can be expanded as in Equation 1.31. If we look for GW at the detector position and consider GW with reduced wavelength larger than the detector size, $\mathbf{k}\cdot\mathbf{x}/\lambda \ll 1$ we get

$$h_{ij}(t) = \sum_{\lambda=+,\times} h_\lambda(t)e^\lambda_{ij}(\mathbf{k}). \tag{2.6}$$

Introducing Equation 2.6 into Equation 2.2 we can write the GW signal, $h(t)$ as

$$h(t) = \sum_{\lambda=+,\times} h^\lambda(t)F_\lambda(\mathbf{k}), \tag{2.7}$$

where the functions F_λ are called detector pattern functions and are defined as

$$F_\lambda(\mathbf{k}) = D^{ij}e^\lambda_{ij}(\mathbf{k}). \tag{2.8}$$

The pattern functions F_λ depend on the arrival direction of the GW, $\mathbf{k} = (\theta, \phi)$ and implicitly on a rotation angle ψ of the plane of the wave respect to the wave incidence direction.

In order to compare the noise with the GW signal, we need an expression for the mean square root of the GW signal. In fact, by using Equation 2.7 we get

$$\langle h^2(t) \rangle = F \int_0^\infty df\, S_h(f), \tag{2.9}$$

where

$$F = \int \frac{d^3k}{4\pi} \sum_{\lambda=+,\times} F^\lambda(\mathbf{k}, \psi) F^\lambda(\mathbf{k}, \psi). \tag{2.10}$$

The factor F is a measure of the detector sensitivity loss due to GWs coming from all directions compared to the sensitivity which can be obtained if GWs come from an optimal direction, $\mathbf{k}_{opt}$. The function $S_h(f)$ is called the *square spectral signal sensitivity* and has the dimensions of Hz^{-1}. By imposing that the signal is above the noise threshold $h(t) > n(t)$ we get

$$S_h(f) > \frac{S_n(f)}{F}. \tag{2.11}$$

Equation 2.11 gives a condition for GW the signal to manifest itself as an excess of noise and eventually detectable. This condition emphasize the role of the factor F on the detectability of the GW signal and therefore an appropriate choice of the detector geometry can minimize the overall noise of the detector.

Each type of detector has different factors F depending essentially on its geometry and on the direction of the propagation of the wave. If we choose for example the wave vector $\mathbf{k}$ to have polar coordinates

$$\mathbf{k} = (\sin\theta \sin\phi, \sin\theta \cos\phi, \cos\theta), \tag{2.12}$$

and using the fact that $\hat{\mathbf{e}}^+ \cdot \hat{\mathbf{e}}^\times = 0$, the coordinates for $\hat{\mathbf{e}}^+$, $\hat{\mathbf{e}}^\times$ are given by

$$\hat{\mathbf{e}}^+ = (-\cos\theta \sin\phi, -\cos\theta \cos\phi, \sin\theta), \qquad \hat{\mathbf{e}}^\times = (-\cos\phi, \sin\phi, 0). \tag{2.13}$$

The detector tensor for the case of interferometers with arms along the directions $\hat{\mathbf{u}}$ and $\hat{\mathbf{v}}$ can be written as

$$D_{ij} = \frac{1}{2}(\hat{\mathbf{u}}_i \hat{\mathbf{v}}_j - \hat{\mathbf{v}}_i \hat{\mathbf{u}}_j). \tag{2.14}$$

With the basis vectors given by Equation 2.13 and the propagation direction given by Equation 2.12 the pattern function are given by [24]

$$F_+(\theta, \phi, \psi) = -\cos\theta \sin 2\phi \sin 2\psi + \frac{1}{2}(1 + \cos^2\theta) \cos 2\phi \cos 2\psi \tag{2.15}$$

$$F_\times(\theta, \phi, \psi) = \cos\theta \sin 2\phi \cos 2\psi + \frac{1}{2}(1 + \cos^2\theta) \cos 2\phi \sin 2\psi. \tag{2.16}$$

After some lengthy calculations, the factor F for interferometers with perpendicular arms reads

$$F = \int \frac{d^3k}{4\pi} \sum_{\lambda=+,\times} F^{\lambda}(\mathbf{k},\psi)F^{\lambda}(\mathbf{k},\psi) = 2/5. \tag{2.17}$$

If the arms of the detector form an angle α the factor F changes as

$$F = \frac{2}{5}\sin^2\alpha. \tag{2.18}$$

This means that the best sensitivity for an interferometer is achieved only when the arms of the detector form a right angle $\alpha = \pi/2$.

In the case of Weber bars or cylindrical bars, the detector tensor can be written as follows

$$D^{ij} = \hat{\mathbf{u}}^i\hat{\mathbf{v}}^j. \tag{2.19}$$

In this case the detector pattern functions can be calculated as in [24]

$$F_+(\theta,\phi,\psi) = \sin^2\theta\cos 2\phi, \tag{2.20}$$

$$F_\times(\theta,\phi,\psi) = \sin^2\theta\sin 2\phi. \tag{2.21}$$

Therefore for Weber bars the detector form factor is $F = 8/15$. Comparison between the form factors of interferometers and Weber bars shows that interferometers are more sensitive for GW detection, reason why (as we will see in the next sections) they are more used for GW detection than Weber bars.

2.2 Noise sources

The Interaction of a GW with a detector is different for resonant mass detector and interferometer. The mean differences are incorporated first in the working mechanism of each of them and second on the materials being used for their construction. This differences lead to different sensitivity levels due to the fact the noise in one group may be further reduced respect to the other. However, there are some noise sources which are common to both groups and in this section we want to discuss the most important of them.

2.2.1 Resonant detectors

The working principle of resonant bars or Weber bars is based on the principle of energy conservation, namely that the energy is transferred to the detector by the GW and we can think of a Weber bar as an energy detection device. A typical Weber bar is composed of aluminum with a typical length of $l \simeq 3$ m, a narrow resonant frequency band between $f \sim 400$ Hz and $f \sim 1.5$ kHz and a mass of the order $M \sim 10^3$ kg.

One of the most important source of noise is the *thermal noise* which arises from the random motion of atoms in the material used. Since a bar can be approximated as an one

dimensional object, the equipartition theorem tells us that the average thermal energy for one mode is simply $k_B T$ where T is the bar temperature and k_B is the Boltzmann constant. If we treat the bar as just as simple harmonic oscillator with constant k and denote with δl the deviation from its normal length l due to thermal noise, the expected RMS value of amplitude of vibration is

$$\langle \delta l^2 \rangle_{th}^{1/2} \simeq \left(\frac{k_B T}{4\pi^2 f_0 M} \right)^{1/2}, \tag{2.22}$$

where we made use of $(1/2)k\delta l^2 = (1/2)M\omega^2 = (1/2)k_B T$ with $\omega = 2\pi f_0$ and f_0 is the bar fundamental oscillation frequency. The most recent resonant detectors such as Auriga or Nautilus are ultra cryogenic and work at $T = 100$ mK and a frequency of $f_0 = 1000$ Hz. At this temperature its RMS vibration amplitude is of the order $\sim 6 \cdot 10^{-18}$ m. This is far larger than the GW amplitude expected from astrophysical sources. Fortunately, the fact that resonant bars are deliberately designed with high mechanical quality factors Q allows much better sensitivity than this naive calculation suggest. In fact, if the material has a high Q, the impulse imparted by a passing GW is dissipated over a timescale $\tau \sim Q/f_0$, so for $Q \sim 10^6, \tau \sim 10^3$ s. This means that a high Q changes the thermal amplitude of vibration of the bar in a random walk with very small steps, taking a time $\tau \sim 10^3$ s. Hence by measuring over many cycles of the resonance, one can reduce the effective noise by a factor comparable to $\sqrt{Q} = 10^3$. This would change the vibration amplitude

$$\langle \delta l^2 \rangle_{th}^{1/2} \simeq \left(\frac{k_B T}{4\pi^2 f_0 M Q} \right)^{1/2} \sim 6 \cdot 10^{-21} \text{m}. \tag{2.23}$$

Since the expected amplitude of GW at earth is about $h_g \simeq 10^{-20}$ ($\delta l_{gw} = h_g l$), ultra cryogenic bars can approach the GW detection level despite thermal noise.

Hitherto we neglected additional sources of noise such as the *sensor noise*. Such a noise arises due to the non triviality of measuring the deposited GW energy. Modern bars, use transducers at the end of the bar in order to convert the bar mechanical energy into electrical energy which after is amplified and recorded. However, amplifiers introduce additional noise which make the weak signal of a GW even harder to detect. If are used transducers with an intrinsic resonant frequency close to the bar resonance frequency, the amplitudes of vibration of the coupled system are largest near f_0, hence the amplifier noise limits the detector sensitivity in a band near f_0.

A fundamental role plays the *quantum noise* due to zero point vibrations of the bar. From simple quantum mechanical arguments the vibration amplitude due to quantum noise is given by

$$\langle \delta l^2 \rangle_{quantum}^{1/2} \simeq \left(\frac{\hbar}{4\pi^2 f_0 M} \right)^{1/2} \simeq 4 \cdot 10^{-21} \text{m}. \tag{2.24}$$

We can see that as far as better sensitivity is obtained by reducing the thermal noise there is always present a quantum noise which is not possible to overcome due to the

uncertainty principle. In this direction it has been proposed that by exploiting quantum squeezing one can somehow improve in sensitivity [25, 26].

2.2.2 Interferometers

In the previous section we saw that due to different noise sources, most of resonant mass detectors have great difficulty on achieving a vibration sensitivity of the order of $\sim 10^{-21}$ m. Due to this limitation other detection methods have been proposed during the last 30 years, offering better detection sensitivity. However, resonant mass detectors remain still the favorable method of searching for narrow frequency bandwidths and high frequency GWs.

Ground based interferometers such as Virgo and LIGO use laser light to measure changes in the difference between the lengths of two nearly perpendicular arms. If we consider for example a GW with a characteristic amplitude of $h_g \sim 10^{-21}$ the length change of the detector as a response of the GW is $\delta l_{gw} = hl = 4 \cdot 10^{-18}$ m, where we took $l = 4$ km. As in the case of resonant mass detectors, *thermal noise* is still present for interferometers too. In fact, as we can see from Figure 2.2, the mirrors used for the light reflection do not completely reflect it and part of the light is absorbed by them. Moreover, the beam splitter suffers the same problem and as consequence the splitter and the mirrors by absorbing part of the light, increase their internal temperature and changes in the index of refraction. Due to thermal-refractive noise, the lensing system undergoes to random fluctuations which influence the detection efficiency of the detector. Other consequence of thermal noise is that it causes vibrations of the mirrors and to the suspending pendulum which can mask GWs. In the case of the pendulum suspensions, thermal noise vibrations are active near the frequency of few Hz and the mirrors have thermal vibrations frequency of the order of kHz. Due to this limitations arising from thermal noise, detection frequency band of interferometers is limited in the frequency range of few Hz up to few kHz.

Thermo-noise effects limit the amount of laser power used in the detector and since photons used for this scope are quantum wave packets, the laser light undergoes to random fluctuations which can mimic the GW signal causing the so called *shot noise*. In fact, by increasing the number of photons the laser beam can be described as an almost classical field where quantum fluctuations are negligible. This suggest that the shot noise improves by increasing the photon number N. The accuracy expected in this case would simply be $\delta l_{shot} \simeq \lambda\!\!\!^{-}/\sqrt{N}$. However, by increasing N, the radiation pressure would increase as $\sqrt{N}$, so one should find a good compromise in the number of photons being used but also by increasing the mass of the mirrors. For this purpose, Advanced LIGO is going to use mirror bars of 40 kg against 11 kg used for initial LIGO, in order to cope with the increased laser power ($\sim$ 10 W). With the present laser power is still difficult to reduce the shot noise below $\delta l \sim 10^{-16}$ m so the only escape is still via quantum squeezing.

Other important noise sources for interferometers can all be classified as *mechanical*

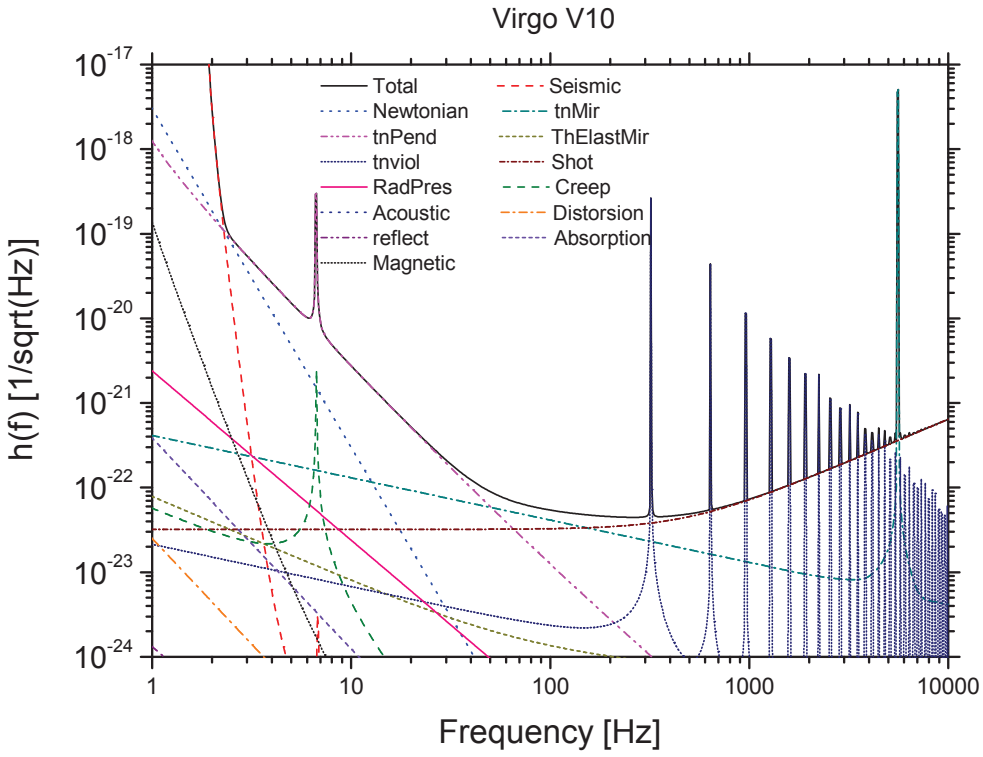

Figure 2.3: Virgo design sensitivity curve with all sources of noise included (courtesy of the Virgo collaboration.)

noise which derive from such as external mechanical vibrations of the detecting system, bounce back and forth of the light used and local changes of the Newtonian gravitational field. The last one can cause tidal forces on the detector as the GW itself does but even more important, it causes gravity waves (seismic waves) due to its inhomogeneity. An important consequence of global mechanical noise is that it decreases with increasing GW frequency by limiting the possibility of detection of the low part of the GW spectrum below few Hz. This is the main reason why looking for lower frequencies one is obliged to go to space for their detection.

2.3 Ground based interferometers

During the last 30 years have been a great effort devoted to the construction of resonant mass detectors and large scale interferometers. In the previous section we discussed the principal sources of noise and saw that the path for detection of GWs is one of the

most challenging in modern science. The principal reasona are due to the weak signal of GWs expected on earth, typically smaller than $h_g \sim 10^{-21}$ and to the physical limits of the detection system which are of quantum origin. In this section we discuss about GW detectors around the globe, including first generation of large interferometers and planned space interferometers.

2.3.1 Virgo

The Virgo interferometer is a Michelson laser interferometer, built in 2003 in Cascina, near Pisa in Italy Figure 2.4 as a collaboration between the Italian INFN and French CNRS. It consist of two perpendicular arms of 3 km each and uses multiple reflections between mirrors located at the extremities of each arm in order to extend the effective optical length of each arm up to 120 kilometers.

Figure 2.4: The Virgo interferometer located in Cascina, Pisa, Italy.

The frequency range of Virgo extends from 10 Hz up to 6 kHz. This range as well as the very high sensitivity should allow detection of gravitational radiation produced by supernovae and coalescence of binary systems in the Milky Way and in outer galaxies, for instance from the Virgo cluster. In Figure 2.3 is shown the planned sensitivity of Virgo before its construction and in Figure 2.5 is shown its last run in September 5, 2011, namely Virgo Science Run 4 (VSR4). In May 2008 started the first Virgo upgrade with new technologies, Virgo+ and performed two science runs VSR3 and VSR4 before its end in November 2011.

During VSR4, Virgo reached finally its design sensitivity of nearly $h_f \sim 10^{-22}$ $\mathrm{Hz}^{-1/2}$ in the frequency range from 100 Hz up to few kHz. Virgo+ will still work until its design sensitivity is reached as shown in Figure 2.5. Meanwhile, Virgo is pointing to more ambitious project on significantly upgrading the existing Virgo+ detector and at the end October 2011and after they plan starting installation of the Advanced Virgo detector. Its goal is to gain sensitivity of two orders of magnitude with respect to the

Virgo initial design over the frequency band 10 Hz-10 kHz, Figure 2.6, and at the end 2014 starting taking data.

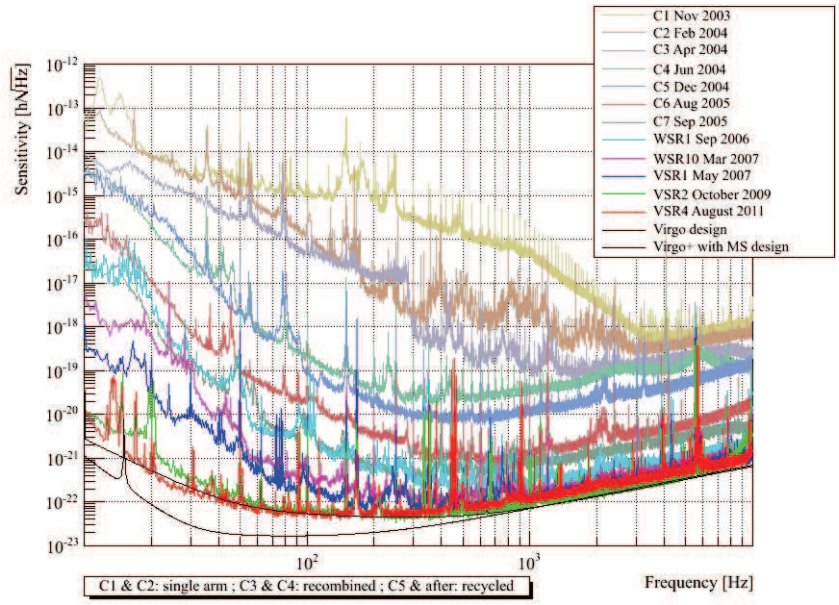

Figure 2.5: Virgo last plot with all sensitivities curve since the first Virgo commissioning run (courtesy of the Virgo collaboration.)

2.3.2 LIGO

The Laser Interferometer Gravitational-Wave Observatory (LIGO) is a joint project of Calthec and MIT aiming to detect GWs of astrophysical and cosmological origin. It consist of two widely separated interferometers located in Hanford (LIGO, Handford), Washington and in Livingston, Luisiana (LIGO, Livingston)

Each observatory support two orthogonal arms of 4 km length and started taking data in September 2002. At the Hanford Observatory, a second interferometer operates in parallel with the primary interferometer. This second detector is half the length at 2 kilometers, and its Fabry-Pérot arm cavities have the same optical finesse and thus half the storage time. With half the storage time, the theoretical strain sensitivity is as good as the full length interferometers above 200 Hz but only half as good at low frequencies. After 5 years of science runs, LIGO reached its design sensitivity goal (over $h_f \sim 10^{-21}$ $\mathrm{Hz}^{-1/2}$) at the end of 2005, Figure 2.8 in a frequency bandwidth of 100 Hz. The fifth science run S5 ended on 30 September 2007.

As its companion Virgo, after the completion of Science Run 5, initial LIGO was upgraded with certain Advanced LIGO technologies that resulted in an improved-performance configuration dubbed Enhanced LIGO. Its aim was a best-effort goal of achieving twice the sensitivity of initial LIGO by the end of the run. Enhanced LIGO started its science

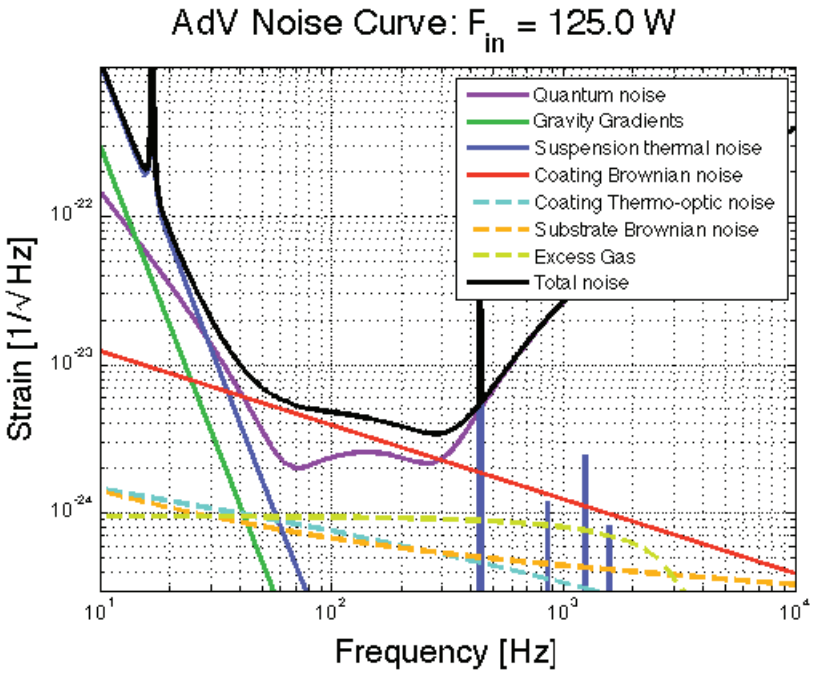

Figure 2.6: Advanced Virgo design sensitivity curve (courtesy of the Virgo collaboration.)

Figure 2.7: LIGO, Livingston, Luisiana (courtesy of the LIGO collaboration.)

run S6 in July 2009 and it concluded in October 2010. The strain sensitivity for S6 is shown in Figure 2.9.

From November 2010, Enhanced LIGO was disassembled and immediately work proceeded on construction of Advanced LIGO. It will take at least four years for its construction and it is scheduled start running from 2014. Advanced LIGO is a result of an international collaboration between, the LIGO Laboratory funded by the National Science Foundation with contributions from the GEO 600 Collaboration, Adelaide Universities in Australia and with participation by the LIGO Scientific Collaboration. This new detector is designed to improve the sensitivity of initial LIGO by more than a factor of 10, and is currently being installed at both LIGO Observatories, replacing the original detectors. Advanced LIGO design strain sensitivity is shown in Figure 2.10. Advanced LIGO is suppose to detect GWs from in spiraling neutron stars (NS) and black hole (BH) binaries, BH+BH mergers and ring downs, supernovae, Gamma ray-bursts, neutron star spinning and stochastic background.

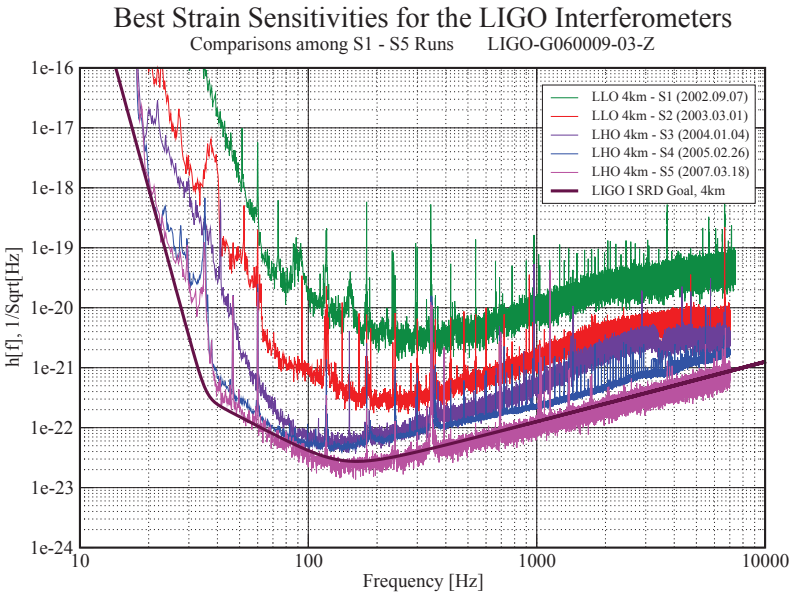

Figure 2.8: Strain sensitivity h_f as a function of frequency for LIGO since runs S1-S5 interferometers (courtesy of the LIGO collaboration).

2.3.3 GEO 600

GEO 600 is a gravitational wave interferometer located near Sarsted, Germany. It has two perpendicular arms of 600 m each and was built in 2001 as a collaboration between Max-Panck institute für Quantenoptik in Garching and the University of Glasgow. In

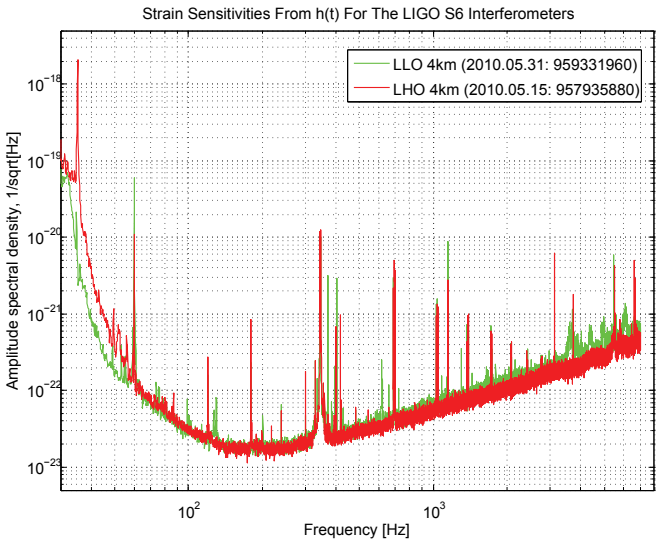

Figure 2.9: Strain sensitivity h_f as a function of frequency for LIGO S6 interferometers (courtesy of the LIGO collaboration).

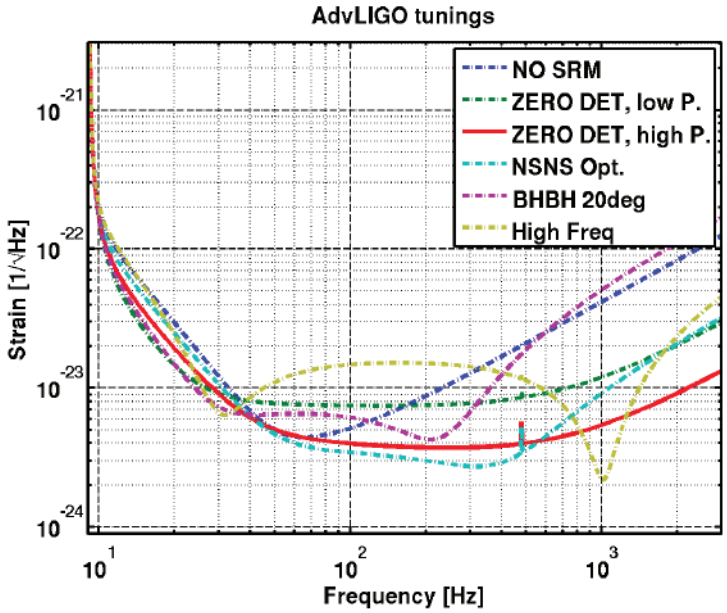

Figure 2.10: Advanced LIGO strain sensitivity curve (red color) as a function of frequency (courtesy of the LIGO collaboration).

2006, GEO600 has reached the design sensitivity, but up to now no signal has been detected. The next aim is to reduce the remaining noise by another factor of about 10, until 2014.

Figure 2.11: GEO600 land area, Sarsted, Germany (courtesy of GEO600 collaboration).

GEO 600 can not match the sensitivity of LIGO or Virgo but it has pioneered several innovations to be used in Advanced LIGO. In fact, since its first run in 2001, LIGO has been collaborating with GEO 600 and both pool and analyze their data jointly. Since 2007 Virgo and LIGO started pooling and analyzing data jointly with the LIGO scientific collaboration even though Virgo is not part it. GEO 600 provides a rather good opportunity to change the spectral characteristics of the detector response, especially due to the shot noise limitation, therefore in the high frequency range of the available bandwidth.

GOE 600 scope is to detect GWs from BH binaries, supernova and stochastic background. Its strain sensitivity is shown in Figure 2.12 and it can be clearly seen that it is very sensitive in the frequency range 50 Hz up to 1.5 kHz. During the enhancement period of Virgo and LIGO, GEO 600 has been the only high sensitive interferometer running in order to detect any possible GW signal from nearby galaxies. At present time, it is operating at high duty factor in *AstroWatch* mode, primarily in case of a nearby galactic supernova, as the Virgo and LIGO detectors undergo to major upgrades.

2.4 Space based interferometers

As we discussed in section 2.2 one of the most important noise sources at frequencies below 1 Hz is due to changes in the Newtonian gravitational potential (Gravity Gradients) on the timescale of the measurements and to seismic noise, see for example Figure 2.6. Most of astrophysical sources of GWs are likely to emit a continuos spectrum of GWs that extends below 1 Hz and since their amplitude at earth is much smaller than gravity gradient noise, their detection at earth would be impossible. For this reason during last 20 years have been proposed several space based interferometers such as LISA, DE-

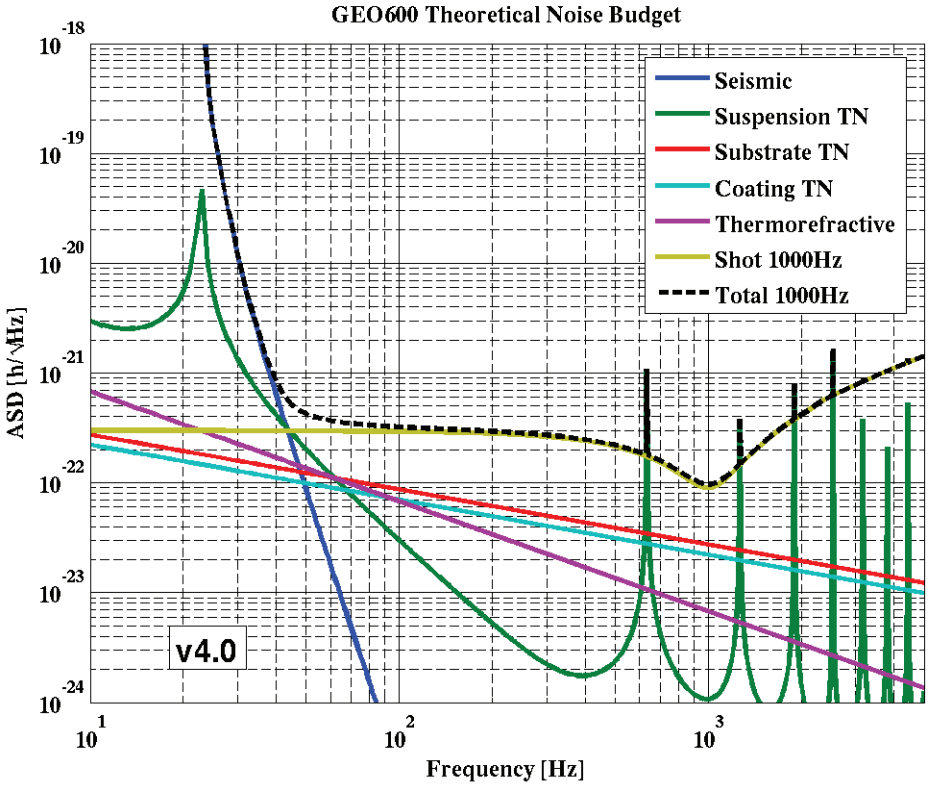

Figure 2.12: GEO600 land area, Sarsted, Germany (courtesy of GEO600 collaboration).

CIGO, BBO, eLISA/NGO etc. In this section we discuss their characteristics and their possible outcomes.

2.4.1 LISA

The Laser Interferometer Space Antenna (LISA) is a joint ESA-NASA project to develop and operate a space-based gravitational wave detector sensitive at frequencies between 0.03 mHz and 0.1 Hz. It was first proposed to ESA in 1993, in the framework of ESA's long term space science program Horizon 2000. Due to fundings reasons in regard of LISA launch time, ESA proposed to NASA a joint collaboration in order to accelerate the construction processes and launching time. However, after many years of discussions about its launching time, remain still unknown when it will be launched with probable launch time between 2018-2026.

LISA will consist of three free-flying spacecrafts arranged in an array that orbits the sun at a distance of 1 AU, about 20° behind the earth in its orbit. It would have arms of $5 \cdot 10^6$ km long and that would be longer than half wavelength for any GWs above 30 mHz. LISA arms form an equilateral triangle in a plane tilted at 60° to the

ecliptic Figure 2.13 and its orbit around the sun preserves this arrangement with the array rotating backwards once per year as the spacecraft orbit the sun. In each arm there is light passing from one array to the other, thus forming a Michelson interferometer and each array can measure the GW polarization directly.

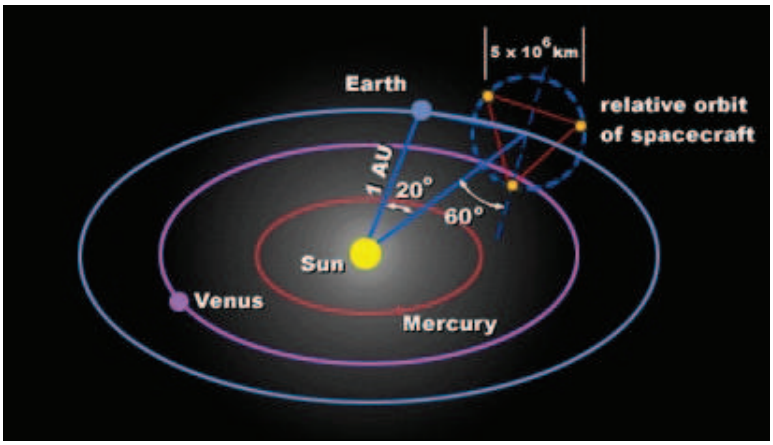

Figure 2.13: LISA spacecraft in orbit (courtesy of ESA).

Being in space, LISA in not free from source noises such as forces from the sun which include both solar radiation pressure and the solar wind. These effect are minimized by using drag-free technology. The two main categories of gravitational-wave sources for LISA are the galactic binaries and the massive black holes (MBHs) expected to exist in the centre of most galaxies. In order to detect these GWs, LISA main goal is to reach a strain sensitivity of $h_f = 4 \cdot 10^{-21}$ Hz$^{-1/2}$ at $f = 1$ mHz, see Figure 2.14. LISA best sensitivity is between 3 Hz and 30 mHz. Above 30 mHz, the sensitivity degrades because the wavelength of the GW becomes shorter than twice the arm length of $5 \cdot 10^6$ km. At low frequencies instead, the noise curve rises because of spurious forces on the test masses.

On April 8, 2011 it was announced that NASA would likely be unable to continue participating in the LISA project due to funds cuts from US government. Revised mission concepts from the New European Gravitational Observatory (NGO) have been considered in a selection process commencing in February 2012 and the initial LISA project has been informally re-named eLISA/NGO [27]. Fortunately found cuts from NASA does not seem to have impact on eLISA performance, so what we discussed above about LISA performance and sensitivity still remain valid for eLISA.

2.4.2 DECIGO/BBO

The Deci-hertz Interferometer Gravitational Wave Observatory (DECIGO) [28, 29, 30] is a proposed space-based Japanese interferometer that will bridges the gap between the ground based interferometers (Virgo, LIGO...) and LISA. It can play a role of follow-up

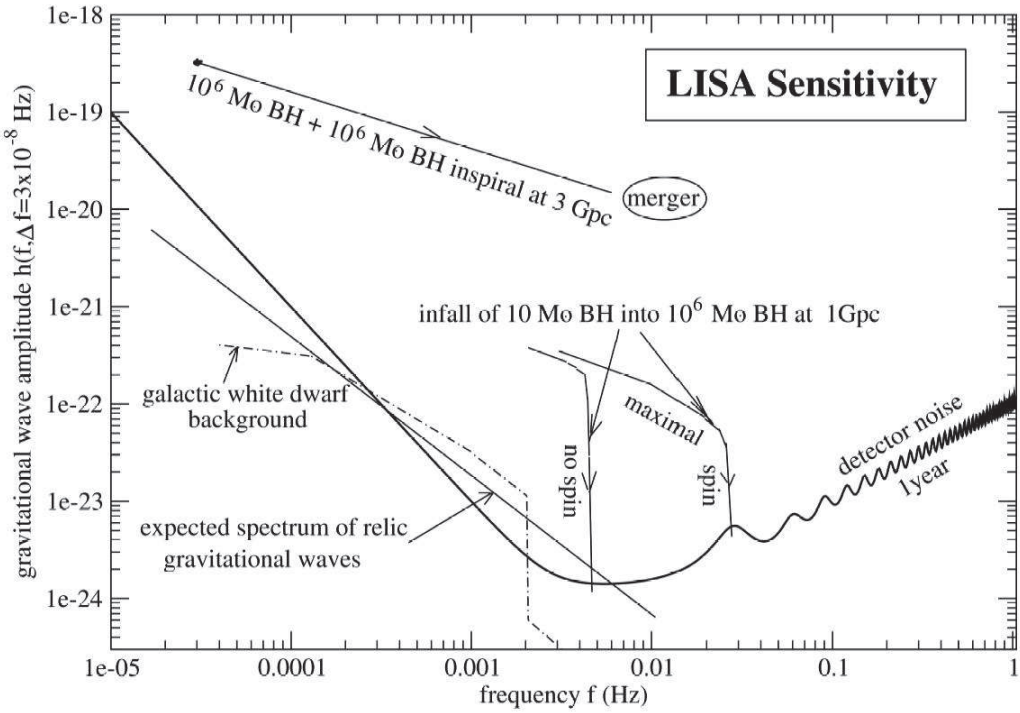

Figure 2.14: Gravitational wave amplitude as a function of frequency for the space-based interferometer LISA (courtesy of ESA).

for LISA by observing inspiral sources that have moved above the LISA band, and can also play a role of predictor for terrestrial detectors by observing in-spiral sources that have not yet moved into the terrestrial detector band. The goal of DECIGO is to detect various sources of gravitational waves mainly between 0.1 Hz and 10 Hz and open a new window of observation for gravitational wave astronomy.

DECIGO consist of three three drag-free spacecrafts separated by arm length of 1000 km each. Each arm consist of a differential Fabry-Perot Michelson interferometer and mass mirrors of mass of 100 kg and mirror diameter of 1 m, see Figure 2.15.

As in the case of LISA, the sensitivity of DECIGO is limited by radiation pressure and solar winds for frequencies below 0.15 Hz. For frequencies above 0.15 noise is dominated by the shot noise. The strain sensitivity curve is shown in Figure 2.16. After three years of corelations in orbit, DECIGO aim is to reach a sensitivity of the order of $h_f \sim 10^{-25}$ Hz$^{-1/2}$. Other ambitious programs for DECIGO is to reach a very high sensitivity of the oder $h_f \sim 10^{-27}$ Hz$^{-1/2}$ after 5 years of data correlation [28]. This project is dubbed the Ultimate DECIGO.

Another post LISA follow on mission which has been proposed to the NASA is the Bing Bang Observer (BBO) [31]. The BBO will be an extremely sensitive antenna that is designed to detect the Gravitational Wave Background (GWB) left by the Big

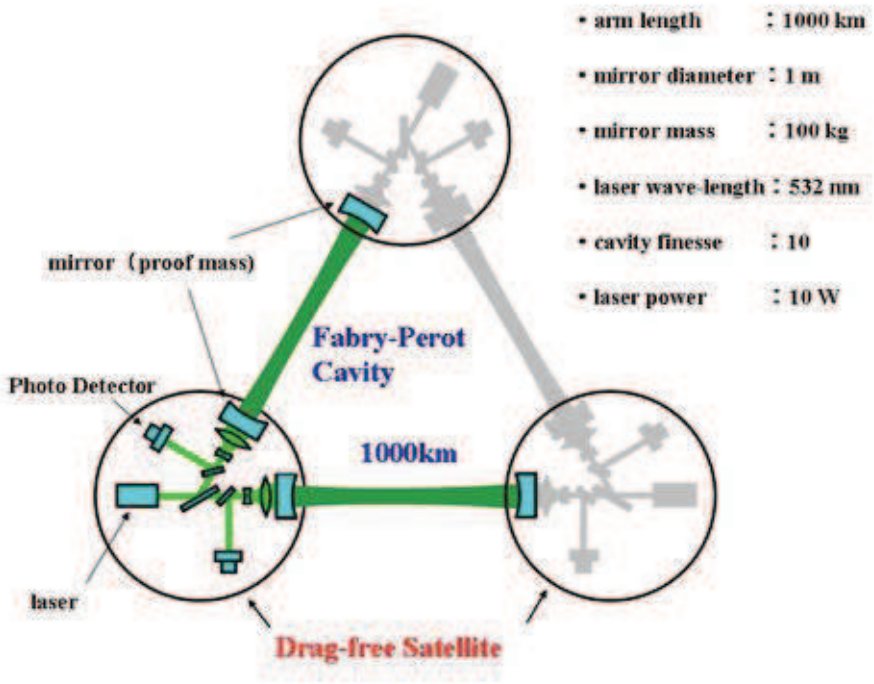

Figure 2.15: DECIGO conceptual design (courtesy of DECIGO collaboration).

Bang. BBO should be able to provide information about the earliest moments in the history of the Universe. The ambitions goal of BBO is to detect GWs left from an early inflationary epoch. As DECIGO, BBO will fill the gap between the Avanced Virgo, LIGO and LISA. It aim to detected GWs in the frequency band of 100 mHz up to 10 Hz and reach a sensitivity of a factor 100 respect to LISA.

The BBO will consist of 3 drag-free masses of 10 kg each and arms of $5 \cdot 10^7$ m. It will be launched at a distance 1 AU from the sun with a tilted angle of 60° respect to the ecliptic. BBO schedule is dived into two stages where the first one will consist of three spacecrafts and will be launched probably around 2025 with five year long mission. The second stage will consist of twelve spacecrafts and three constellations and will be launched around 2029. At the time of writing there is no ongoing BBO research and it remain more an idea than a project.

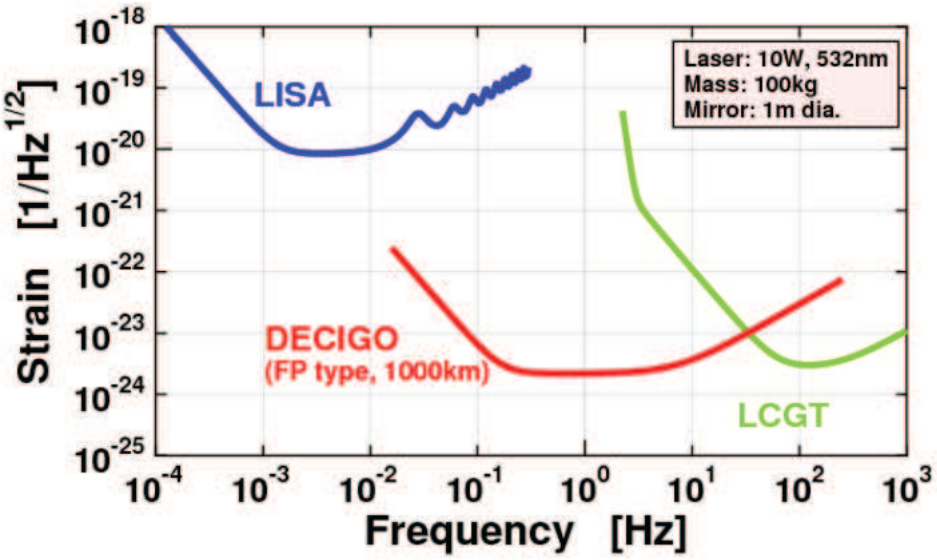

Figure 2.16: Sensitivity curve as a function of frequency for DECIGO (courtesy of DECIGO collaboration). Is also shown for comparison sensitivity curves for LIGO and LISA.

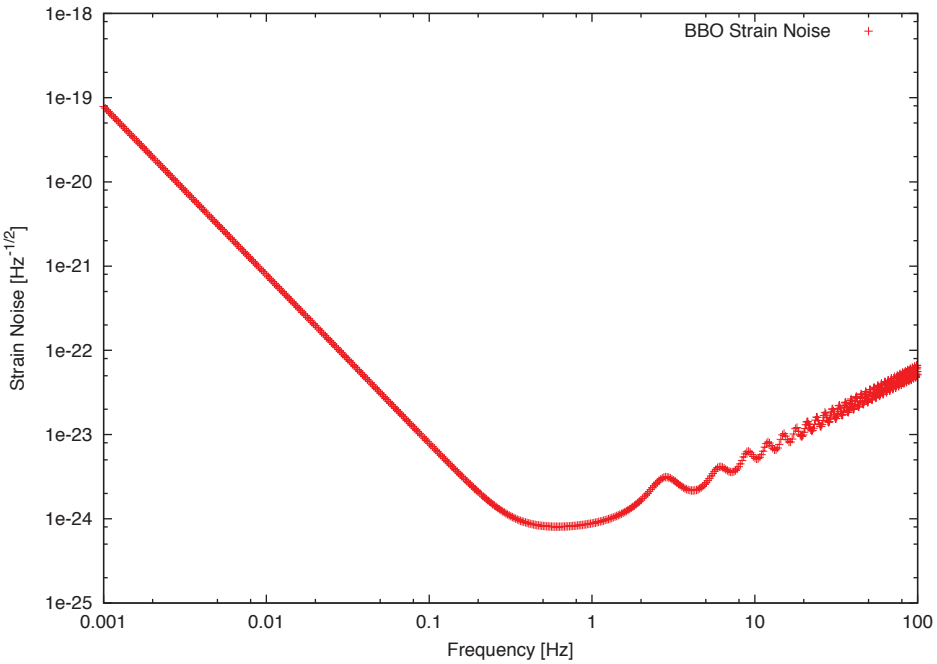

Figure 2.17: Sensitivity curve as a function of frequency for BBO generated with (LISA curve generator) (courtesy of LISA collaboration) and with BBO technical parameters given in Tab. II of [32].

Chapter 3

Stochastic backgrounds of GWs from the early universe

In the previous chapter we presented very fundamentals concepts regarding GW detectors and their present status. Among their target sources of GWs such as compact objects like neutron stars, BH, white dwarfs and supernovae, there is a stochastic background of GWs from the early Universe. This expected background of GWs as will see in the next sections, should not be a surprise since a very well known predicted and detected background from the early Universe is the Cosmic Microwave Background (CMB). In fact, as we will see various models of the early Universe predict different backgrounds of GWs and their detection would have profound impact on the early Universe cosmology and on high energy physics. Such a background would give us a temporal snapshot of the early Universe at the time of their emission because it would reach us completely virgin due to the weak interaction of gravitons with the cosmological plasma. In fact, as far as thermodynamic equilibrium is concerned the interaction rate of gravitons with each other Γ_g has to be greater than the Hubble parameter H, $\Gamma_g > H$. In general for a species in thermal equilibrium the interaction rate given by $\Gamma_g = n\langle\sigma v\rangle$ where $n \sim T$, $v = 1$ with T being the plasma temperature. By pure dimensional reasons the scattering cross section for gravitons is $\sigma \sim G\langle E\rangle^2 \sim GT^2$ and since the Universe after the Bing Bang is believed to have been radiation dominated, the Hubble constant in this epoch would simply be $H \sim T^2/m_{\rm Pl}$ where $G = 1/m_{\rm Pl}^2$ with $m_{\rm Pl}$ being the Planck mass, see Appendix A. Requiring that the expansion rate H is equal to the interaction rate Γ_g the decoupling temperature for the graviton is below the Planck mass or Planck scale

$$\Gamma_g/H \simeq (T/m_{\rm Pl})^3. \tag{3.1}$$

Equation 3.1 tells us that after the Bing Bang gravitons are completely out of equilibrium with matter and their spectrum would remain completely unchanged by the Universe expansion, making them very appealing to detect.

In this chapter we are going to discuss very fundamental quantities related to the stochastic background such as its energy density, strain amplitude, its GW amplitude etc. Moreover we discuss the most important models of graviton production in the early Universe and their possible detection.

3.1 Intrinsic quantities of the stochastic background

Most sources of GWs from the early universe and present day universe are uncorrelated with each other. Furthermore their emission of GWs can be regarded as a random process over time, so in general a GW would be an incoherent superposition of GWs emitted from different sources. However, there are also other mechanisms such as vacuum fluctuations during the inflationary epoch which can not be characterized as emitted from different sources. In any case in both processes their GWs background is characterized by random processes of emission and such a background is called *stochastic*.

In order to see more closely what we do mean with a stochastic background, let us recall that in the TT gauge a general GW can be written as follows

$$h_{ij}(\mathbf{x},t) = \sum_{\lambda=+,\times} \iint d\omega\, d\hat{\mathbf{n}}\, h_\lambda(\omega,\hat{\mathbf{n}}) e^\lambda_{ij}(\hat{\mathbf{n}}) e^{-i(\omega t - \mathbf{k}\cdot\mathbf{x})} \tag{3.2}$$

where $\mathbf{k} = k\hat{\mathbf{n}}$ with $\hat{\mathbf{n}}$ being the direction of wave propagation. The wave amplitudes $h_\lambda(\omega,\hat{\mathbf{n}})$ are random variables and are characterized statistically by their ensemble average. In general, when dealing with a stochastic background one assumes few hypothesis which characterize it. Such a background is assumed to be homogeneous, Gaussian, isotropic and unpolarized. Homogeneity means that the two point correlation functions must depend only to the time difference and not to the absolute values of time, namely $\langle h_\lambda(t)\, h_{\lambda'}(t')\rangle \propto \delta(t-t')$ or in Fourier space

$$\langle h_\lambda(f)\, h^*_{\lambda'}(f')\rangle \propto \delta(f-f'). \tag{3.3}$$

A Gaussian background is characterized by the fact that all N-point correlation functions can be decomposed as a sum and product of the two point function $\langle h_\lambda(t)\, h_{\lambda'}(t')\rangle$. This of course is valid only when the number of stochastic variables is very large $N \to \infty$, while for a limited number of variables (GW sources) this approximation do not hold anymore and higher point correlators are needed. Another important hypothesis is concerned with the isotropy of the GW background. As in the case of the CMB which is very isotropic with deviation from it of the order of $\sim 10^{-5}$, we can expect that even a stochastic background of GWs (SBGWs) can be isotropic. In this case the two point correlation function at two different directions is proportional to

$$\langle h_\lambda(f,\hat{\mathbf{n}})\, h^*_{\lambda'}(f',\hat{\mathbf{n}}')\rangle \propto \delta(\hat{\mathbf{n}}-\hat{\mathbf{n}}'), \tag{3.4}$$

where the proportionality constant must not depend on the propagation direction, $\hat{\mathbf{n}}$. The last hypothesis concerns the polarization of SBGWs which we assume to be unpolarized.

In this case the two point function $\langle h_\lambda(f,\hat{\mathbf{n}})\, h^*_{\lambda'}(f',\hat{\mathbf{n}}')\rangle \propto \delta_{\lambda\lambda'}$ with the proportionality coefficient independent of the polarization index λ. In general under the above hypothesis we must have for the two point correlation function

$$\langle h_\lambda(f,\hat{\mathbf{n}})\, h^*_{\lambda'}(f',\hat{\mathbf{n}}')\rangle = \delta(f-f')\,\delta_{\lambda\lambda'}\frac{\delta(\hat{\mathbf{n}},\hat{\mathbf{n}}')}{4\pi}\frac{1}{2}S_h(f), \tag{3.5}$$

where $S_h(f)$ is called the spectral density or power spectrum of GWs. It has the dimension of Hz^{-1} and satisfies $S_h(f) = S_h(-f)$. Using both Equation 3.2 and Equation 3.5, the two point correlation function for $h_{ij}(\mathbf{x}=0,t)$ is given by

$$\langle h_{ij}(t)\, h^{ij}(t)\rangle = 4\int_0^\infty S_h(f). \tag{3.6}$$

Next step is to relate the GWs power spectrum $S_h(f)$ whith the GWs energy density ρ_{gw}, Equation 1.53. Let Ω_{gw} be the GW density parameter which is defined as

$$\Omega_{\mathrm{gw}} \equiv \frac{\rho_{\mathrm{gw}}}{\rho_c}, \tag{3.7}$$

where $\rho_c = 1.878\cdot 10^{-29} h_0^2$ g/cm^3 is the critical energy density Equation A.42, where we wrote the present Hubble parameter as $H_0 = 100h_0$ km/s/Mpc with $h_0 \simeq 0.70$ a parameter which arises due to the uncertainty on the Hubble parameter, H_0 [33]. The spectral distribution of ρ_{gw} can be written as follows

$$\rho_{\mathrm{gw}} = \int_0^\infty d(\log f)\frac{d\rho_{\mathrm{gw}}}{d\log f}. \tag{3.8}$$

Making use of Equation 3.8, Equation 3.7 can be written as

$$\Omega_{\mathrm{gw}} = \int_0^\infty d(\log f)\Omega_{\mathrm{gw}}(f), \tag{3.9}$$

where $\Omega_{\mathrm{gw}}(f)$ is called spectral density parameter or density parameter as a function of frequency

$$\Omega_{\mathrm{gw}}(f) = \frac{1}{\rho_c}\frac{d\rho_{\mathrm{gw}}}{d\log f}. \tag{3.10}$$

Using the ergodic theorem, we can replace the time average in Equation 1.53 with its ensemble average and get

$$\rho_{\mathrm{gw}} = \frac{1}{8\pi G}\int_0^\infty d(\log f)\, f(2\pi f)^2\, S_h(f). \tag{3.11}$$

Comparing Equation 3.8 with Equation 3.11 and using Equation 3.10 we get

$$\Omega_{\mathrm{gw}} = \frac{4\pi^2}{3H_0^2} f^3 S_h(f). \tag{3.12}$$

Equation 3.12 gives an important relation between the density parameter of GWs and their power spectrum. In complete analogy with Equation 2.4 we can define the characteristic amplitude of a SBGWs as

$$\langle h_{ij}^2(t)\rangle = 2\int_0^\infty d(\log f)\, h_g^2(f), \tag{3.13}$$

where we made use of Equation 3.2. $h_g(f)$ is the amplitude of SBGWs and should be not confused with detector output $h(t)$ Equation 2.7 due to the interaction of the GW with the detector. By comparing Equation 3.13 with Equation 3.6 we get the following relation between the power spectrum S_h and the GW amplitude h_g

$$h_g^2(f) = 2fS_h(f). \tag{3.14}$$

Inserting into Equation 3.12 we get the following important relation between h_g and $\Omega_{\rm gw}$

$$h_g(f) = 1.263\cdot 10^{-18}\left(\frac{1\text{Hz}}{f}\right)\sqrt{h_0^2\Omega_{\rm gw}}. \tag{3.15}$$

We may note that the GW density parameter is written as a combination of h_0 and $\Omega_{\rm gw}$, namely $h_0^2\Omega_{\rm gw}$. This is a standard way of writing the density parameter in GW astronomy. This way of writing the density parameter* get rid of the uncertainty arising in ρ_c since it is expressed through the Hubble parameter. Equation 3.15 can be used to evaluate the minimum density parameter which a single GW detector can reach. In fact, by using Equation 2.11 and both Equation 2.5 and Equation 3.1 we get

$$h_g(f) \geqslant \sqrt{2f/F}\, h_f \tag{3.16}$$

Using Equation 3.16 into Equation 3.15 we get the following relation

$$h_0^2\Omega_{\rm gw}^{\rm min}(f) \geqslant \frac{1.25\cdot 10^{-8}}{F}\left(\frac{f}{1\text{Hz}}\right)^3\left(\frac{h_f}{10^{-22}\text{Hz}^{-1/2}}\right)^2. \tag{3.17}$$

Equation 3.17 gives the minimum density parameter detectable by a single detector. It depends essentially on the detector strain sensitivity and on the form factor F.

3.2 Phenomenological bounds on the stochastic background of GWs

In this section we discuss some (not all!) phenomenological bounds on the density parameter in GWs in different frequency bands. This bounds are extremely important since they can constrain various GWs models and also new theories which predict new particles at the early stages of the universe, such as supersymmetry etc. In the next sections we are going to discuss the WMAP bound which is based essentially on bounds on the CMB anisotropies and the BBN bound which is based on the number of neutrino families present at nucleosynthesis time.

*From now with density parameter we mean $h_0^2\Omega_{\rm gw}$ instead of $\Omega_{\rm gw}$.

3.2.1 WMAP bound

CMB observations can be used to bound the number density of relic gravitons present at the time of decoupling. In fact, at our current understanding, CMB presents small temperature anisotropies of the order of $\delta T/T \sim 10^{-5}$ in different directions in the sky. These anisotropies may arise due to various effects such as, our peculiar velocity respect to the cosmic fluid (the so called dipole anisotropy), the peculiar velocity of the matter that might have scattered the CMB, inhomogeneities in the Newtonian potential at recombination, intrinsic homogeneities of the CMB at recombination time, geodesic deviation of photons from the time of recombination up to present epoch the so called Sachs-Wolfe effect and maybe due to re-ionization of the universe.

All the above mentioned processes operate on different length scales. For example, let us assume that inhomogeneities in the gravitational potential at recombination vary on a length scale l. The angle subtended by this length scale on the sky at present would be

$$\theta = \frac{l}{d_A(z)}, \tag{3.18}$$

where $d_A(z)$ is the angular diameter distance. In the case when $z \gg 1$ the angular distance is given by [34]

$$d_A(z) = \frac{2H_0^{-1}}{z\,\Omega}, \tag{3.19}$$

where Ω is the total density parameter, see Appendix A. Thus the angle subtended by the length scale l today would be

$$\theta \simeq \left(\frac{lz}{H_0^{-1}}\right)\left(\frac{\Omega}{2}\right). \tag{3.20}$$

Taking the length scale $l = H^{-1}(t_{rec}) = H_0^{-1}(\Omega\, z_{rec})^{-1/2} z_{rec}^{-1}$, the angle subtended on the sky by the recombination epoch would be

$$\theta_{rec} = 0.87^{\circ}\Omega^{1/2}\left(\frac{1090}{z_{rec}}\right)^{1/2}. \tag{3.21}$$

So, the angle about $\theta \sim 1^{\circ}$ on the sky correspond to the horizon size at recombination epoch. The microphysical processes took place at small angular size $\theta < 1^{\circ}$ while the macro physics took place at large scales $\theta > 1^{\circ}$.

Before going to the WMAP bound on the present day density parameter, let us estimate the frequency range of GWs that could create CMB anisotropies. All modes that crossed the horizon starting from recombination till present epoch could create CMB anisotropies. In fact, CMB observations show a peak in the power spectrum corresponding to an angle in the sky of $\theta \sim 1^{\circ}$, namely at recombination time. Since GWs once enter inside horizon would decay due to universe expansion, $h_g \sim 1/a$, their strongest contribution is expected to come from long tensor modes which enter horizon after recombination or shortly before it. However, in principle even GWs which enter horizon

before recombination could lead to CMB anisostropies but also other mechanism are more likely to produce these anisotropies such as adiabatic perturbations, density perturbations etc. So, in principle CMB anisotropies on large scales $\theta > 1^\circ$ are exclusively produced by GWs which enter horizon after recombination. Present day GW modes which are entering horizon would have a frequency $f \simeq H_0 = 3 \cdot 10^{-18}$ Hz. On the other hand a mode which entered horizon at recombination time would have a frequency at recombination $f_{rec} = H(t_{rec}) = H_0(1 + z_{rec})^{3/2}$. Its present frequency would be

$$f \lesssim H_0 \, z_{rec}^{1/2} \simeq 10^{-16}\text{Hz}. \tag{3.22}$$

So the frequency range to look for large scale CMB anisotropies is in the interval

$$3 \cdot 10^{-18}\text{Hz} \lesssim f \lesssim 10^{-16}\text{Hz}. \tag{3.23}$$

Based on the above discussion, the amplitude of a GW crossing the horizon at $t = t_{rec}$ and scale $k(\theta)$ with θ being the angle subtended on the sky by the GW wavelength, is given by

$$h_g(t_{rec}, k(\theta)) = \left(\frac{\delta T}{T_0}\right)_\theta . \tag{3.24}$$

Let us now derive the expression for the density parameter for GWs entering inside horizon at a time $t_{\rm hor}$. The amplitude of these GWs today would be

$$h_g(f, t_0) = \frac{a(t_{\rm hor})}{a(t_0)} h_g(f, t_{rec}), \tag{3.25}$$

where $a(t_{\rm hor})$ is the scale factor at horizon entering. Writing $a(t_{\rm hor})/a(t_0) = a(t_{\rm hor})/a(t_{rec}) z_{rec}$ and taking into account that during matter domination the scale factor goes as $a \propto t^{3/2}$ we can easily get the following expression for the GW amplitude at present epoch

$$h_g(f, t_0) \simeq \left(\frac{H_0}{2f}\right)^2 \left(\frac{\delta T}{T_0}\right)^2, \tag{3.26}$$

where T_0 is the present day CMB medium temperature. Inserting Equation 3.26 into Equation 3.12, we get

$$\Omega_{\rm gw}(f) \simeq \left(\frac{H_0}{f}\right)^2 \left(\frac{\delta T}{T_0}\right)^2. \tag{3.27}$$

Taking $\delta T/T_0 \sim 10^{-5}$ (WMAP) at large angular scales we get the following bound

$$\Omega_{\rm gw}(f) < 10^{-10} \left(\frac{H_0}{f}\right)^2 \qquad (3 \cdot 10^{-18}\text{Hz} < f < 10^{-16}\text{Hz}). \tag{3.28}$$

The WMAP bound is shown in Figure 3.1

3.2.2 Bing Bang Nucleosynthesis bound

CMB observations severely constraint the density parameter at long wavelengths as we saw in the previous section and can be used as a probe for different GW models. However, another important bound which constrain the number density of gravitons produced before Bing Bang Nucleosynthesis (BBN), is the so called BBN bound on gravitational waves. This bound relies on the fact that any new relic particle present at the time of BBN could contribute to the energy density of the universe and thus, could have modified its evolution and have impact on nucleosynthesis of light elements.

An important role on the BBN bound is played by the effective number of massless degrees of freedom g_* at BBN. Roughly speaking more effective particles present at BBN in comparison to the standard model would have impact on the freeze out temperature and on the production of ^{4}He. The abundance of ^{4}He is strictly connected with the number density of neutrons at BBN. The number density of neutrons to the number density of protons in thermal equilibrium is expressed through

$$\frac{n}{p} = \exp(-Q/T), \tag{3.29}$$

where $Q = m_n - m_p = 1.3$ MeV is the mass difference. Thermal equilibrium is maintained by the weak interactions

$$n \leftrightarrow p + e^- + \bar{\nu}, \tag{3.30}$$

$$e^+ + n \leftrightarrow p + \bar{\nu}, \tag{3.31}$$

$$\nu + n \leftrightarrow p + e^-, \tag{3.32}$$

as far as the interaction rate is greater than the Hubble parameter, $\Gamma_{int} > H$. Once the temperature reaches the value of freeze out T_f, the interaction between the particles can not compete anymore with the universe expansion and therefore the ratio of neutrons to protons would freeze at the temperature T_f with ratio $n/p = \exp(-Q/T_f)$. Estimation of the freeze out temperature can be calculated by requiring that $\Gamma_{int} = H$, where for $T \gg Q$ the weak interactions rate is approximately $\Gamma_{int} \sim G_F^2 T^5$. In this case we can take the Hubble parameter as in Equation A.29 with the energy density given by Equation A.57 and get the following estimate for the freeze out temperature

$$T_f \simeq \left(\frac{8\pi^3 g_*}{90}\right)^{1/6} \left(\frac{1}{G_F^2 m_{\rm Pl}}\right)^{1/3}. \tag{3.33}$$

We can see that apart from some constant factors, the freeze out temperature goes like $T_f \propto g_*^{1/6}$ and more effective massless particles at BBN would eventually lead to an increase of T_f. An increase of the freeze out temperature would increase the number density of free neutrons leading to an overproduction of ^{4}He. Since BBN prediction on the abundance of primordial ^{4}He is in good agreement with the observed abundance, theoretical predictions on the abundance of ^{4}He can be used to constrain different models which predict additional degrees of freedom at BBN.

One of the most important features of BBN is that the freeze out temperature calculated above is in reality smaller than the binding energy of light nuclei. For a given atomic specie the binding energy is $B_A = Zm_p + (A-Z)m_n - m_Z$ where Z is the atomic number, A is the mass number. In the case of ^{4}He the binding energy is 28.3 MeV and the temperature which the mass fraction of ^{4}He is of the order of unity is 0.28 MeV. Due to this reason nucleosynthesis took place mostly for temperatures $T < 1$ MeV. At this temperatures the only relativistic particles are 3 species of neutrinos, 3 species of antineutrinos, $e^{\pm}$ and the photon. Let N_ν denotes the number of neutrino or antineutrino species in thermal equilibrium at temperature $T_i = T$. The effective number of degrees of freedom would be Equation A.59

$$g_*(N_\nu) = 2 + \frac{7}{8}(4 + 2N_\nu), \tag{3.34}$$

where the factor 2 takes into account of the two polarization or helicity states of the photon, the factor 4 takes into account those of the electron and the positron and the factor 2 takes into account the neutrino and the antineutrino species. In the standard model of particle physics, the number of neutrino families are 3, thus the effective number of degrees of freedom accounts for $g_*(3) = 43/4$. If there is an extra specie at BBN it is likely to decouple before the temperature reaches the value of $T \sim 1$ MeV, so the particle temperature is small in comparison to the photon temperature at BBN. If for example a specie decouples at $T_D > 300$ GeV, we would have that $g_*(T_D) > 106.75$. The ratio of the specie temperature to the photon temperature at BBN would be $(T_i/T)^4 \leqslant (10.75/106.75)^4 = 0.047$, thus this new specie would have very small contribution to the effective degrees of freedom at BBN. Now, let us suppose that these extra specie(s) exist at BBN, then the effective number of degrees of freedom at $T \sim 1$ MeV would be

$$g_* = g_*^{(S)} + \sum_{i=\text{new bosons}} g_i \left(\frac{T_i}{T}\right)^4 + \sum_{i=\text{new fermions}} g_i \left(\frac{T_i}{T}\right)^4, \tag{3.35}$$

where $g_*^{(S)} = 2 + 7/8(4 + 2N_\nu)$ is the number of degrees of freedom of the standard model with $N_\nu = 3$. With a fourth generation of neutrino specie $N_\nu \leqslant 4$ at the same temperature as the photon $T_i = T$, we would have that $g_*^{(S)} \leqslant g_*(N_\nu \leqslant 4)$ where the contribution of the other extra species (apart a fourth generation of neutrinos) is small as we already discussed. Denoting with N the *number of effective neutrino species*, the bound $g_*(N) \geqslant g_*^{(S)}$ gives

$$\sum_{i=\text{new bosons}} g_i \left(\frac{T_i}{T}\right)^4 + \sum_{i=\text{new fermions}} g_i \left(\frac{T_i}{T}\right)^4 \leqslant \frac{7}{4}(N - N_\nu). \tag{3.36}$$

Let us assume that the only extra Bosonic specie is the graviton with $g_i = 2$ and $(T_i/T)^4 = \rho_{\text{gw}}/\rho_\gamma$. Then we get the following bound on the energy density at BBN

$$\rho_{\text{gw}}(t_{BBN}) \leqslant \frac{7}{8}\rho_\gamma(t_{BBN})(N - N_\nu). \tag{3.37}$$

Since both energy density of photons and gravitons goes with the scale factor as $\sim 1/a^4$ and making use of Equation A.64 and Equation 3.37 we can easily get the graviton energy density at present time $t = t_0$

$$\rho_{\rm gw}(t_0) \leqslant 0.22\,\rho_\gamma(t_0)(N - N_\nu). \tag{3.38}$$

From CMB observations the total density parameter in photons at present is given by [34]

$$h_0^2\Omega_\gamma(t_0) = 2.47 \cdot 10^{-5}, \tag{3.39}$$

and using the definition of the total density in GWs, Equation 3.7, we get the bound on the present total density parameter in GWs,

$$h_0^2\Omega_\gamma(t_0) \leqslant 5.7 \cdot 10^{-6}(N - N_\nu). \tag{3.40}$$

It is important to note that Equation 3.40 is a bound on the density parameter integrated over all frequencies which were already inside horizon at BBN. In fact, BBN took place roughly speaking at $t \sim 1$ s and $T \sim 1$ MeV. The lowest frequency at that time would be equal to the Hubble parameter at BBN, $f_* \sim H(t_*) = 1/2t_*$ for a RD universe and $t_* = t_{BBN}$. So the lowest frequency (the longest wavelength) at BBN, would be for $t_* \sim 1$ s, $f_* \sim 0.5$ Hz. Using the fact that the entropy per co-moving volume is conserved, the lowest frequency at BBN would have a present day value of

$$f = f_* \left(\frac{a_*}{a_0}\right) \sim 10^{-10}\,\text{Hz}, \tag{3.41}$$

where we made explicit use of Equation 4.26 with $g_*(T_*) = 10.75$ and $g_*(T_0) = 3.36$. Thus, the bound, Equation 3.40, is valid in the present day frequency range of 10^{-10} Hz $\lesssim f < \infty$. A plot of the BBN bound on GWs is shown in Figure 3.1.

3.3 Models of relic graviton production

Stochastic background of relic gravitational waves can be produced by several mechanisms. The theoretical predictions are model depended due to the uncertainties in the cosmological framework and on the values of the redshift from the production epoch. Below we briefly describe some of the production scenarios. For a more detailed review on stochastic background of GWs production mechanisms and their spectra the reader can be found in [35, 36, 37].

3.3.1 Boguliobov transformation and vacuum amplification

It was established long ago that gravitational waves could be produced in cosmology due to an amplification of vacuum fluctuations by external gravitational field (quantum particle production). It was first studied in [12] and first applied to an inflationary model in [13]. The gravitational waves could be quite efficiently produced at inflation. Their

spectrum at large wavelengths is independent on the details of inflationary models. The frequency band of these gravitons today is quite wide and the associated density parameter is very low.

First calculations of the GW power spectrum from inflationary models treated the quantum mechanical two-point function as two-point statistical average of an ensemble of classical fields where the fields evolve according to the classical equations of motions. However, such a mixed treatment raised some subtle questions since it was not clear to what extend one could apply them in order to derive the power spectrum [38]. A full quantum mechanical treatment was derived in [39]. Before going to the De Sitter epoch we first show how gravitational waves are created in FLRW universe and discuss how amplification of quantum fluctuations arises.

We start by specializing in the FLRW metric Equation A.1 and write it as

$$ds^2 = a^2(\eta)(-d\eta^2 + \delta_{ij}\, dx^i dx^j), \tag{3.42}$$

where we consider a flat space-time with curvature $k = 0$ and introduced the conformal time τ which is defined as

$$d\tau = dt/a(t). \tag{3.43}$$

Tensor perturbations in a spatially-flat FLRW universe are described by the line element

$$ds^2 = a^2(\eta)[-d\eta^2 + (\delta_{ij} + h_{ij})\, dx^i dx^j], \tag{3.44}$$

where h_{ij} are tensor perturbations in the FLRW metric. Here we still work in the TT gauge and expand the tensorial perturbations in Fourier integral as follows

$$h_{ij}(\mathbf{x}, \eta) = \sqrt{8\pi G} \sum_{\lambda=+,\times} \int \frac{d^3k}{(2\pi)^3 \sqrt{2k}}\, h_\lambda(\mathbf{k}, \eta) e^\lambda_{ij}(\mathbf{k})\, e^{i\mathbf{k}\cdot\mathbf{x}}, \tag{3.45}$$

where $\mathbf{x}, \mathbf{k}$ are respectively the co-moving coordinate and the co-moving wave-vector. The normalization coefficient in front of expansion, Equation 3.45 has been chosen appropriately in order to match with the Einstein-Hilbert action for the fields h_λ.

The Einstein field equations in vacuum for the fields h_{ij} are given by Equation 1.21 where in the TT gauge $h_{ij} = \bar{h}_{ij}$ and the d'Alambert operator in curved space-time is given by

$$\Box h_{ij} = \nabla_\mu \nabla^\mu h_{ij}. \tag{3.46}$$

Introducing the expansion Equation 3.45 into Equation 3.46 we may notice that the polarization tensor depend only on the propagation direction and the operator ($\Box$) acts only on h_λ (which is a scalar field) and on the exponential term. In curved space-time the wave equation for a general scalar field ϕ reads

$$\Box\phi = \frac{1}{\sqrt{-g}} \partial_\mu (\sqrt{-g} g^{\mu\nu} \partial_\nu)\phi = 0, \tag{3.47}$$

where g is the metric determinant. Taking into account of the line element Equation 3.42 the metric tensor has the form $g_{\mu\nu}$=diag $(-a^2, a^2, a^2, a^2)$ and $\sqrt{-g} = a^8$. After some

straightforward calculations the wave equation for the fields $h_\lambda(\mathbf{k},\eta)$ or Lifshitz equations [40] are given by

$$h''_\lambda(\mathbf{k},\eta) + 2\frac{a'(\eta)}{a(\eta)}h'_\lambda(\mathbf{k},\eta) + k^2 h_\lambda(\mathbf{k},\eta) = 0, \tag{3.48}$$

where the $(')$ symbol indicate a derivative respect to conformal time η. Lifshitz equation, Equation 3.48, can be written in a more fashionable way by writing the fields $h_\lambda(\mathbf{k},\eta)$ in terms of the functions $\phi_\lambda(\mathbf{k},\eta)$ as

$$h_\lambda(\mathbf{k},\eta) = \frac{1}{a(\eta)}\phi_\lambda(\mathbf{k},\eta). \tag{3.49}$$

Inserting Equation 3.49 into the Lifshitz equation, it becomes

$$\phi''_\lambda(\mathbf{k},\eta) + \left(k^2 - \frac{a''}{a}\right)\phi_\lambda(\mathbf{k},\eta) = 0. \tag{3.50}$$

Equation 3.50 is a Bessel-Riccati differential equation and its general solution can be written as

$$\phi_\lambda(\mathbf{k},\eta) = a(\mathbf{k})\xi(k\eta) + a'(\mathbf{k})\xi^*(k\eta), \tag{3.51}$$

where ξ is a function of $k\eta$ which is in general expressed in terms of the Hankel functions of the first and second kind and $(^*)$ denotes complex conjugate. Imposing that ϕ are real functions, substituting $\mathbf{k} \to -\mathbf{k}$ we get that $a'(-\mathbf{k}) = a^\dagger(\mathbf{k})$. Here $a(\mathbf{k})$ and $a^\dagger(\mathbf{k})$ are respectively the annihilation and creation quantum mechanical operators. Taking into account of Equation 3.49, the mode expansion for the fields h_{ij}, Equation 3.45, is

$$\begin{aligned} h_{ij}(\mathbf{x},\eta) = \sqrt{8\pi G}\sum_{\lambda=+,\times}\int \frac{d^3k}{(2\pi)^3\sqrt{2k}}\frac{1}{a(\eta)}\Big[a_\lambda(\mathbf{k})\xi(k\eta)e^\lambda_{ij}(\mathbf{k})\,e^{i\mathbf{k}\cdot\mathbf{x}} \\ + a^\dagger_\lambda(\mathbf{k})\xi^*(k\eta)e^\lambda_{ij}(\mathbf{k})\,e^{-i\mathbf{k}\cdot\mathbf{x}}\Big], \end{aligned} \tag{3.52}$$

where we used the fact that $e^\lambda_{ij}(\mathbf{k}) = e^{*\lambda}_{ij}(\mathbf{k})$.

Let us now go one step further on calculating the amount of gravitons produced in different epochs during the universe expansion. Suppose that $\{a(\mathbf{k}), a^\dagger(\mathbf{k})\}$, $\{b(\mathbf{k}), b^\dagger(\mathbf{k})\}$ are respectively the annihilation and creation operators which enters expansion, Equation 3.52, for two different cosmological regimes. The two sets of annihilation operators are related through the Bogoliubov transformation

$$a(\mathbf{k}) = \sum_{\mathbf{q}}[\alpha(\mathbf{k},\mathbf{q})b(\mathbf{q}) + \beta^*(\mathbf{k},\mathbf{q})b^\dagger(\mathbf{q})], \tag{3.53}$$

where α,β are two complex numbers. Since we are dealing with gravitons (bosons), we have that

$$[a(\mathbf{k}), a^\dagger(\mathbf{q})] = \delta(\mathbf{k}-\mathbf{q}), \qquad [b(\mathbf{k}), b^\dagger(\mathbf{q})] = \delta(\mathbf{k}-\mathbf{q}). \tag{3.54}$$

Inserting Equation 3.53 into the first commutator Equation 3.54 we get the following relation between the coefficients α, β for $\mathbf{k} = \mathbf{q}$

$$|\alpha|^2 - |\beta|^2 = 1. \tag{3.55}$$

After some straightforward manipulations we can express the annihilation operator $b(\mathbf{k})$ as a linear combination of $\{a(\mathbf{k}), a^\dagger(\mathbf{k})\}$

$$b(\mathbf{k}) = \sum_{\mathbf{q}} [\alpha^*(\mathbf{k},\mathbf{q})a(\mathbf{q}) - \beta^*(\mathbf{k},\mathbf{q})a^\dagger(\mathbf{q})]. \tag{3.56}$$

Let us assume that $\{a(\mathbf{k}), a^\dagger(\mathbf{k})\}$ are the annihilation and creation operators during inflation and $\{b(\mathbf{k}), b^\dagger(\mathbf{k})\}$ are the annihilation and creation operators during the radiation dominated (RD) epoch. The number operator in the RD epoch is given by

$$N_b(\mathbf{k}) \equiv b^\dagger(\mathbf{k})b(\mathbf{k}) = N_a(\mathbf{k}) + 2|\beta|^2 \left[N_a(\mathbf{k}) + \frac{1}{2} \right] - \alpha\beta^*(a^\dagger)^2 - \alpha^*\beta(a^2). \tag{3.57}$$

Consider for example that the universe during the inflationary epoch was in a state $|\phi_a\rangle$ with particle number N_a. In order to have a physical insight on vacuum amplification let us consider two kind of perturbations during the inflationary epoch. There are perturbations with physical wavelength $\lambda_{phy} \gg H^{-1}$ and $\lambda_{phy} \ll H^{-1}$ where H^{-1} is the Hubble horizon. A sudden change in the universe expansion is accompanied with a sudden change in the Hubble parameter since it governs the dynamics of the expansion. Consequently, physical wavelengths which are inside the Hubble radius would see the dynamic change as adiabatic while wavelengths greater than the Hubble radius would see it as a sudden transition. In the latter case the state of the universe $|\phi_a\rangle$ would not change for those wavelengths because they are very few affected, however during the transition would change the creation and annihilation operators. Thus, in the latter case we would have for state of the universe

$$|\phi_a\rangle, \text{before transition} \qquad |\phi_b\rangle = |\phi_a\rangle, \text{after the transition.} \tag{3.58}$$

Taking the expectation value of Equation 3.57 on the state $|\phi_a\rangle$ and using the fact that it does not change for long wavelengths, the number of particle creation during the transition is given by

$$N_b = N_a + 2|\beta|^2 \left[N_a + \frac{1}{2} \right]. \tag{3.59}$$

Equation 3.59 is an important result since it gives the number of particle creation during changes in the Hubble parameter. We may also notice that even in the case when $N_a = 0$ (total absence of particles during inflation) the half vacuum fluctuations are amplified through the factor β. This mechanism of particle creation (gravitons in this case) is called *amplification of vacuum fluctuations*.

3.3.2 de Sitter universe

The mechanisms of graviton production by a time depended gravitational field is very important for GW generation during various inflationary models. Due to amplification of vacuum fluctuations, we saw that long wavelengths which enter horizon during changes in the Hubble parameter are amplified and shorter wavelengths change adiabatically with time with no further amplification. In this section we want to compute the density parameter of GWs generated during the transition from a de Sitter epoch to the RD epoch.

The de Sitter solution of Einstein field equations is a particular solution which the matter and energy content of the universe is completely neglected. However, into the Einstein field equations is included a cosmological term Λ which is assumed to be constant. Introduction of a cosmological constant would modify the Friedemann equation, Equation A.29, in the following way

$$H^2 = \frac{8\pi G\rho}{3} - \frac{K}{a^2} + \frac{\Lambda}{3}. \tag{3.60}$$

In the de Sitter universe $K = 0$, $\rho = 0$ and the dynamics of expansion is governed by the cosmological constant Λ with a Hubble parameter constant in time

$$H = \sqrt{\Lambda/3}. \tag{3.61}$$

The scale factor in this case is given by

$$a(t) = a(t_i)e^{Ht}. \tag{3.62}$$

where t_i is the initial time when expansion startes. Therefore we can realize that the de Sitter universe is a universe which scale factor a increases exponentially. In terms of the conformal time η, the scale factor in the de Sitter universe reads

$$a(\eta) = -\frac{1}{H\eta}, \tag{3.63}$$

where $-\infty < \eta < \eta_1$ with η_1 being the cosmological time of transition from the de Sitter universe to the RD universe. In the RD universe the scale factor is $a(t)\propto t^{1/2}$ and in terms of conformal time it reads

$$a(\eta) = \frac{1}{H\eta_1^2}(\eta - 2\eta_1), \tag{3.64}$$

where $\eta_1 < \eta < \eta_{\rm eq}$ with $\eta_{\rm eq}$ being the equilibrium time between the RD epoch and the MD epoch.

With the scale factors given by Equation 3.63, Equation 3.64 we solve Equation 3.50 in the de Sitter universe and in the RD universe. The general solution of Equation 3.51 in the de Sitter universe with $a''/a = 2/\eta^2$ is given by

$$\phi(\mathbf{k},\eta) = e^{-ik\eta}\left(1 - \frac{i}{\kappa\eta}\right), \qquad -\infty < \eta < \eta_1, \tag{3.65}$$

and in the RD epoch $a''/a = 0$ we get

$$\phi(\mathbf{k},\eta) = \left[\alpha(\mathbf{k})e^{-ik\eta} + \beta(\mathbf{k})e^{ik\eta}\right], \qquad \eta_1 < \eta < \eta_{\rm eq}. \tag{3.66}$$

Requiring that both ϕ and ϕ' are continuous function during the transition at $\eta = \eta_1$ we get the following expression for the Boguliobov coefficients [36, 39]

$$\alpha(\mathbf{k}) = 1 - \frac{1}{k\eta_1} - \frac{1}{2k^2\eta_1^2}, \qquad \beta(\mathbf{k}) = \frac{1}{2k^2\eta_1^2}. \tag{3.67}$$

If we assume that during the de Sitter expansion gravitons were missing, $n_a = 0$, the number of produced gravitons after transition would be

$$n_b = |\beta|^2 = \frac{1}{4k^4\eta_1^4}. \tag{3.68}$$

Further we can connect the density parameter at present with the number density of the produced gravitons. Let $n(\mathbf{x},\mathbf{k})$ be the number density of gravitons per cell of the phase space. In the case of an isotropic and homogeneous universe it depends only on the graviton energy or frequency, $n(\mathbf{x},\mathbf{k}) = n(\omega)$ where ω is the graviton energy. For Bose particles, the energy density is

$$\rho_{\rm gw} = \frac{2}{(2\pi)^3}\int d^3k\, n(\omega)\,\omega = 16\pi^2\int_0^\infty d(\log f) f^4\, n(f), \tag{3.69}$$

where the factor 2 in front of the integral takes into account that the graviton is a spin 2 particle and $\omega = 2\pi f$. The density parameter at present as a function of the frequency and the graviton number density is given by

$$h_0^2\Omega_{\rm gw}(f) \simeq 3.5\cdot 10^{-19}\left(\frac{n}{10^{30}}\right)\left(\frac{f}{1{\rm Hz}}\right)^4. \tag{3.70}$$

Now we need to express the graviton number density as a function of present day frequency f. First we may note that the term in the denominator in Equation 3.68, namely $k\eta$ is roughly speaking the ratio of the horizon size at the end of the de Sitter epoch to the physical wavelength $a(t)/k$. In fact, we can write

$$k|\eta_1| = k_{\rm phys}(t_0)a(t_0)|\eta_1| = 2\pi f a(t_0)|\eta_1| = \frac{2\pi f}{H}\frac{a(t_0)}{a(t_1)}. \tag{3.71}$$

Using Equation 4.26 and Equation 4.27 we get

$$k|\eta_1| = 10^{-11}\left(\frac{m_{\rm Pl}}{H}\right)^{1/2}\left(\frac{f}{1\ {\rm Hz}}\right). \tag{3.72}$$

Inserting Equation 3.72 into Equation 3.68 we get the following expression for the graviton number density at present

$$n_b \simeq 2.5\cdot 10^{43}\left(\frac{H}{m_{\rm Pl}}\right)^2\left(\frac{1\ {\rm Hz}}{f}\right)^4, \tag{3.73}$$

and inserting Equation 3.73 into Equation 3.74 we get the following expression for the present density parameter of GWs produced during the transition from the de Sitter epoch to RD epoch

$$h_0^2\Omega_{\rm gw}^{dS}(f) \simeq 8.75\cdot 10^{-6}\left(\frac{H}{m_{\rm Pl}}\right)^2. \tag{3.74}$$

We can see from the above result that the density parameter does not depend on the graviton frequency but it only depends on the value of the Hubble constant at the de Sitter epoch. As far as we know from the present theory of inflation, it ended roughly speaking at an energy scale or temperature of $T_b \sim 10^{-4}m_{\rm Pl}$, so the present day density parameter in GWs would be $h_0^2\Omega_{\rm gw}^{dS}(f) \simeq 10^{-13}$. We may also note that Equation 3.72 can be written as $k|\eta_1| = f_b^4/4f^4$ where f_b is a cut-off frequency in the GHz range

$$f_b = 10^{11}\left(\frac{H}{m_{\rm Pl}}\right)^{1/2}\text{Hz}. \tag{3.75}$$

The above calculations hold only during the transition from the de Sitter to the RD epoch but the same amplification of the graviton number happens even during the transition from the RD to the MD epoch. Here we do not show the calculations because they are similar to those done for the transition from the de Sitter to the RD epoch but we do present only the final result. Typical scales which are amplified in this case are those with wavelength of the order of the horizon size at the time of the RD and the MD equilibrium, since after that time the universe became MD. It is interesting at this stage to find the frequency of modes which entered horizon at $t = t_{\rm eq}$. Therefore one can find the following relation between the Hubble parameter at equilibrium and the equilibrium time [41]

$$t_{\rm eq} = 4(\sqrt{2}-1)/3H_{\rm eq} \tag{3.76}$$

The condition for a mode to enter horizon is $\lambda\!\!\!^{-}_{\rm eq} \simeq H_{\rm eq}^{-1}$ implies a equilibrium frequency at present $f_{\rm eq} = H_{\rm eq}/2\pi(1+z_{\rm eq})$. Knowing that $1+z_{\rm eq} = 2.32\cdot 10^4\,(h_0^2\Omega)$ and $t_{\rm eq} = 4.4\cdot 10^{10}\,(h_0^2\Omega)^{-2}$ s we get the value of the equilibrium frequency at present

$$f_{\rm eq} \simeq 10^{-16}\,(h_0^2\Omega)\text{Hz}. \tag{3.77}$$

On the other hand the lowest part of the graviton spectrum which would have been amplified corresponds to modes which are entering inside horizon at present epoch with wavelength $\lambda\!\!\!^{-} \simeq H_0^{-1}$. The frequency of these modes is $f = H_0/2\pi = 3\cdot 10^{-18}$ Hz. Consequently, the frequency range of gravitons which are created during the RD to the MD epoch is $3\cdot 10^{-18}$ Hz $< f < 10^{-16}\,(h_0^2\Omega)$ Hz. The corresponding density parameter at present is given by [12, 39]

$$h_0^2\Omega_{\rm gw}^{RD-MD}(f) \simeq 10^{-5}\left(\frac{f_{\rm eq}}{f}\right)^2\left(\frac{H}{m_{\rm Pl}}\right)^2. \tag{3.78}$$

Both Equation 3.74 and Equation 3.78 give the density parameter in two different frequency ranges which are complementary to each other, namely Equation 3.74 is valid for $10^{-16}\,(h_0^2\Omega)$ Hz $< f < 10^9$ Hz and Equation 3.78 being valid for $3\cdot 10^{-18}$ Hz $< f < 10^{-16}\,(h_0^2\Omega)$ Hz.

3.3.3 Gravitons from the slow-roll inflation

A near scale-invariant spectrum over a wide range of frequencies is a key prediction of the standard inflationary model [42, 43]. The relative amplitude of GWs spectrum to density perturbations spectrum is usually expressed in terms of the ratio, r, of tensor to scalar perturbations. From observations of WMAP, the current limit on B-mode of the CMB polarization demands $r \lesssim 0.22$ which rule out some models of inflation [44, 45]. The spectrum of GWs can be expressed in terms of the tensorial spectral index, n_t, and is almost flat in the frequency range 2×10^{-15} Hz $< f < f_{max} \simeq 10^{10}$ Hz. The density parameter is proportional to a power of the frequency:

$$h_0^2 \Omega_{GW}(f) \propto f^{n_t}. \tag{3.79}$$

Since the tensorial spectral index is negative, $n_t < 0$, the spectrum is decreasing rather than flat. Depending on inflationary model the value of the tensorial spectral index changes and there are some models which predict $r \sim 10^{-3}$.

3.3.4 Pre-heating phase

At the end of inflation the energy of the inflaton field ϕ is spent to generate new particles and heat the Universe. The first estimate of the density parameter of GWs during the pre-heating phase was done in [46] who found the density parameter of the order $h_0^2 \Omega_{GW} \sim 10^{-11}$ for the gravitational waves with the present day frequency $f \sim 10^6$ Hz, in the models with quartic potential, $\lambda\phi^4$. Later, this mechanism was reconsidered in [47, 48] who studied the models with the potentials of the form $\lambda\phi^4$ and $m^2\phi^2$. The authors have found numerically that $h_0^2 \Omega_{GW} \sim 10^{-10}$ in the frequency range $f \sim 10^8 - 10^9$ Hz.

3.3.5 First order phase transitions

At the end of inflation, first-order phase transitions could have generated a large amount of gravitational waves. At such transitions the bubble nucleation of true vacuum states and percolation can occur accompanied by the bubble collisions. In a series of papers [49, 50, 51, 52] the energy of gravitational waves generated from bubble collisions at strongly first-order phase transitions was estimated and the results were later extended to the electroweak first-order phase transitions. The amount of GWs from strongly first-order phase transition at its end is of the order $1.3 \cdot 10^{-3}(\tau/H)$, where τ is the duration of the phase transition, H is the Hubble constant, and the peak frequency is $\omega_*^{peak} = 3.8/\tau$. The present day density parameter of GWs produced at the electroweak first-order phase transition was found to be of the order $\Omega_{GW} \sim 10^{-22}$ with characteristic frequency $f \sim 4 \cdot 10^{-3}$. Since later it has been found out, that there is no first order electroweak phase transition in the standard model [53], the mechanism was reconsidered in [54]. The authors estimated the GW production in the temperature range 100 GeV-10^7 GeV. The spectrum of the GWs today in this temperature range extends from 10^{-3} Hz to 10^2

Hz. The associated density parameter was found to be quite large, $h_0^2\Omega_{GW}(f_{peak}) \sim 10^{-9}$ depending on the parameters of the model.

3.3.6 Topological defects and cosmic strings

Practically in all inflationary models the gravitational wave spectrum is almost flat in the frequency range from 10^{-15} Hz$< f < f_{max} \simeq 10^{10}$ Hz with some variations coming from pre-heating and reheating phases for which the frequency is peaked near GHz region. There are other mechanisms of GWs production e.g. by cosmic strings which predict almost flat spectrum in a wide range of frequencies. Many of the proposed observational tests for the existence of cosmic strings are based on their gravitational interactions [55, 56]. Particularly interesting are GWs produced by closed string loops which oscillate in relativistic regime. The spectrum of the GWs produced by such relativistic oscillations is almost flat in the region 10^{-8} Hz$< f < f_{max} \simeq 10^{10}$ Hz with a peak at low frequency near $f \sim 10^{-12}$ Hz. The density parameter in the frequency range $f \gg 10^{-4}$ Hz, according to [57], is equal to:

$$h_0^2\Omega_{GW}(f) \simeq 10^{-8}\left(\frac{G\mu}{10^{-8}}\right)^{1/2}\left(\frac{\gamma}{50}\right)^{1/2}\left(\frac{\alpha}{0.1}\right)^{1/2}, \tag{3.80}$$

where $G\mu$, α and γ are respectively the string tension, the initial loop size as a fraction of the Hubble radius and the radiation efficiency. From the pulsar timing data the authors of [58] constrained the density parameter of GWs from the cosmic strings in the frequency range $f \gg 10^{-6}$ Hz and put the limit

$$h_0^2\Omega_{GW}(f) \lesssim 10^{-8}. \tag{3.81}$$

It is generally assumed that at the end of inflation the inflaton oscillates and eventually decays. If non-topological solitons, the so called Q-balls, are produced at the inflaton decay, such Q-balls could be a source of GWs. According to the calculations of [59] the density parameter of such GWs would be of the order of $h_0^2\Omega_{GW} \sim 10^{-9}$ with a peak frequency $f \sim 10^{10}$ Hz.

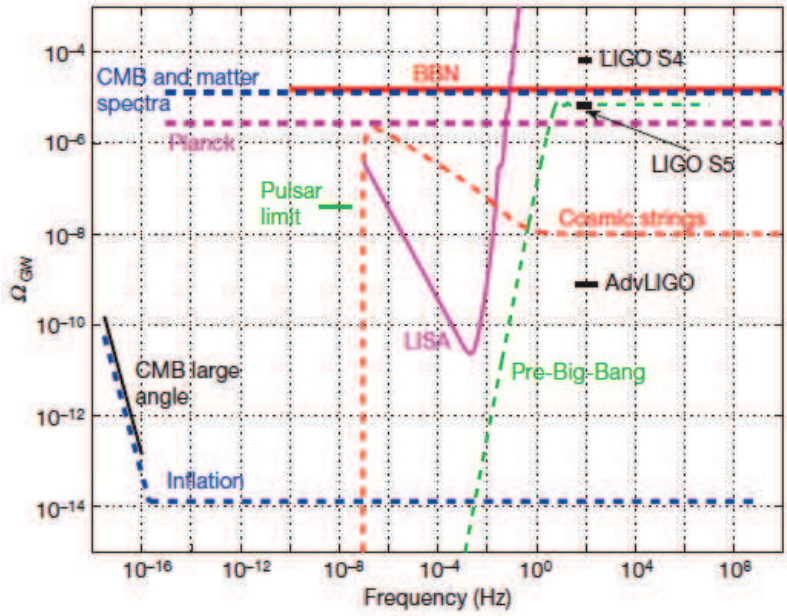

Figure 3.1: $\log[h_0^2\Omega_{GW}(\mathrm{f})]$ vs. log(f [Hz]) for different models of production of stochastic background of GWs as given in [60].

Chapter 4

Relic gravitons from primordial black holes

In this chapter we discuss one more source of gravitational wave (GW) in the early Universe, namely, the interaction between primordial black holes (PBHs). We consider relatively light PBH, such that they evaporated before BBN and so they are not constrained by the light element abundances. Cosmological scenario with early formed and evaporated primordial black holes producing gravitons was considered in [61]. Here we will remain in essentially the same frameworks and study in addition the GW emission in different processes with PBH.

Not taking into account the gray body factor, the life-time of evaporating black hole with initial mass M, is equal to [62, 63]:

$$\tau_{BH} = \frac{10240\,\pi}{N_{eff}} \frac{M^3}{m_{Pl}^4}, \tag{4.1}$$

where the Planck mass is $m_{Pl} = 2.176 \cdot 10^{-5}$ g and N_{eff} is the number of particle species with masses smaller than the black hole temperature:

$$T_{BH} = \frac{m_{Pl}^2}{8\pi M}. \tag{4.2}$$

To avoid a conflict with BBN the black holes should had been evaporated before cosmological time $t \approx 10^{-2}$ s [64] and thus their mass would be bounded from above by

$$M < 1.75 \cdot 10^8 \left(\frac{N_{eff}}{100}\right)^{1/3} \text{ g}. \tag{4.3}$$

The temperature of such PBHs should be higher than $3 \cdot 10^4$ GeV and correspondingly $N_{eff} \geqslant 10^2$. On the other hand, as is discussed in what follows, the PBH mass is bounded from below e.g. by Equation 4.16. This is the mass range of PBHs considered

here. Such PBH are not constrained by any astronomical data, which are applicable to heavier ones [64, 65].

Primordial black holes should interact in the early Universe creating gravitational radiation. Below we estimate the efficiency of GW emission in several processes with PBH. In section 4.1 some mechanisms of PBH production and PBH evolution in the early Universe are briefly described. We stress, in particular, a very important role played by the clumping of PBH due to gravitational instability at the matter dominated stage. In section 4.2 we consider the initial interaction between the PBHs when they started to "feel" each other and accelerate with respect to the background cosmological expansion. In section 4.3 the quantum bremsstrahlung of gravitons at PBH collisions is discussed, which is quite similar to the electromagnetic bremsstrahlung at Coulomb scattering of electrically charged particles. Next, in section 4.4 we consider the classical emission of GW at accelerated motion of a pair of BHs in their mutual gravitational field. In section 4.5 we evaluate the energy loss of PBHs due to their mutual interaction. It may be relevant to the estimation of the probability of formation of PBH binaries. The gravitational radiation from PBH binaries in high density clusters is discussed in section 4.6. In section 4.7 we calculate the present day energy density of gravitons produced at PBH evaporation.

4.1 Production and evolution of PBH in the early universe.

Formation of primordial black holes from the primordial density perturbations in the early Universe was first considered by in [66] and later in [67, 68]. PBHs would be formed when the density contrast, $\delta\rho/\rho$, at horizon was of the order of unity or, in other words, when the Schwarzschild radius of the perturbation was of the order of the horizon scale. If PBH was formed at the radiation dominated stage, when the cosmological energy density was $\rho(t) = 3m_{Pl}^2/(32\pi t^2)$, and the horizon was $l_h = 2t$, the mass of PBH would be:

$$M(t) = m_{Pl}^2 t \simeq 4 \cdot 10^{38} \left(\frac{t}{\text{sec}}\right) \text{ g} \tag{4.4}$$

where t is the time elapsed since Big Bang.

The fraction of the cosmological energy density of PBH produced by such mechanism depends upon the spectrum of the primordial density perturbations. We denote this fraction Ω_p and take it as a free parameter of the model. The data on the large scale structure of the Universe and on the angular fluctuations of the cosmic microwave background radiation (CMB) show that the spectrum of the primordial density fluctuations is almost flat Harrison-Zeldovich one. For such spectrum the probability of PBH production is quite low and $\Omega_p \ll 1$. However, the flatness of the spectrum is verified only for astronomically large scales, comparable with the galactic ones. The form of the spectrum for masses below 10^{10} g is not known. Inflation predicts that the spectrum remains flat for all the scales but there exist scenarios with strong deviation from flatness at small scales. In particular, in ref. [69, 70] a model of PBH formation has been proposed which

leads to log-normal mass spectrum of the produced PBH:

$$\frac{dN}{dM} = C \exp\left[\frac{(M - M_0)^2}{M_1^2}\right], \tag{4.5}$$

where C, M_0, and M_1 are some model dependent parameters. Quite naturally the central value of PBH mass distribution may be in the desired range $M_0 < 10^9$ g. In this model the value of Ω_p may be much larger than in the conventional model based on the flat spectrum of the primordial fluctuations. We will not further speculate on the value of Ω_p and on the form of the mass spectrum of PBH. In what follows we assume for an order of magnitude estimate that the spectrum is well localized near some fixed mass value and that Ω_p is an arbitrary parameter. Different mechanisms of PBH production are reviewed e.g. in [71, 72].

We assume that PBHs were produced in radiation dominated (RD) Universe, when the cosmological energy density was equal to

$$\rho_R = \frac{3m_{Pl}^2}{32\pi t^2}. \tag{4.6}$$

If we neglect the PBH evaporation and possible coalescence, their number density would remain constant in the co-moving volume, $n_{BH}(t)a^3(t) = const$. In what follows the instant decay approximation for evaporation is used. The cosmological evolution of PBHs with more realistic account of their decay was studied in [73].

Since the black holes were non-relativistic at production, their relative contribution to the cosmological energy density rose as the cosmological scale factor, $a(t)$:

$$\Omega_{BH}(t) = \Omega_p \left(\frac{a(t)}{a_p}\right), \tag{4.7}$$

where a_p is the value of the scale factor at the PBH production and at RD-stage $a(t)/a_p = (t/t_p)^{1/2}$. The moment t_p of the black hole production is connected with the PBH mass through Equation 4.4. Hence

$$t_p = \frac{M}{m_{Pl}^2}. \tag{4.8}$$

Thus if PBHs lived long enough, they would dominate the cosmological energy density and the Universe would become matter dominated at $t > t_{eq}$, where

$$t_{eq} = \frac{M}{m_{Pl}^2 \Omega_p^2} = \frac{r_g}{2\Omega_p^2}, \tag{4.9}$$

and $r_g = 2M/m_{Pl}^2$ is the gravitational (Schwartzschild) radius of a black hole. In what follows we assume that all PBHs have the same mass M, but the results can be simply generalized by integration over the PBH mass spectrum. Evidently at RD stage the number density of PBHs drops as:

$$n_{BH}(t) = n_p \left(\frac{a_p}{a(t)}\right)^3 = n_p \left(\frac{t_p}{t}\right)^{3/2}, \tag{4.10}$$

while at MD stage

$$n_{BH}(t) = n_p \left(\frac{t_p}{t_{eq}}\right)^{3/2} \left(\frac{t_{eq}}{t}\right)^2 . \tag{4.11}$$

Cosmological mass fraction of BH as a function of time behaves as

$$\Omega_{BH}(t) = \frac{n_{BH}(t)M}{\rho_c} = \frac{16\pi}{3} r_g t^2 n_{BH}(t) , \tag{4.12}$$

i.e. $\Omega_{BH} \sim t^{1/2}$ at RD stage. After the onset of the PBH dominance, Ω_{BH} approached unity and remained constant till the PBH evaporation when Ω_{BH} quickly dropped down to zero and the universe became dominated by relativistic particles produced by PBH evaporation. All relics from the earlier RD stage would be diluted by the redshift factor $(t_{eq}/\tau_{BH})^{2/3}$. In particular the energy density of GWs produced at inflation would be diminished by this factor with respect to the standard predictions. Such dilution may cause problems with baryogenesis. However, these problems may be resolved if baryogenesis took place at the process of PBH evaporation through the mechanism suggested in [74] and quantitatively studied in [75, 76]. Somewhat similar model of baryogenesis by heavy particle decay (e.g. by bosons of GUT) created at PBH evaporation was considered in [77, 78, 79, 80].

To survive till equilibration the PBHs should live long enough so that their evaporation time t_{ev} would be larger than t_{eq} or $\tau_{BH} > t_{eq} - t_p$ which can be translated into the bound on the PBH mass:

$$M > \left(\frac{N_{eff}}{3.2 \cdot 10^4}\right)^{1/2} m_{Pl} \left(\frac{1}{\Omega_p^2} - 1\right)^{1/2} \simeq 5.6 \cdot 10^{-2} \left(\frac{N_{eff}}{100}\right)^{1/2} \frac{m_{Pl}}{\Omega_p} \tag{4.13}$$

where $\Omega_p \ll 1$ and M is mass of PBHs at production *. Both constraints, Equation 4.3 and Equation 4.13 would be satisfied if

$$\Omega_p > 0.7 \cdot 10^{-14} \left(\frac{N_{eff}}{100}\right)^{1/6} . \tag{4.14}$$

For example, if $\Omega_p = 10^{-10}$, the black holes should be heavier than $1.2 \cdot 10^4$ g.

When the Universe became dominated by non-relativistic PBHs, primordial density perturbations, $\Delta = \delta\rho/\rho$, should rise as the cosmological scale factor. They could reach unity at cosmological time t_1 satisfying the condition:

$$\Delta_{in} \left(\frac{t_1}{t_{eq}}\right)^{2/3} \sim 1 , \tag{4.15}$$

*In fact in equation (4.13) there must be the PBHs mass at the equilibrium time, $M(t_{eq})$. Due to evaporation the PBH mass as a function of time is given by $M(t) = M(t_p)(1 - t/\tau_{BH})^{1/3}$ and it is easy to see that for $\tau_{BH} > t_{eq}$ it gives $M = M(t_p) \simeq M(t_{eq})$, so hereafter we refer to M as the mass of PBH at production.

where Δ_{in} is the initial magnitude of the primordial density perturbations. To be more accurate, the evolution of density perturbations depends upon the moment when they cross horizon, see below, Equation 4.19. For the moment we neglect this complication to make some simple estimates.

The initial density contrast is usually assumed to be of the order of $\Delta_{in} \sim 10^{-5} - 10^{-4}$ which is not necessarily true at small scales and may be much larger, especially in the model of [69, 70]. Evidently the BH life-time, τ_{BH}, must be long enough, so that the density fluctuations in BH matter would rise up to the values of the order of unity. The condition $t_{ev} > t_1$ or equivalently $\tau_{BH} > t_1 - t_p$ leads to the following restriction on the PBH mass:

$$M > M_{low} = \left(\frac{N_{eff}}{3.2 \cdot 10^4}\right)^{1/2} \frac{m_{Pl}}{\Omega_p \Delta_{in}^{3/4}} \simeq 1.2 \cdot 10^3 \text{ g} \left(\frac{10^{-6}}{\Omega_p}\right) \left(\frac{10^{-4}}{\Delta_{in}}\right)^{3/4} \left(\frac{N_{eff}}{100}\right)^{1/2} \quad (4.16)$$

We can see that Equation 4.16 puts a stronger lower limit on PBHs mass than Equation 4.13. The limits are comparable only if $\Delta_{in} \approx 1$. Using Equation 4.16 and (4.3) we get a stronger than Equation 4.14 restriction on Ω_p:

$$\Omega_p > 0.7 \cdot 10^{-11} \left(\frac{10^{-4}}{\Delta_{in}}\right)^{3/4} \left(\frac{N_{eff}}{100}\right)^{1/6}. \quad (4.17)$$

After Δ reached unity, the rapid structure formation would take place and high density clusters of PBHs would be formed. As we see in what follows, generation of gravitational waves would be especially efficient from such high density clusters of primordial black holes.

Let us assume that the spectrum of perturbations is the flat Harrison-Zeldovich one and that a perturbation with some wave length λ crossed horizon at moment t_{in}. The mass inside horizon at this moment was:

$$M_b(t_{in}) = m_{Pl}^2 t_{in}. \quad (4.18)$$

It is the mass of the would-be high density cluster of PBHs. This initial time is supposed to be larger than t_{eq} Equation 4.9, i.e. the horizon crossing took place already at MD-stage. For flat spectrum of perturbations density contrast, $\Delta = \delta\rho/\rho$, at horizon crossing is the same for all wave lengths. After horizon crossing the perturbations would continue to grow up as the scale factor, $\Delta(t) = \Delta_{in}(t/t_{in})^{2/3}$. Such rise would continue till moment $t_1(t_{in})$ such that:

$$\Delta[t_1(t_{in})] = \Delta_{in}[t_1(t_{in})/t_{in}]^{2/3} = 1 \text{ or } t_1(t_{in}) = t_{in}\Delta_{in}^{-3/2}. \quad (4.19)$$

The radius of the PBH cluster rose almost as the cosmological scale factor till $t = t_1(t_{in})$. After the density contrast has reached unity the cluster would decouple from the common cosmological expansion. In other words, the cluster stopped to expand together with the universe and, on the opposite, it would begin to shrink when gravity takes over

the free streaming of PBHs. So the cluster size would drop down and both n_{BH} and ρ_b would rise. The density contrast would quickly rise from unity to $\Delta_b = \rho_b/\rho_c \gg 1$, where ρ_c and ρ_b are respectively the average cosmological energy density and the density of PBHs in the cluster (bunch). It looks reasonable that the density contrast of the evolved cluster could rise up to $\Delta = 10^5 - 10^6$, as in the contemporary galaxies. After the size of the cluster stabilized, the number density of PBH, n_{BH}, as well as their mass density, ρ_{BH}, would be constant too. But the density contrast, Δ_b would continue to rise as $(t/t_1)^2$ because ρ_c drops down as $1/t^2$. From time $t = t_1$ to $t = \tau_{BH}$ the density contrast would additionally rise by the factor:

$$\Delta(\tau_{BH}) = \Delta(t_1)\left(\frac{\tau_{BH}}{t_1}\right)^2 = \Delta(t_i)\left(\frac{M}{M_{low}}\right)^4, \tag{4.20}$$

where t_1 and M_{low} are given by Equation 4.15 and Equation 4.16 respectively.

The size of the high density clusters of PBH would be

$$R_b = \Delta_b^{-1/3} t_1^{2/3} t_{in}^{1/3} \tag{4.21}$$

and the average distance between the PBHs in the bunch can be estimated as:

$$d_b = (M/M_b)^{1/3} R_b = \Delta_b^{-1/3} t_1^{2/3} r_g^{1/3} = 2^{-2/3} \Delta_b^{-1/3} \Delta_{in}^{-1} \Omega_p^{-4/3} r_g \,. \tag{4.22}$$

It does not depend upon t_{in}. Here Equation 4.15 and Equation 4.9 have been used. The virial velocity inside the cluster would be

$$v = \sqrt{\frac{2M_b}{m_{Pl}^2 R_b}} = 2^{1/2} \Delta_b^{1/6} \Delta_{in}^{1/2} \approx 0.14 \left(\frac{\Delta_b}{10^6}\right)^{1/6} \left(\frac{\Delta_{in}}{10^{-4}}\right)^{1/2}. \tag{4.23}$$

So PBHs in the cluster can be moderately relativistic. Later, when $t = \tau_{BH}$, black holes would decay producing relativistic matter and the Universe would return to the normal RD regime. However, the previous history of the earlier RD stage would be forgotten.

For the future discussion it is convenient to introduce the average distance between the PBHs at arbitrary time, $d = n_{BH}^{-1/3}$, where $n_{BH} = \rho_{BH}/M$ is the number density of PBHs. Since

$$\Omega_p = \frac{\rho_p}{\rho_c} = \frac{32\pi t_p^2 M n_p}{3 m_{Pl}^2} = \frac{32\pi}{3}\left(\frac{t_p}{d_p}\right)^3, \tag{4.24}$$

the average distance between PBHs at the production moment is equal to

$$d_p = (4\pi/3)^{1/3} r_g \Omega_p^{-1/3} \,. \tag{4.25}$$

When the mutual gravitational attraction of PBH may be neglected, d rises as cosmological scale factor, $a(t)$.

Gravitational waves produced in the early universe will be hopefully registered in the present epoch. The sensitivity of GW detectors strongly depends upon the frequency

of the signal. The frequency f_* of GW produced at time t_* during PBH evaporation, is redshifted down to the present day value, f, according to:

$$f = f_* \left[\frac{a(t_*)}{a_0}\right] = 0.34\, f_* \frac{T_0}{T_*} \left[\frac{100}{g_S(T_*)}\right]^{1/3}, \tag{4.26}$$

where $T_0 = 2.725$ K [81] is the temperature of the cosmic microwave background radiation at the present time, $T_* \equiv T(t_*)$ is the plasma temperature at the moment of radiation of the gravitational waves, and $g_S(T_*)$ is the number of species contributing to the entropy of the primeval plasma at temperature T_*. It is convenient to express T_0 in frequency units, $T_0 = 2.7\,\mathrm{K} = 5.4 \cdot 10^{10}$ Hz.

The temperature of the primeval plasma after the PBH evaporation can be approximately found from:

$$\rho = \frac{m_{Pl}^2}{6\pi t^2} = \frac{\pi^2 g_*(T_*) T_*^4}{30}, \tag{4.27}$$

where $g_*(T_*) \approx 10^2$ is the contribution of different particle species to the energy density at temperature T_* and $t_1 < t < t_{ev}$. For relativistic plasma $g_*(T) = g_S(T)$. Since $t_{ev} = \tau_{BH} + t_p \simeq \tau_{BH}$, we obtain from Equation 4.27 at time $t_* = \tau_{BH}$:

$$T_*(\tau_{BH}) = \left[\frac{30}{6\pi^3 g_S(T_*)}\right]^{1/4} \left(\frac{N_{eff}}{3.2 \cdot 10^4}\right)^{1/2} \frac{m_{Pl}^{5/2}}{M^{3/2}}. \tag{4.28}$$

Substituting the numbers we find:

$$T_*(\tau_{BH}) \approx 0.011 m_{Pl} \left[\frac{100}{g_S(T_*)}\right]^{1/4} \left(\frac{N_{eff}}{100}\right)^{1/2} \left(\frac{m_{Pl}}{M}\right)^{3/2}. \tag{4.29}$$

For comparison at the PBH production moment the temperature of the primeval plasma was:

$$T_p \approx 0.2 m_{Pl} \left(\frac{m_{Pl}}{M}\right)^{1/2}. \tag{4.30}$$

Using Equation 4.26 and Equation 4.29, we find that the present day frequency of the GWs, emitted at T_*, Equation 4.28 with frequency f_*, would be equal to:

$$f = 1.7 \cdot 10^{12}\mathrm{Hz} \left[\frac{100}{g_S(T_*)}\right]^{1/12} \left(\frac{100}{N_{eff}}\right)^{1/2} \left(\frac{f_*}{m_{Pl}}\right) \left(\frac{M}{m_{Pl}}\right)^{3/2}. \tag{4.31}$$

If we take the maximum frequency of the emitted gravitons $f_{max*} \approx r_g^{-1} = m_{Pl}^2/2M$, the GW maximum frequency today would be:

$$f_{max} \approx 8.6 \cdot 10^{11}\mathrm{Hz} \left(\frac{M}{m_{Pl}}\right)^{1/2} = 5.8 \cdot 10^{16}\,\mathrm{Hz} \left(\frac{M}{10^5 \mathrm{g}}\right)^{1/2}. \tag{4.32}$$

4.2 Onset of GW radiation

Once PBHs enter inside each other cosmological horizon[†] they start to interact and thus to radiate gravitational waves due to their mutual acceleration. The corresponding time moment t_h is determined by the condition $2t_h = d(t_h)$ and remembering that it happened still at RD stage, we find

$$t_h = \frac{1}{2}\left(\frac{4\pi}{3}\right)^{2/3} r_g \Omega_p^{-2/3}. \tag{4.33}$$

For $t > t_h$, the curvature effects can be neglected and the PBH motion is completely determined by the Newtonian gravity:

$$\ddot{\mathbf{r}} = -\frac{M_{BH}}{m_{Pl}^2 r^2}\frac{\mathbf{r}}{r} \tag{4.34}$$

with the initial conditions $r_i \equiv |\mathbf{r}_i| = d(t_i)$ and $|\dot{\mathbf{r}}_i| = H(t_i)|\mathbf{r}_i|$, where $\mathbf{r}$ is the position vector of PBHs. For $t_i = t_h$ their relative initial velocity $|\dot{\mathbf{r}}_i| = v_i = 1$ and non-relativistic approximation is invalid. To avoid that we should choose $t_i > t_h$ such that $v_i \ll 1$. The solution of the equation of motion demonstrates that the effects of mutual attraction at this stage and production of GW are weak.

After PBHs enter inside each other horizon and Newtonian gravity can be applied, their acceleration toward each other becomes essential when their Hubble velocity drops below the capture velocity. The corresponding time moment, t_c, when it happened, is determined from the condition:

$$\frac{1}{2}v^2(t_c) \equiv \frac{1}{2}[H(t_c)d(t_c)]^2 \lesssim \frac{M_{BH}}{m_{pl}^2 d(t_c)}. \tag{4.35}$$

If it took place at the RD regime, the corresponding time moment would be equal to:

$$t_c = \frac{8\pi^2}{9}\frac{r_g}{\Omega_p^2}, \tag{4.36}$$

and the density parameter of PBHs at $t = t_c$ would be

$$\Omega_{BH}(t_c) = \Omega_p\left(\frac{t_c}{t_p}\right)^{1/2} = \frac{4\pi}{3} > 1\,. \tag{4.37}$$

Thus at $t = t_c$ the universe is already matter dominated and we have to use the non-relativistic expansion law, $a \sim t^{2/3}$, starting from the moment $t = t_{eq}$, Equation 4.9. Accordingly the average distance between BHs, when $t > t_{eq}$, grows as:

$$d(t) = d_p\left(\frac{t_{eq}}{t_p}\right)^{1/2}\left(\frac{t}{t_{eq}}\right)^{2/3}. \tag{4.38}$$

[†]The cosmological horizon is the distance which PBHs started interacting with each other exchanging gravitons and should not be confused with the black hole event horizon.

Now we find that the condition that the Hubble velocity, $v_H = (2/3t_c)d_c$ is smaller than the virial one, for average values, reads:

$$\frac{4d_p^3}{9r_g t_p^{3/2} t_{eq}^{1/2}} < 1\,. \tag{4.39}$$

One can see that this condition is never fulfilled. However, this negative result does not mean that the acceleration of BHs and GW emission are suppressed, because of the mentioned above effect of rising density perturbations.

4.3 Bremsstrahlung of gravitons.

PBH scattering in the early Universe should be accompanied by the graviton emission almost exactly as the scattering of charged particles is accompanied by the emission of photons. The cross-section of the graviton bremsstrahlung in particle collisions was calculated in [82] for the case of two spineless particles (here black holes) with masses m and M under assumption that $m \ll M$. In non-relativistic approximation, $\mathbf{p}^2 \ll m^2$, the differential cross section reads:

$$\mathrm{d}\sigma = \frac{64M^2m^2}{15m_{pl}^6}\frac{\mathrm{d}\xi}{\xi}\left[5\sqrt{1-\xi} + \frac{3}{2}(2-\xi)\ln\frac{1+\sqrt{1-\xi}}{1-\sqrt{1-\xi}}\right], \tag{4.40}$$

where ξ is the ratio of the emitted graviton frequency, $\omega = 2\pi f$, to the kinetic energy of the incident black hole, i.e. $\xi = 2m\omega/\mathbf{p}^2$. We will use Equation 4.40 for an order of magnitude estimate assuming that it is approximately valid for arbitrary m and M, in particular, for $m \sim M$.

The energy density of gravitational waves emitted at the time interval t and $t + \mathrm{d}t$ in the frequency range ω and $\omega + \mathrm{d}\omega$ is given by

$$\frac{\mathrm{d}\rho_{GW}}{\mathrm{d}\omega} = v_{rel}n_{BH}^2\omega\left(\frac{\mathrm{d}\sigma}{\mathrm{d}\omega}\right)\mathrm{d}t\,, \tag{4.41}$$

where n_{BH} is the number density of PBH and v_{rel} is their relative velocity. The energy emitted in the frequency interval $\omega \in [0, \omega_{max}]$ per unit time is proportional to the integral

$$I(\omega_{max}) = \frac{\mathbf{p}^2}{2m}\int_0^{\xi max} d\xi\left[5\sqrt{1-\xi} + \frac{3}{2}(2-\xi)\ln\frac{1+\sqrt{1-\xi}}{1-\sqrt{1-\xi}}\right]. \tag{4.42}$$

The maximum value of the frequency of the emitted gravitons should be smaller than either the kinetic energy of the colliding BHs, $E_{kin} = p^2/(2M)$ or the BH inverse gravitational radius, $1/r_g = m_{Pl}^2/2M$, depending on which of the two is smaller. Their ratio is $E_{kin}r_g = M^2v^2/m_{Pl}^2$, so for $M < m_{Pl}v^{-1}$ the maximum frequency would be the PBH kinetic energy and in this case $\xi_{max} = 1$. It corresponds to the situation when PBH

is nearly captured. It looses practically all its kinetic energy, which goes to the graviton. For PBHs in the high density clusters, when $v \sim 0.1$, the maximum frequency would be $\omega_{max} \sim 1/r_g$ for all PBHs heavier than $10m_{Pl}$. In this case $\xi_{max} = (m_{Pl}/Mv)^2$.

The first, rather exotic case, when $M < m_{Pl}/v$ can be realized only if $\Omega_p \geqslant 0.01$, see Equation 4.13. If $\xi_{max} = 1$, then $\omega_{max} \sim \mathbf{p}^2/2m$ and the integral can be taken analytically:

$$I(\omega_{max} = p^2/2M) = \frac{25}{3}\frac{\mathbf{p}^2}{2m} = \frac{25}{3}\omega_{max}. \tag{4.43}$$

In this case the energy taken by GWs is of the order of the kinetic energy of PBH and correspondingly $\Omega_{GW} \sim Mn_{bh}v^2/\rho_{BH} = v^2$.

Below we will consider more natural situation when $M > m_{Pl}\, v^{-1}$. Integral Equation 4.42 in the limit of small ξ_{max} is

$$I(\omega_{max} = 1/r_g) = \frac{p^2}{2M}\,\xi_{max}\,[8 + 3\ln(4/\xi_{max})] \tag{4.44}$$

This expression is accurate within 30% up to $\xi_{max} = 1$. So in what follows we will use this result as $I(\omega_{max}) \approx 25\omega_{max}/3$, keeping in mind that normally $\omega_{max} = 1/r_g \ll p^2/2M$.

The fraction of the cosmological energy density of the emitted gravitational waves which has been produced during time interval t and $t + \mathrm{d}t$, which is smaller than or comparable to the cosmological time $t_1 \lesssim t \lesssim t_{ev} \simeq \tau_{BH}$, can be obtained by the integration of Equation 4.41 over ω from 0 to ω_{max} taking into account that the energy density of GWs goes with the redshift as $(1+z)^{-4}$, and the integration over cosmological time, t, which is connected with the redshift by the relation[‡]

$$\mathrm{d}t = -\frac{\mathrm{d}z}{H_*\,(1+z)\,[\Omega_{BH*}(1+z)^3 + \Omega_{r*}(1+z)^4]^{1/2}}\,, \tag{4.45}$$

where H_*, Ω_{BH*}, and Ω_{r*} are respectively the Hubble parameter, the matter density parameter, and the radiation density parameter evaluated at cosmological time $t_* = \tau_{BH}$, just before the PBH decay. Recall that we use the instant decay approximation, so the Universe at $t = \tau_{BH}$ was still at MD stage. In this case all quantities such as H_* and ρ_c are taken at this stage: $H_* = 2/3t_*$, $\rho_c = m_{Pl}^2/6\pi\tau_{BH}^2$, $\Omega_{BH*} = 1$, and $\Omega_{r*} = 0$.

We need to calculate the energy density of GWs at the moment of the PBH evaporation. The rate of GW production is given by Equation 4.41. To take into account the redshift of the energy density of the gravitational waves we have to divide $d\rho_{GW}/d\omega$ by $(1+z)^4$, to substitute $\omega = (1+z)\omega_*$, where ω_* is the GW frequency at $t = \tau_{BH}$, and to express time through the redshift as $\mathrm{d}t = (3/2)\tau_{BH}(1+z)^{-5/2}\mathrm{d}z$. As a result we obtain at $t_* = \tau_{BH}$:

$$\mathrm{d}\rho_{GW}(\tau_{BH}) = \frac{32M^2 v_{rel}}{5m_{Pl}^6}[\rho_{BH}^{(cluster)}]^2\tau_{BH}(1+z)^{-13/2} f[\omega_*(z+1)]\mathrm{d}[(1+z)\omega_*]\mathrm{d}z \tag{4.46}$$

[‡]In this paper we consider flat space with curvature $k = 0$ and neglect cosmological constant, $\Lambda = 0$.

Here $\rho_{BH}^{(cluster)}$ is the energy density of the PBHs in the cluster (which is denoted above as ρ_b). Note that $\rho_{BH}^{(cluster)} = const$ before the PBH decay. We parametrize this quantity as $\rho_{BH}^{(cluster)} = \rho_{BH}^{(c)}(\tau_{BH})\Delta(\tau_{BH})$, where $\rho_{BH}^{(c)}(\tau_{BH}) = m_{Pl}^2/(6\pi\tau_{BH}^2)$ is the average cosmological energy density of PBH and $\Delta(\tau_{BH})$ is given by Equation 4.20, see also the discussion above this equation. Function $f(\omega)$ is the function of $\xi = 2m\omega/p^2$ in the square brackets of Equation 4.40.

To find the cosmological energy fraction of GWs at $t = \tau_{BH}$ we need to integrate the expression above over frequency, using Equation 4.43, and over redshift and to divide it by the total average cosmological energy density $\rho_{BH}^{(c)}(\tau_{BH}) = m_{Pl}^2/(6\pi\tau_{BH}^2)$. Since we have to average over the whole cosmological volume, one factor Δ disappears and we remain with the first power of Δ. So the cosmological energy fraction of GWs would be:

$$\Omega_{GW}(\omega_{max}, \tau_{BH}) \approx 16Q \left(\frac{v_{rel}}{0.1}\right) \left(\frac{\Delta}{10^5}\right) \left(\frac{N_{eff}}{100}\right) \left(\frac{\omega_{max}}{M}\right) . \tag{4.47}$$

Here coefficient Q reflects the uncertainty in the cross-section due to the unaccounted for Sommerfeld enhancement [83, 84]. Note that Δ may be considerably larger than 10^5.

With $v_{rel} = 0.1$, $\Delta = 10^5$, $Q = 100$, and $f_{max} = r_g^{-1}$ the fraction of the cosmological energy density of the GWs emitted by the bremsstrahlung of gravitons from the PBHs collisions, when the Universe age was equal to the life-time of the PBH, could reach:

$$\Omega_{GW}(\tau_{BH}) \sim 3.8 \cdot 10^{-17} \left(\frac{10^5\ \mathrm{g}}{M}\right)^2 . \tag{4.48}$$

It looks that for very light PBH, $M < 50 m_{Pl}$, the fraction of GW might exceed unity, which is evidently a senseless result. However, one should remember the lower bound on the PBH mass Equation 4.16 and that $m_{Pl}/M < \Omega_p/20$ and $m_{Pl}/M < 10^{-7}(\Omega_p/10^{-6})$.

It may be interesting to calculate the contribution to $\Omega_{GW}(\tau_{BH})$ from the earlier period before the cluster formation. The mass density of PBHs at that stage was equal to the cosmological energy density but since it was quite high and the effect is proportional to the density squared, the contribution from this period might be non-negligible. The result can be obtained from Equation 4.46, where ρ_{BH} is taken equal to the average cosmological energy density. Since ρ_c evolves with time we need to insert into the integral over $\mathrm{d}z$ the factor $(1+z)^6$ where the redshift is taken from some initial time, presumably $t_i = t_{eq}$, down to the moment of the cluster formation, t_1. So the energy density of gravitational waves produced by bremsstrahlung from $t = t_{eq}$, Equation 4.9, till $t = t_1$, Equation 4.15 would be:

$$\mathrm{d}\rho_{GW}^{(1)} = \frac{32M^2 v_{rel}}{5m_{Pl}^6} [\rho_{BH}^{(c)}(t_1)]^2 t_1 (1+z)^{-1/2} f[\omega_*(z+1)] \mathrm{d}[(1+z)\omega_*] \mathrm{d}z\,, \tag{4.49}$$

where $\rho_{BH}^{(c)} = m_{Pl}^2/(6\pi t_1^2)$ and $(1+z)$ runs from 1 up to $(t_1/t_{eq})^{2/3}$. We have introduced an upper index (1) to indicate that this is the energy density of GWs generated before the cluster formation time $t = t_1$. The integration over z gives the enhancement factor

$(1+z_{max})^{1/2} = (t_1/t_{eq})^{1/3}$. According to Equation 4.9 and Equation 4.15, this ratio is $\Delta_{in}^{-1/2} \sim 10^2$. Another enhancement factor comes from a larger cosmological energy density $\rho^{(c)}(t_1) = \rho^{(c)}(\tau_{BH})(\tau_{BH}/t_1)^2$. The other factor $\rho^{(c)}_{BH}(t_1)$ disappears in the ratio $\Omega_{GW} = \rho_{GW}/\rho^{(c)}$. On the other hand, Ω_{GW} is redshifted by $(\tau_{BH}/t_1)^{2/3}$. Correspondingly

$$\frac{\Omega^{(1)}_{GW}(\tau_{BH})}{\Omega_{GW}(\tau_{BH})} = \frac{11\Delta_{in}^{-1/2}}{\Delta(\tau_{BH})}\frac{v^{(1)}_{rel}}{v_{rel}}\left(\frac{\tau_{BH}}{t_1}\right)^{1/3}, \tag{4.50}$$

where the coefficient 11 came from the ratio of the integrals over z of Equation 4.46 and Equation 4.49 and

$$\left(\frac{\tau_{BH}}{t_1}\right)^{1/3} = \left(\frac{32170}{N_{eff}}\right)^{1/3}\Omega_p^{2/3}\left(\frac{M}{m_{Pl}}\right)^{2/3}. \tag{4.51}$$

The ratio of relative velocities of PBHs before and after the cluster formation, $v^{(1)}_{rel}/v_{rel}$, is tiny, according to the estimates of section 4.2, and this introduces another strong suppression factor to the production of GWs at an earlier stage. In accordance with Equation 4.20 the density contrast rises as $\Delta = \Delta(t_1)(\tau_{BH}/t_1)^2$, where $\Delta(t_1)$ is supposed to be large, say, $10^4 - 10^5$ due to the fast rise of density perturbations at MD stage after they reached unity. Thus the generation of GWs in high density PBH clusters is much more efficient than at the earlier stage.

The density parameter of the gravitational waves at the present time is related to cosmological time t_* as:

$$\Omega_{GW}(t_0) = \Omega_{GW}(t_*)\left(\frac{a(t_*)}{a(t_0)}\right)^4\left(\frac{H_*}{H_0}\right)^2, \tag{4.52}$$

where $H_0 = 100h_0$ km/s/Mpc is the Hubble parameter and $h_0 = 0.74 \pm 0.04$ [33, 85]. Using expression for redshift Equation 4.26 and taking the emission time $t_* = \tau_{BH}$ we obtain:

$$\Omega_{GW}(t_0) = 1.67\times 10^{-5}h_0^{-2}\left(\frac{100}{g_S(T(\tau_{BH}))}\right)^{1/3}\Omega_{GW}(\tau_{BH}). \tag{4.53}$$

Now using both equations Equation 4.48 and Equation 4.53 we find that the total density parameter of gravitational waves integrated up to the maximum frequency is:

$$h_0^2\Omega_{GW}(t_0) \approx 0.6\cdot 10^{-21}\,K\left(\frac{10^5\,\mathrm{g}}{M}\right)^2, \tag{4.54}$$

where K is the numerical coefficient:

$$K = \left(\frac{v_{rel}}{0.1}\right)\left(\frac{\Delta}{10^5}\right)\left(\frac{N_{eff}}{100}\right)\left(\frac{Q}{100}\right)\left(\frac{100}{g_S(T(\tau_{BH}))}\right)^{1/3}. \tag{4.55}$$

Presumably K is of order unity but since Δ may be much larger than one, see Equation 4.20, K may also be large.

4.4 GW from PBH scattering. Classical treatment.

Classical radiation of gravitational waves by non-relativistic masses is well described in quadrupole approximation, see e.g. books [17, 16, 86]. However, as we have seen, in high density clusters of PBH, their relative velocity could be high, see Equation 4.23, and relativistic corrections may be non negligible. This problem was studied by Peters [87], who considered emission of the GWs by two bodies with masses M and m, where the former is supposed to be heavy and at rest and the latter, lighter one, moves with velocity v. For non-relativistic motion, when $v \ll 1$, and the minimal distance between the bodies is larger than their gravitational radii, the energy of gravitational waves emitted in a single scattering process is equal to:

$$\delta E_{GW} = \frac{37\pi}{15}\frac{M^2 m^2 v}{b^3 m_{Pl}^6}, \qquad v \ll 1\,, \tag{4.56}$$

where b is the impact parameter.

For the relativistic motion, $1 - v^2 < 1$, the emitted energy is:

$$\delta E_{GW} = \frac{M^2 m^2}{b^3 m_{Pl}^6 (1-v^2)^{3/2}}\,. \tag{4.57}$$

The frequency of the emitted gravitational waves in this process is peaked near $\omega \sim 2\pi/\delta t$, where δt is the transition time which, for non-relativistic motion is $\delta t = b/v$ according to ref. [87], while for the relativistic one it is equal to $\delta t \sim b(1-v^2)^{1/2}$. For an order of magnitude estimate let us take $M \sim m$, then the radiated energy, as a function of frequency, would be:

$$\delta E_{GW}(\omega) \approx \frac{M^4}{m_{Pl}^6}\,\omega^3\,. \tag{4.58}$$

This and the previous equations are true for sufficiently large impact parameter, $b \gg r_g$ for which the space-time between the scattered PBHs may be considered as flat and their gravitational mass defect can be neglected. The energy loss in a single scattering event cannot be larger than

$$\delta E_{max} = \frac{p\,q}{M}\,, \tag{4.59}$$

where $p = M v_{rel}$ is the relative momentum of two scattered PBHs and q is the momentum transfer which by an order of magnitude is $q = 1/b$. Here and in what follows we use non-relativistic approximation. So equations Equation 4.56 and Equation 4.57 can be true only for

$$b > b_{min} = \sqrt{\frac{37\pi}{15}}\,\frac{M^2}{m_{Pl}^3}\,. \tag{4.60}$$

For smaller impact parameters the radiation of gravitational waves would be considerably stronger but the approximation used becomes invalid. For the (near) “head-on”

collision of black holes a bound state of two BH (a binary) or a larger black hole could be formed and the energy loss might be comparable to the BH mass due to gravitational mass defect. However, we are interested in gravitational waves at the low frequency part of the spectrum, such that they could be registered by existing or not-so-distant-future GW detectors. For such low frequency gravitational waves the approximation used here is an adequate one.

The differential cross-section of the gravitational scattering of two PBHs in non-relativistic regime, $q^2 \ll 2M^2$, can be taken as:

$$\mathrm{d}\sigma = \frac{M^2}{m_{Pl}^2}\frac{\mathrm{d}q^2}{q^4} = \frac{2M^2}{m_{Pl}^2} b\mathrm{d}b\,. \tag{4.61}$$

The differential energy density of GWs emitted at time and frequency intervals $[t,\ t+\mathrm{d}t]$ and $[\omega,\ \omega+\mathrm{d}\omega]$ respectively can be calculated as follows. The rate of the energy emission by GWs is

$$\mathrm{d}\dot{\rho}_{GW} = \mathrm{d}\sigma n_{BH}^2 v_{rel}\delta E_{GW}\,, \tag{4.62}$$

where we take for δE non-relativistic expression Equation 4.56. We assume that the impact parameter is related to the radiated frequency as $\omega = 2\pi v_{rel}/b$, as is discussed below Equation 4.57. With $b\mathrm{d}b = b^3\mathrm{d}\omega/(2\pi v_{rel})$ we find:

$$\mathrm{d}\rho_{GW} = \frac{74\pi v_{rel}}{15}\rho_{BH}^2\frac{M^4}{m_{Pl}^8}\frac{\mathrm{d}\omega}{2\pi}\mathrm{d}t\,. \tag{4.63}$$

The energy density parameter of GW at the moment of BH evaporation can be obtained integrating this expression over time and frequency. Thus we obtain:

$$\Omega_{GW}(\tau_{BH}) = 2\cdot 10^{-10}\left(\frac{v_{rel}}{0.1}\right)^2\left(\frac{\Delta_b}{10^5}\right)\left(\frac{N_{eff}}{100}\right)\left(\frac{10^5\,\mathrm{g}}{M}\right)\,. \tag{4.64}$$

If we do not confine ourselves to the impact parameter bounded by condition Equation 4.60 and allow for $b \sim r_g$, the energy density of GWs at the moment of PBHs evaporation might be comparable to unity.

Let us now take into account the redshift of GWs emitted at different moments during the the life-time of the high density clusters. The energy density of GWs emitted at some time t is redshifted to the moment of BH decay as $1/(z+1)^4$. The frequency of GW is redshifted as $\omega = (z+1)\omega_*$, where ω_* is the frequency of GWs at $t = \tau_{BH}$. Integration over time or redshift is trivial and we find from equation Equation 4.63 that the energy density parameter of gravitational waves per logarithmic interval of frequency or the spectral density parameter, Equation 3.10, at time $t = \tau_{BH}$ is equal to:

$$\Omega_{GW}(f_*;\tau_{BH}) \approx 8.5\left(\frac{v_{rel}}{0.1}\right)\left(\frac{\Delta_b}{10^5}\right)\left(\frac{N_{eff}}{100}\right)\left(\frac{M}{m_{Pl}^2}\right) f_*\,. \tag{4.65}$$

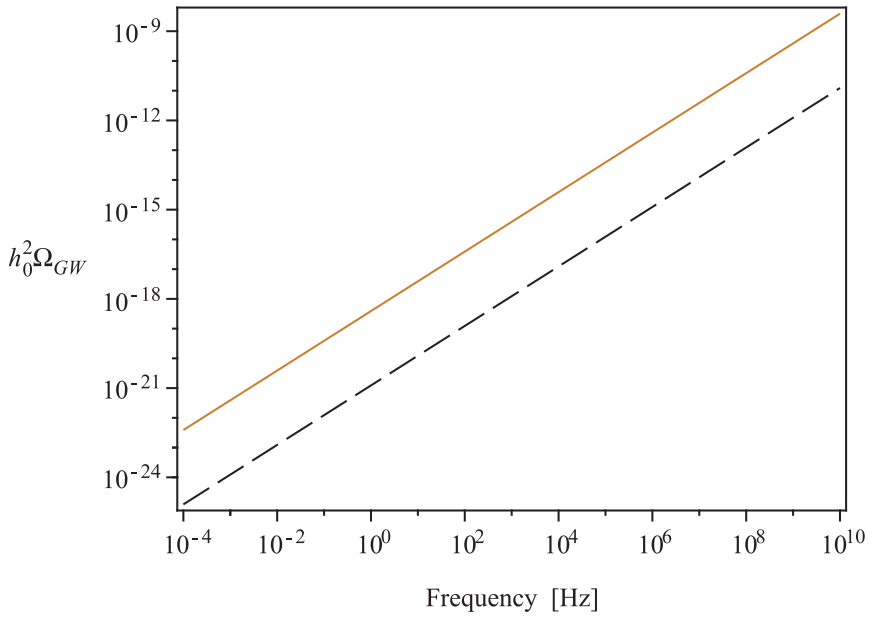

Figure 4.1: Log-log plot of density parameter today, $h_0^2\Omega_{GW}$, as a function of expected frequency today in classical approximation for $N_{eff} \sim 100$, $g_S \sim 100$, $\Delta_b \sim 10^5$, and $v_{rel} \sim 0.1$ for different values of PBH mass $M \sim 1$ g (solid line) and $M \sim 10^5$ g (dashed line).

Now using Equation 4.31 and Equation 4.53 we can calculate the relative energy density of GWs per logarithmic frequency at the present time:

$$h_0^2\Omega_{GW}(f;t_0) \approx 1.23 \cdot 10^{-12}\alpha' \left(\frac{f}{\text{GHz}}\right)\left(\frac{10^5\,\text{g}}{M}\right)^{1/2}, \tag{4.66}$$

where α' is the coefficient at least of order of unity:

$$\alpha' = \left(\frac{v_{rel}}{0.1}\right)\left(\frac{\Delta_b}{10^5}\right)\left(\frac{N_{eff}}{100}\right)^{3/2}\left(\frac{100}{g_S(T(\tau_{BH}))}\right)^{1/4}. \tag{4.67}$$

It may be much larger if $\Delta_b \gg 10^5$.

As we mentioned above, the classical approximation is valid if the impact parameter is bounded from below by Equation 4.60. Since the frequency of the radiated GWs is of the order of v/b, the maximum present day frequency of GWs, produced at cosmological time $t = \tau_{BH}$, for which the classical non-relativistic approximation is still valid, would be:

$$f_{max} \sim 9 \cdot 10^5\text{Hz}\left(\frac{v_{rel}}{0.1}\right)\left(\frac{100}{g_S(T(\tau_{BH}))}\right)^{1/12}\left(\frac{100}{N_{eff}}\right)^{1/2}\left(\frac{10^5\,\text{g}}{M}\right)^{1/2}. \tag{4.68}$$

For $M = 10^5$ g the minimum impact parameter is $b_{min} \approx 10^{-13}$ cm. The frequency of the order of 1 Hz today corresponds to the impact parameter 6 orders of magnitude larger.

If we demand that the impact parameter should be smaller than the average distance between PBHs in the clusters, then using equations Equation 4.22 and Equation 4.60 we find that it can be true if the following condition is fulfilled:

$$\Omega_p < 1.8 \cdot 10^{-6} \left(\frac{10^5 \mathrm{g}}{M}\right)^{3/4} \left(\frac{10^5}{\Delta_b}\right)^{1/4} \left(\frac{10^{-4}}{\Delta_{in}}\right)^{3/4} . \tag{4.69}$$

4.5 Energy loss of PBHs

We calculate here the total energy loss of PBHs in the high density clusters, in order to understand how probable could be the formation of the PBH binaries. First, let us estimate the total energy loss of PBHs due to the graviton bremsstrahlung. The loss of the kinetic energy per unit time due to the graviton emission is:

$$-\left(\frac{\mathrm{d}E_{kin}}{\mathrm{d}t}\right)_{brem} = n_{BH} v_{rel} \int_0^{\omega_{max}} \mathrm{d}\omega\, \omega \left(\frac{\mathrm{d}\sigma}{\mathrm{d}\omega}\right)_{brem} , \tag{4.70}$$

where ω_{max} is defined in section 4.3. The total loss of kinetic energy of a single PBH during the time interval equal to the PBH life-time, $\delta E_{kin} = -\dot{E}_{kin}\tau_{BH}$, normalized to the original kinetic energy of the PBH can be estimated as

$$\frac{\delta E_{kin}}{E_{kin}} = 6 \cdot 10^4 \kappa_2 \left(\frac{m_{Pl}}{M}\right)^2 , \tag{4.71}$$

where

$$\kappa_2 = \left(\frac{0.1}{v_{rel}}\right) \left(\frac{\Delta_b}{10^5}\right) \left(\frac{N_{eff}}{100}\right) \left(\frac{Q}{10}\right) . \tag{4.72}$$

Clearly the energy loss is essential for very light PBHs which could form dense clusters only if Ω_p is sufficiently high, see Equation 4.16.

The energy loss due to classical GW emission might be somewhat more efficient. According to the previous section the energy loss by a single PBH per unit time is:

$$\Delta\dot{E}_{class} = n_{BH} v \int_{b_{min}}^{\infty} db \left(\frac{\mathrm{d}\sigma}{\mathrm{d}b}\right)_{class} \delta E(b) , \tag{4.73}$$

where $\delta E(b)$ and b_{min} are given respectively by Equation 4.56 and Equation 4.60.

Taking the integral over b and time we find for the fractional energy loss of PBH due to classical emission of the gravitational waves:

$$\frac{\Delta E_{class}}{E_{kin}} = 0.9 \cdot 10^3 \frac{\Delta_b}{10^5} \frac{N_{eff}}{100} \frac{m_{Pl}}{M} . \tag{4.74}$$

One should remember however that this energy loss comes from the PBHs scattering with rather large impact parameter $b > b_{min}$. For smaller b, when the simple approximation used in this work is inapplicable, the energy loss might be much larger. Moreover,

according to Equation 4.9, Equation 4.15 and Equation 4.20 the density amplification factor Δ_b may be much larger than 10^5:

$$\Delta_b(\tau_{BH}) = 10^4\,\Delta(t_1)\,\Delta_{in}^3\Omega_p^4\left(\frac{100}{N_{eff}}\right)^2\left(\frac{M}{m_{Pl}}\right)^4, \tag{4.75}$$

where we may expect e.g. that $\Delta(t_1) \sim 10^5$, $\Delta_{in} \sim 10^{-4}$, and $\Omega_p \sim 10^{-6}$.

PBHs in the high density clouds could also loose their energy by dynamical friction, see e.g. book [88]. A particle moving in the cloud of other particles would transfer its energy to these particles due to their gravitational interaction. However, one should keep in mind that the energy redistribution in the case of dynamical friction is essentially different from the energy loss due to gravitational radiation. In the latter case the energy leaks out of the system cooling it down, while dynamical friction does not change the total energy of the cluster. Nevertheless a particular pair of black holes moving toward each other with acceleration may transmit their energy to the rest of the system and became gravitationally captured forming a binary.

For an order of magnitude estimate we will use the Chandrasekhar's formula which is valid for a heavy particle moving in the gas of lighter particles having the Maxwellian velocity distribution with dispersion σ. The deceleration of a BH moving at velocity v_{BH} with respect to the rest frame of the gas is given by

$$\frac{d}{dt}\vec{v}_{BH} = -4\pi\,G_N^2\,M_{BH}\,\rho_b\,\ln\Lambda\,\frac{\vec{v}_{BH}}{v_{BH}^3}\left[erf(X) - \frac{2X\exp(-X^2)}{\sqrt{\pi}}\right], \tag{4.76}$$

where $X \equiv v_{BH}/(\sqrt{2}\sigma)$, erf is the error function, ρ_b is the density of the background particles, and $\ln\Lambda \approx \ln(M_*/M_{BH})$ is the Coulomb logarithm, which is defined as in [88]:

$$\ln\Lambda = \ln\frac{b_{max}m_{Pl}^2\,\sigma^2}{M_{BH}+m}.$$

Here b_{max} is the maximum impact parameter, σ^2 is the mean square velocity of the gas and m is the mass of particles in the gas. Numerical simulations show that b_{max} can be assumed to be of the order the radius of the cloud, R_b, which is given by equation Equation 4.21. Since $\sigma^2 \sim M_b/(m_{Pl}^2 R_b)$, a reasonable estimate of Λ is M_b/M_{BH}.

Equation 4.76 was solved in [89] in two limits $v > \sigma$ and $v < \sigma$. In both cases the characteristic dynamical friction time was of the order of:

$$\tau_{DF} = \frac{\sigma^3 m_{Pl}^4}{4\pi\,M_{BH}\rho_b\ln\Lambda} \approx \left(\frac{\sigma}{0.1}\right)^3\left[\frac{25}{\ln(10^{-6}/\Omega_p)}\right]\left(\frac{100}{N_{eff}}\right)\left(\frac{M}{1\,\mathrm{g}}\right)\left(\frac{10^6}{\Delta}\right)\tau_{BH}, \tag{4.77}$$

For PBH masses below a few grams dynamical friction would be an efficient mechanism of PBH cooling leading to frequent binary formation. Moreover, dynamical friction could result in the collapse of small PBHs into much larger BH with the mass of the order of M_b, Equation 4.18. This process would be accompanied by a burst of GW emission.

4.6 Gravitational waves from PBH binaries

Binary systems of PBH could be formed with non-negligible probability in the high density clusters. As we have seen in the previous section, PBHs could loose their energy due to emission of gravitational waves and due to dynamical friction [88]. As a result they would be mutually captured. Determination of the capture probability is a complicated task, which could probably be solved by numerical simulation. Since it is outside of the scope of the present work, we simply assume that the mass or number fraction of PBH binaries in the high density bunches of PBH is equal to ϵ, where ϵ is a dimensionless parameter which is hopefully not too small in comparison with unity.

Gravitationally bound systems of two massive bodies in circular orbit are known to emit gravitational waves with stationary rate and fixed frequency which is twice the rotation frequency of the orbit. In this approximation orbital frequency, ω_{orb}, and orbit radius, R, are fixed. Luminosity of GW radiation from a single binary in the stationary approximation is well known, see e.g. book [17]:

$$L_s \equiv \dot{E} = \frac{32 M_1^2 M_2^2 (M_1 + M_2)}{5 R^5 m_{Pl}^8} = \frac{32}{5} m_{Pl}^2 \left(\frac{M_c \, \omega_{orb}}{m_{Pl}^2} \right)^{10/3} , \tag{4.78}$$

where M_1, M_2 are the masses of two bodies in the binary system and M_c is the chirp mass which is defined as

$$M_c = \frac{(M_1 \, M_2)^{3/5}}{(M_1 + M_2)^{1/5}} \tag{4.79}$$

and

$$\omega_{orb}^2 = \frac{M_1 + M_2}{m_{Pl}^2 R^3} . \tag{4.80}$$

In the case of elliptic orbit with large semi-axis a and eccentricity e the luminosity is somewhat larger (if $R = a$):

$$L_e = \frac{32 M_1^2 M_2^2 (M_1 + M_2)}{5 a^5 m_{Pl}^8 \, (1 - e^2)^{7/2}} \left(1 + \frac{73 e^2}{24} + \frac{37 e^4}{96} \right) . \tag{4.81}$$

The emission of GWs costs energy which is provided by the sum of the kinetic and potential energy of the system. To compensate the energy loss the radius of the binary system decreases and the frequency rises making the stationary approximation invalid. As a result the system goes into the so called inspiral regime. Ultimately the two rotating bodies coalesce and produce a burst of gravitational waves. To reach this stage the characteristic time of the coalescence should be shorter than the life-time of the system. In our case it is the life-time of PBH with respect to the evaporation.

In the inspiral regime the initially circular orbit may remain approximately circular if radial velocity of the orbit, $\dot{R}$, is much smaller than the tangential velocity, $\omega_{orb} R$. This regime is called quasi-circular motion and is valid as long as (see e.g. book [18]):

$$\dot{\omega}_{orb} \ll \omega_{orb}^2 . \tag{4.82}$$

Equation 4.82 can be translated into the lower bound on the radius of the orbit:

$$R \gg r_g^{(eff)} = \frac{M_1 + M_2}{m_{Pl}^2}, \tag{4.83}$$

which is the condition of the validity of the Newtonian approximation. It was shown by Peters [90] that the orbits with initial $e_0 = 0$ would remain quasi-circular as far as condition Equation 4.82 is fulfilled, while for the orbits with $e_0 \neq 0$ the eccentricity rapidly approaches zero due to back reaction of the gravitational radiation.

Most probably binaries are formed in elliptic orbits with high eccentricity. However in the calculation of the GW emission by binaries we assume for simplicity that all orbits are circular. The result would be a lower bound on GW emission, hopefully not too far from the real case.

In what follows we will consider both stationary and inspiral regimes since they both might be realized for different values of the parameters. We will use the instant decay approximation, when the PBH mass is supposed to be constant till $t = \tau_{BH}$ and then BH would instantly disappear. The case of the realistic decrease of PBH mass will be considered elsewhere.

The stationary orbit approximation is valid if time of coalescence, τ_{co}, is much larger than the BH life-time, $\tau_{co} > \tau_{BH}$. The former can be found as follows (see e.g. book [17]). According to the virial theorem the total (kinetic plus potential) energy of the system is $E = -M_1 M_2/(2Rm_{Pl}^2)$. Since luminosity, Equation 4.78 is $L_s = -dE/dt$, the radius varies with time according to

$$\dot{R} = -\frac{64 M_1 M_2 (M_1 + M_2)}{5 R^3 m_{Pl}^6}. \tag{4.84}$$

Correspondingly

$$R(t) = R_0 \left(\frac{t_0 + \tau_{co} - t}{\tau_{co}} \right)^{1/4}, \tag{4.85}$$

where R_0 is the initial value of the radius, t_0 is the initial time, and the coalescence time is given by:

$$\tau_{co} = \frac{5 R_0^4 m_{Pl}^6}{256 M_1 M_2 (M_1 + M_2)}. \tag{4.86}$$

The condition $\tau_{co} > \tau_{BH}$ can be translated into the lower bound on R (for $M_1 = M_2$):

$$R > R_{min} = 4.6 \cdot 10^5 \left(\frac{100}{N_{eff}} \right)^{1/4} \left(\frac{M}{10^5\,\mathrm{g}} \right)^{1/2} r_g. \tag{4.87}$$

Keeping in mind that the frequency of GWs emitted at circular motion of the binary is twice the orbital frequency, $f_s = \omega_{orb}/\pi$ we find from Equation 4.80 that lower bound, Equation 4.87 leads to the following upper bound on the GW frequency:

$$f_s < \omega_{max}/\pi \approx 2 \cdot 10^{24}\mathrm{Hz} \left(\frac{N_{eff}}{100} \right)^{3/8} \left(\frac{10^5\,\mathrm{g}}{M} \right)^{7/4}. \tag{4.88}$$

On the other hand, the radius of the binary orbit should be smaller than the average distance between PBHs in the cluster, Equation 4.22 and probably quite close to it. Using Equation 4.22 and Equation 4.87 we find:

$$\frac{R_{min}}{d_b} = 1.3 \cdot 10^{-5} \left(\frac{\Delta_b}{10^5}\right)^{1/3} \left(\frac{\Delta_{in}}{10^{-4}}\right) \left(\frac{\Omega_p}{10^{-6}}\right)^{4/3} \left(\frac{M}{10^5 g}\right)^{1/2}. \tag{4.89}$$

So it seems natural that $R_{min} \ll d_b$ and the PBH binaries should be mostly in the quasi-stationary regime. R_{min} would be equal to d_b roughly speaking for quite large mass fraction of the produced PBHs, $\Omega_p > 10^{-3}$. The condition $R_{min} = d_b$ gives a lower bound on orbital frequency, ω_{orb}:

$$\omega_{orb} > \omega_{min} \approx 9.4 \cdot 10^{17} \mathrm{sec}^{-1} \left(\frac{\Delta_b}{10^5}\right)^{1/2} \left(\frac{\Delta_{in}}{10^{-4}}\right)^{3/2} \left(\frac{\Omega_p}{10^{-6}}\right)^{2} \left(\frac{10^5\,\mathrm{g}}{M}\right). \tag{4.90}$$

During the inspiral phase, for which $\tau_{co} < \tau_{BH}$, we expect that binaries emit GWs in the frequency range:

$$2 \cdot 10^{24} \mathrm{Hz} \left(\frac{N_{eff}}{100}\right)^{3/8} \left(\frac{10^5\,\mathrm{g}}{M}\right)^{7/4} < f < 0.6 \cdot 10^{33} \mathrm{Hz} \left(\frac{10^5\,\mathrm{g}}{M}\right). \tag{4.91}$$

The upper bound corresponds to $\omega \sim 1/r_g$.

The frequency spectrum of the gravitational waves in inspiral but quasi-circular motion can be found in the adiabatic approximation as follows. Since the gravitational waves are emitted in a narrow band near twice the orbital frequency, the spectrum of the luminosity, Equation 4.78, can be approximated as:

$$\mathrm{d}\dot{E} = \frac{32 M_1^2 M_2^2 (M_1 + M_2)}{5 R^5(t) m_{Pl}^8} \delta\left(\omega - 2\omega_{orb}(R)\right) \mathrm{d}\omega \tag{4.92}$$

To find the energy spectrum we have to integrate this expression over time from initial time, $t_{min} = t_0$, to maximum time $t_{max} = min[\tau_{BH} + t_p, \tau_{co} + t_0]$, where t_0 and t_p are respectively the time of the binary formation (it may be different for different binaries but here we neglect this possible spread) and the time of PBH formation (it is different for PBH with different masses). Note that the coalescence time, τ_{co} is also different for binaries with different initial radius R_0.

Using Equation 4.80 and Equation 4.84 and the expression for the differential time $\mathrm{d}t = (\mathrm{d}R/\mathrm{d}t)^{-1}(\mathrm{d}R/\mathrm{d}\omega_{orb})\mathrm{d}\omega_{orb}$, we find:

$$\frac{\mathrm{d}E}{\mathrm{d}\ln\omega} = \frac{2^{1/3}\omega^{2/3}}{3} \frac{M_1 M_2}{m_{Pl}^{4/3}(M_1 + M_2)^{1/3}} \tag{4.93}$$

in agreement with [18] and [91]. This expression is valid for the frequencies in the interval determined by Equation 4.80 with $R_{max} = R_0$ and $R_{min} = R(t_{max})$.

In Equation 4.93 we have not taken in account the redshift which is different for different frequencies and thus this leads to spectrum distortion. According toEquation 4.80 and Equation 4.85, frequency ω is emitted at the time moment:

$$t(\omega) = t_0 + \tau_{co}\left[1 - \left(\frac{\omega_{min}}{\omega}\right)^{8/3}\right], \tag{4.94}$$

where

$$\omega_{min} = 2\left(\frac{M_1 + M_2}{m_{Pl}^2}\right)^{1/2} R_0^{-3/2} \tag{4.95}$$

is the minimal frequency emitted at initial moment $t = t_0$. To the moment of the PBH evaporation the frequency of the GWs emitted at $t = t(\omega)$ is redshifted by the frequency dependent factor:

$$\omega_* = \frac{\omega}{1 + z(\omega)} = \left[\frac{t(\omega)}{t_p + \tau_{BH}}\right]^{2/3} \omega, \tag{4.96}$$

where ω_* is the frequency of GWs at $t = t_p + \tau_{BH}$. This equation implicitly determines ω as a function of ω_*.

The spectrum of the gravitational waves at PBH evaporation can be obtained from Equation 4.93 dividing it by $(1 + z)$ (the redshift of the graviton energy, E) and with substitution $\omega = (z + 1)\omega_*$. Correspondingly

$$\mathrm{d}\omega = \frac{z + 1}{1 - \omega_*(\mathrm{d}z/\mathrm{d}\omega)}\,\mathrm{d}\omega_* \tag{4.97}$$

As a result we find:

$$\frac{\mathrm{d}E_*}{\mathrm{d}\ln\omega_*} = \frac{2^{1/3}\omega_*^{2/3}}{3}\frac{M_1 M_2}{m_{Pl}^{4/3}(M_1 + M_2)^{1/3}}\frac{[1 - \omega_*(\mathrm{d}z/\mathrm{d}\omega)]^{-1}}{(1 + z)^{1/3}}. \tag{4.98}$$

Here $z(\omega)$ should be taken as a function of ω_* according to Equation 4.96 and ω_* varies between ω_{min} and ω_{max} divided by the corresponding red-shift factor. In particular, $\omega_{*(min)} = \omega_{min}[t_0/(t_p + \tau_{BH})]^{2/3}$. Note that R_0 enters explicitly into Equation 4.98), while in Equation 4.93 it enters only through the limits in which ω varies. Because of that the frequency spectrum depends upon the distribution of binaries over their initial radius, R_0. As is shown below, it is especially profound in the case of long coalescence time when the frequency spectrum of a single binary with fixed R is close to delta-function.

In the stationary approximation, when the change of the orbit radius can be neglected, we expect that a single binary emits GWs in a narrow band of frequencies close to twice the orbital frequency. However the distribution of binaries over their initial radius, $\mathrm{d}n_{BIN} = F(R_0)\mathrm{d}R_0$ spreads up the spectrum. Here $\mathrm{d}n_{BIN}$ is the number density of binaries with the radius in the interval $[R_0, R_0 + \mathrm{d}R_0]$. Since in this approximation the

radius is approximately constant we do not distinguish between R and R_0. The cosmological energy density of the gravitational waves emitted per unit time is equal to:

$$\mathrm{d}\dot{\rho}_{GW}^{(stat)} = \frac{2F(R)\,R}{3}\frac{n_{BH}^{c}}{n_{BH}^{b}}\frac{\mathrm{d}\omega}{\omega}L_s\,, \tag{4.99}$$

where n_{BH}^{b} is the number density of PBH in the high density bunch (cluster), n_{BH}^{c} is the average cosmological number density of PBH, $R = R(\omega_{orb})$ according to Equation 4.80, and we used the relation $\mathrm{d}R = -2(R/3)\,(\mathrm{d}\omega/\omega)$. Distribution, $F(R)$, is normalized as:

$$\int \mathrm{d}RF(R) = n_{BIN} = \epsilon n_{BH}^{b}\,. \tag{4.100}$$

We assume for simplicity that $F(R)$ does not depend upon R in some interval $[R_1, R_2]$ and vanishes outside it. So $F(R) = \epsilon n_{BH}^{b}/(R_1 - R_2)$.

A more realistic fit to the PBH distribution over radius could be a Gaussian one:

$$F(R) = \frac{1}{\sqrt{2\pi}\,\sigma}\epsilon n_{BH}\exp\left[-(R-\langle R\rangle)^2/2\sigma^2\right]\,, \tag{4.101}$$

where σ is the mean-square deviation of R from the average value $\langle R\rangle$.

The small factor n_{BH}^{c}/n_{BH}^{b} enters Equation 4.99 because we are interested in the cosmological energy density of GWs averaged over the whole universe volume. The cosmological number density of PBH is expressed through their energy density as $n_{BH} = \rho_{BH}/M = \rho_c(t)/M$. The number density of binaries in the cluster is parametrized according to:

$$n_{BIN}(t) = \epsilon(t)\,n_{BH}^{b}(t) = \epsilon(t)\,\rho_c(t)\Delta(t)/M\,, \tag{4.102}$$

where, we remind, $\rho_c(t)$ is the total cosmological energy density and $\Delta(t) = \rho_b/\rho_c \gg 1$ is the density contrast of the cluster. The time dependence of n_{BH}^{b} disappears when the cluster reaches the stationary state, see discussion in section 4.1, and $\Delta(t)$ evolves according to Equation 4.20. When the stationary orbit approximation is valid, ϵ remains constant.

Collecting all the factors and integrating Equation 4.99 over time with an account of the frequency redshift, $\omega = \omega_*(1+z)$ and the total redshift of the energy density of GWs, $\rho_{GW}(t_*) = \rho_{GW}(t)/(1+z)^4$, we find:

$$\mathrm{d}\rho_{GW}^{(stat)}(\omega_*) = \frac{2^{7/3}}{5}\left[\frac{n_{BH}^{c}(\tau_{BH})}{n_{BH}^{b}}\right]\frac{(M_1^2M_2^2)(\tau_{BH}+t_p)}{(M_1+M_2)^{1/3}m_{Pl}^{16/3}}F(R)\omega_*^{5/3}\mathrm{d}\omega_*\int_{x_{min}}^{1}x^{11/6}\mathrm{d}x,$$

where $x = a(t)/a(t_*) = 1/(1+z)$, $x_{min} = a(t_0)/a(t_*)$, t_0 is the time moment of binary formation and we make use of equation Equation 5.49. Dividing this result by the critical energy density just before PBHs complete evaporation, $n_{BH}(\tau_{BH}) \approx \rho_c(\tau_{BH})/M$, we find the cosmological fraction of the energy density of GWs at $t = \tau_{BH}$ per logarithmic

interval of frequency $f = \omega/(2\pi)$ (below we assume that all BHs have equal masses, M):

$$\Omega_{GW}^{(stat)}(f_*;\tau_{BH}) = \frac{3\cdot 2^{17/3}}{85}\,\frac{\epsilon\cdot(t_p+\tau_{BH})}{R_1-R_2}\left(\frac{\pi f_* M}{m_{Pl}^2}\right)^{8/3}[1-x_{min}^{17/6}] \qquad (4.103)$$

where for the sake of a simple estimate we assumed that $F(R) = const$. We assume also that all the binaries are formed at the same time, $t_0 \ll \tau_{BH}$ and so $x_{min} \ll 1$. Note that the frequency of GWs coming from the binaries with radii between R_1 and R_2 is confined according to Equation 4.80.

To make an order of magnitude estimate of the fraction of the energy density of GWs at the moment of PBH evaporation we take $(R_1-R_2) \sim R_1 \sim R(\omega)$, where $R(\omega)$ is determined by equation Equation 4.80 and take into account that the stationary approximation is valid if the radii of the binaries are bounded from below by Equation 4.87. Hence, if the stationary regime is realized, the spectral density parameter today would be:

$$h_0^2\Omega_{GW}^{(stat)}(f;t_0) \approx 10^{-8}\epsilon\left[\frac{N_{eff}}{100}\right]^{2/3}\left[\frac{100}{g_S(T(\tau_{BH}))}\right]^{1/18}\left[\frac{M}{10^5\,\mathrm{g}}\right]^{1/3}\left[\frac{f}{\mathrm{GHz}}\right]^{10/3} \qquad (4.104)$$

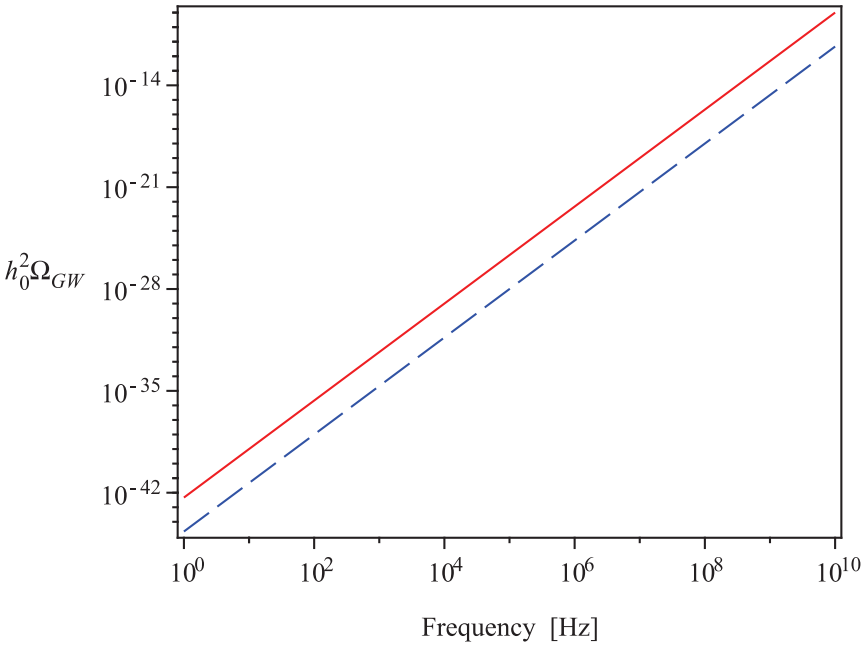

Figure 4.2: Log-log plot of density parameter today $h_0^2\Omega_{GW}$ as a function of expected frequency today for PBHs binaries in the stationary approximation for $\beta \sim 1$, $\epsilon \sim 10^{-5}$, $N_{eff} \sim 100$, $g_S \sim 100$, PBH mass $M \sim 10^7$ g (solid line) and $M \sim 1$ g (dashed line).

The expected range of the present day frequencies of the GWs from the binaries in the stationary approximation is given by Equation 4.90 and Equation 4.88. The emitted

frequency is determined by the binary radius, so a single binary emits GWs with a very narrow spectrum. However, the distribution of binaries over their radius could lead to a significant spread of the spectrum. In principle the frequencies emitted may have any value in the specified above range. The minimal present day frequency of such GWs today can be found by plugging Equation 4.90 into Equation 4.31:

$$f \geqslant 4.3\,\mathrm{Hz}\,\beta\left(\frac{10^5\,\mathrm{g}}{M}\right)^{1/2}, \tag{4.105}$$

where β is given by

$$\beta = \left(\frac{\Delta_b}{10^5}\right)^{1/2}\left(\frac{\Delta_{in}}{10^{-4}}\right)^{3/2}\left(\frac{\Omega_p}{10^{-6}}\right)^{2}\left(\frac{100}{g_S(T(\tau_{BH}))}\right)^{1/12}\left(\frac{100}{N_{eff}}\right)^{1/2}. \tag{4.106}$$

For binaries formed with $R > R_{min}$, see Equation 4.31, Equation 4.87 and Equation 4.88, the frequency of emitted GWs today is bounded from above by:

$$f \leqslant 5.7\cdot 10^7\,\mathrm{Hz}\left(\frac{100}{g_S(T(\tau_{BH}))}\right)^{1/12}\left(\frac{100}{N_{eff}}\right)^{1/8}\left(\frac{10^5\,\mathrm{g}}{M}\right)^{1/4}. \tag{4.107}$$

Let us estimate now the energy density of GWs in the inspiral case, when $\tau_{co} < \tau_{BH}$ and the GW emission from a single binary proceeds in a wide range of frequencies due to shrinking of the binary radius. The radiation frequency spans from $f_{s,min}$, which is the GW frequency at the initial PBH separation, to $f_{s,max}$ which corresponds to GWs emitted at $R \sim r_g$. The energy spectrum of GWs is given by Equation 4.93 where, in what follows, we change to cyclic frequency, $f = \omega/2\pi$.

After the cluster evolution was over, the number density of PBHs in high density clusters remained approximately constant till the PBH evaporation, but in the inspiral phase the fraction of binaries, $\epsilon(t)$, decreased due to their coalescence. So the tail of the distribution function at small initial R_0 is eaten up, and the average value of R drops down. In distribution function, $F(R_0)$, we have to substitute instead R_0 its expression through R and time according to

$$R_0 \to \left[R^4 + \left(\frac{256 M_1 M_2 (M_1+M_2)}{5 m_{Pl}^6}\right)(t-t_0)\right]^{1/4} \tag{4.108}$$

with the corresponding change of $R_0^3 \mathrm{d}R_0 \to R^3 \mathrm{d}R$.

To calculate the cosmological energy fraction of GWs at the PBH evaporation moment we can proceed along the same lines as we have done deriving Equation 4.98 introducing additional factor $F(R_0)\mathrm{d}R_0$ which depends upon time according to Equation 4.108. However, at the level of calculations in the present model with many unknown parameters it can be sufficient to neglect such subtleties and to use a simplified estimate:

$$\frac{\mathrm{d}\rho_{GW}}{\mathrm{d}(\log f_s)} = \epsilon_{co} n^c_{BH}(t)\frac{\mathrm{d}E_{GW}}{\mathrm{d}(\log f_s)}, \tag{4.109}$$

where ϵ_{co} is the fraction of binaries with coalescence time shorter or equal to PBH lifetime. For an estimate by an order of magnitude we assume also that the number of binaries is independent on the redshift. To some extend the decrease of the binary number may be compensated by their continuous formation. We neglect possible difference of binary masses and take $M_1 = M_2$. We approximately take the redshift into account from the moment of the coalescence to the PBH decay, $(z_{co}+1) \approx (\tau_{BH}/\tau_{co})^{2/3}$. This corresponds to the assumption that the binaries radiated all GWs only at the moment of τ_{co}. So the $f_* = f(1+z_{co})$. Thus we obtain as an order of magnitude estimate:

$$\Omega_{GW}(f_*, \tau_{BH}) = \frac{\epsilon_{co}}{3}\left(\frac{\pi f_* M}{m_{Pl}^2}\right)^{2/3}(z_{co}+1)^{-1/3}\,. \tag{4.110}$$

Using Equation 4.31 and Equation 4.53, we find that the energy density parameter of gravitational waves today is equal to:

$$h_0^2\Omega_{GW}(f) \approx 5\cdot 10^{-9}\epsilon_{co}\left(\frac{100}{g_S(T(\tau_{BH}))}\right)^{5/18}\left(\frac{N_{eff}}{100}\right)^{1/3}\left(\frac{f}{10^{12}\mathrm{Hz}}\right)^{2/3}\left(\frac{10^5\,\mathrm{g}}{M}\right)^{1/3}, \tag{4.111}$$

where we neglected possibly weak redshift dilution of GWs by the factor $(\tau_{co}/\tau_{BH})^{2/9}$.

If the system goes to the inspiral phase, then according to equation Equation 4.91 we would expect today a continuous spectrum in the range from $f_{min} \sim 0.9\cdot 10^7$ Hz to $f_{max} \sim 3\cdot 10^{14}$ Hz. However if we take into account the redshift of the early formed binaries from the moment of their formation to the PBH decay, the lower value of the frequency may move to about 1 Hz.

4.7 Gravitons from PBH evaporation

In the previous sections we have considered only gravitational waves emitted through mutual acceleration of PBHs in the high density clusters. On the other hand PBHs could directly produce gravitons by evaporation. This process in connection with creation of cosmological background of relic GWs was considered in [61] and later in [92]. In the last reference a possible clumping of PBHs at the matter dominated stage was also considered. Though such clumping does not influence the probability of the GW emission by PBHs, it may change the mass spectrum of PBHs due to their merging.

The PBHs reduce their mass according to the equation:

$$M(t) = M_0\left(1-\frac{t-t_p}{\tau_{BH}}\right)^{1/3}, \tag{4.112}$$

where M_0 is the initial mass of an evaporating BH and t_p is the time of BH production after Big Bang. Equation 4.112 shows that the BH mass can be approximately considered as constant till the moment of the evaporation and may be approximated as $\theta(t-t_p-\tau_{BH})$. Due to evaporation a BH emits all kind of particles with masses $m < T_{BH}$

and, in particular, gravitons. The total energy emitted by BH per unit time and frequency ω (energy) of the emitted particles, is approximately given by the equation (see, e. g. book [93]):

$$\left(\frac{\mathrm{d}E}{\mathrm{d}t\mathrm{d}\omega}\right) = \frac{2N_{eff}}{\pi}\frac{M^2}{m_{Pl}^4}\frac{\omega^3}{e^{\omega/T_{BH}}-1}\,, \tag{4.113}$$

where T is the BH temperature Equation 4.2. Due to the impact of the gravitational field of BH on the propagation of the evaporated particles, their spectrum is distorted [63] by the so called grey factor $g(\omega)$, but we disregard it in what follows.

Let us now estimate the amount of the gravitational radiation from the graviton evaporation. After their production PBHs started to emit thermal gravitons independently on the PBH clustering. Hence the thermal graviton emission depends only on PBH number density, n_{BH}. The energy density of gravitons in logarithmic frequency band emitted in the time interval t and $t + \mathrm{d}t$ is

$$\frac{\mathrm{d}\rho_{GW}(\omega;t)}{\mathrm{d}\omega} = 10^{-2} n_{BH}(t)\left(\frac{\mathrm{d}E}{\mathrm{d}t\,d\omega}\right)\mathrm{d}t\,, \tag{4.114}$$

where factor 10^{-2} takes into account that about one percent of the emitted energy goes into gravitons. The density parameter of GWs per logarithmic frequency interval at cosmological time $t_* = \tau_{BH}$ can be obtained by integrating Equation 4.114 over redshift with an account of the drop-off of the graviton energy density by $(1+z)^{-4}$ and the redshift of the emitted frequency so that at $t_* = \tau_{BH}$: $\omega = \omega_*(1+z)$. Note that in the instant decay approximation the BH temperature remains constant. One has also to take into account that the number density of PBH behaves as $n_{BH}(t) = n_p(t_p)(1+z)^3$, so if we normalize our result to $n_{BH}(\tau_{BH})$, the integrand should be multiplied by $(1+z)^3$. Finally we obtain:

$$\frac{\mathrm{d}\rho_{GW}(\omega_*,\tau_{BH})}{\mathrm{d}\ln\omega_*} = \frac{0.03N_{eff}M\omega_*^4}{\pi m_{Pl}^4}(3\tau_{BH})\,\rho_{BH}(\tau_{BH})\,I\left(\frac{\omega_*}{T_{BH}}\right)\,, \tag{4.115}$$

where

$$I\left(\frac{\omega_*}{T_{BH}}\right) \equiv \int_0^{z_{max}} \frac{\mathrm{d}z\,(1+z)^{1/2}}{\exp\left[(z+1)\omega_*/T_{BH}\right]-1}\,, \tag{4.116}$$

and

$$1+z_{max} = \left(\frac{\tau_{BH}}{t_{eq}}\right)^{2/3}\left(\frac{t_{eq}}{t_p}\right)^{1/2} = \left(\frac{32170}{N_{eff}}\right)^{2/3}\left(\frac{M}{m_{Pl}}\right)^{4/3}\Omega_p^{1/3}\,, \tag{4.117}$$

where the effective time of integration is equal to $3\tau_{BH}$ because of the instant decay approximation. One can check that in this case the total evaporated energy would be equal to the PBH mass.

The spectral density parameter of GWs at $t = \tau_{BH}$ is equal to:

$$\Omega_{GW}(\omega_*;\tau_{BH}) \approx \frac{2.9\cdot 10^3 M^4\omega_*^4}{\pi\, m_{Pl}^8}\,I\left(\frac{\omega_*}{T_{BH}}\right)\,. \tag{4.118}$$

The spectrum is not a thermal one, though rather similar to it. It has more power at small frequencies due to redshift of higher frequencies into lower band and less power at high ω_*. The spectral density parameter reaches maximum at $\omega_*^{peak}/T_{BH} = 2.8$. Accordingly the maximum value of the spectral density parameter when PBHs completely evaporated is equal to:

$$\Omega_{GW}^{peak}(\omega_*^{peak}; \tau_{BH}) \approx 3.8 \cdot 10^{-3} \,. \tag{4.119}$$

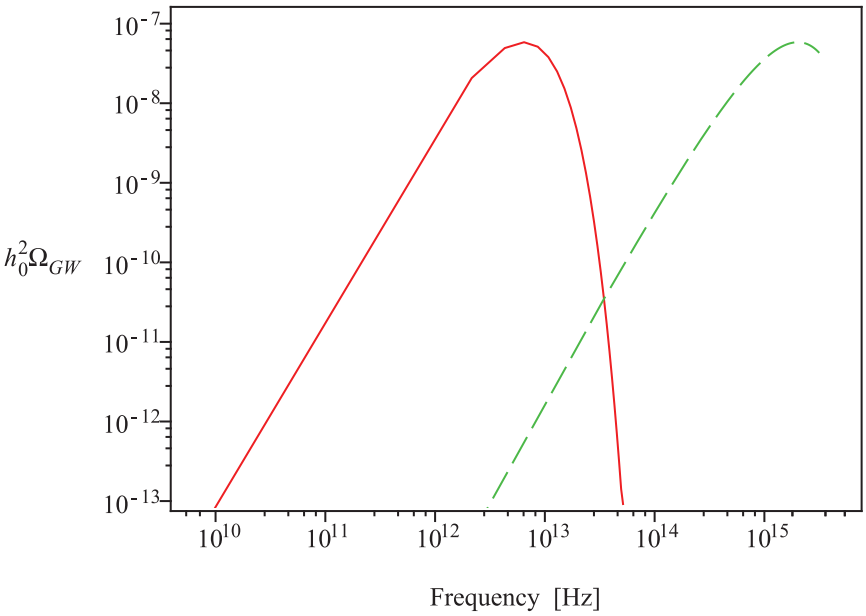

Figure 4.3: Log-log plot of the density parameter per logarithmic frequency, $h_0^2\Omega_{GW}(f;t_0)$, as a function of frequency today, f, for the case $g_S \sim 100$, $N_{eff} \sim 100$, black hole mass $M = 1$ g (solid line) and black hole mass $M = 10^5$ g (dashed line). We can see that the spectrum has a maximum which is sharp and of order $h_0^2\Omega_{GW}(f_{peak}) \sim 10^{-7}$.

Integrating Equation 4.118 first over ω_* and then over redshift, we find that the total fraction of energy of GWs is 0.006 which is reasonably (in view of the used approximations) close to the expected 0.01. At BBN the energy fraction of such GWs would be about 0.005. So the total number of additional effective neutrino species would be close to 0.045, where 0.03 comes from neutrino heating by e^+e^- annihilation and 0.01 comes from the plasma corrections (see e.g. review [94]). Of course the GWs produced by the considered mechanism are safely below the BBN bound [60]. Using Equation 4.53 and taking into account the redshift from $t = \tau_{BH}$ to the present time, we find that the total density parameter of GWs today due to PBH evaporation would be about 10^{-7}.

The total energy density of GWs from the PBH evaporation is quite large but it is concentrated at high frequencies. According to Equation 4.31 the redshifted peak

frequency emitted at time $t_* = \tau_{BH}$ becomes today:

$$f^{(peak)} = 2 \cdot 10^{15}\,\text{Hz} \left(\frac{g_S(T(\tau_{BH}))}{100}\right)^{1/12} \left(\frac{100}{N_{eff}}\right)^{1/2} \left(\frac{M}{10^5\,\text{g}}\right)^{1/2}. \quad (4.120)$$

The energy density of GWs at small f drops down in accordance with Equation 4.119. The spectral density today can be calculated from Equation 4.118 with an account of the redshift to the present day:

$$h_0^2 \Omega_{GW}(f; t_0) = 1.36 \cdot 10^{-27} \left(\frac{N_{eff}}{100}\right)^2 \left(\frac{10^5\,\text{g}}{M}\right)^2 \left(\frac{f}{10^{10}\,\text{Hz}}\right)^4 \cdot I\left(\frac{2\pi \cdot f}{T_0}\right), \quad (4.121)$$

where we used $\omega = 2\pi f$ and T_0 is the BH temperature redshifted to the present time:

$$T_0 = \left[\frac{a(\tau_{BH})}{a(t_0)}\right] T_{BH} = 4.53 \cdot 10^{15}\,\text{Hz} \left(\frac{100}{g_S(T(\tau_{BH}))}\right)^{1/12} \left(\frac{100}{N_{eff}}\right)^{1/2} \left(\frac{M}{10^5\,\text{g}}\right)^{1/2}. \quad (4.122)$$

Chapter 5

Mixing of gravitons with photons in the post recombination epoch

In chapter 4 we discussed some GW production mechanisms by PBH. These different mechanisms produce a spectrum which extends from few Hz up to 10^{18} Hz creating a rather substantial background of GWs of high density parameter $\Omega_{\rm gw}$. The lover part of the spectrum ($\sim$ 1 Hz) is potentially detectable by the future space interferometers DECIGO/BBO, see subsection 2.4.2. However, the high frequency part of the spectrum (BH evaporation) is not covered by any present day interferometer but different prototypes of high frequency GW detectors are under construction (at very initial stage), which in the future may reach an adequate sensitivity at these high frequencies.

In this chapter we discuss an alternative way on detecting the high frequency part of the spectrum which does not look very difficult due to the process of GW transformation into photons in external magnetic field. In pioneering paper [95] the inverse process of photon to graviton transformation in magnetic field was studied. It followed by several works dedicated to graviton to photon transition [96, 97, 98, 99, 100]. Below we calculate the probability of GWs transformation into electromagnetic radiation in the primordial magnetic field after the hydrogen recombination and argue that the registration of this radiation might be feasible. The calculations presented in the following sections regarding the intensity of the electromagnetic radiation closely follow those described in [101].

This chapter is organized as follows. In section 5.1 we derive equations of motions for the graviton-photon system in static magnetic field in the case when the graviton wavelength is smaller than the magnetic field coherence length. In section 5.2 we derive the mixing probability for graviton to photon oscillation using the wave function approximation. The oscillation probability is analogous to oscillation between neutrinos with different flavors. In section 5.3 we calculate oscillation probability at a qualitative level using the wave function approximation at various stages during the cosmological

history, namely at recombination and the contemporary epoch. In section 5.4 we do the same thing as in section 5.3, using the density matrix approach in order to take into account coherence breaking due to scattering of photons in plasma. In section 5.5 we discuss observable effects of graviton to photon conversion at the present time and in section 5.6 we discuss the graviton to photon oscillation in the resonant case.

5.1 Equations of motions of the graviton-photon system

The total action describing gravitational and electromagnetic fields is given by the sum of two terms:

$$\mathcal{S} = \mathcal{S}_g + \mathcal{S}_{em}, \tag{5.1}$$

where $\mathcal{S}_g$ is the usual Einstein-Hilbert action equal to:

$$\mathcal{S}_g = \frac{1}{\kappa^2}\int \mathrm{d}^4x\,\sqrt{-g}R \tag{5.2}$$

and $\mathcal{S}_{em}$ is the action of the electromagnetic field minimally coupled to gravity:

$$\mathcal{S}_m = -\frac{1}{4}\int \mathrm{d}^4x\,\sqrt{-g}\,g^{\mu\rho}g^{\nu\sigma}F_{\mu\nu}F_{\rho\sigma} + \frac{\alpha^2}{90m_e^4}\int \mathrm{d}^4x\,\sqrt{-g}\,[(F_{\mu\nu}F^{\mu\nu})^2 + \frac{7}{4}(\tilde{F}_{\mu\nu}F^{\mu\nu})^2]\,. \tag{5.3}$$

The first term above is the Maxwell action and the second quartic one is the Heisenberg-Euler contribution [102, 103] originating from the electron box diagram. This term describes nonlinear corrections to the classical electrodynamics in the limit of low photon frequencies, $\omega \ll m_e$. As we will see below the second term gives the photon an effective refraction index in vacuum with external magnetic field. Using this expression for the action confines the validity of the results presented here to sufficiently low frequencies. However, they can be easily generalized to higher ω.

The essential quantities are defined as follows: $\kappa \equiv \sqrt{16\pi G}$, $G \equiv 1/m_{Pl}^2$ is the Newton constant, $m_{Pl} = 1.2\cdot 10^{19}$ GeV* , $\alpha = e^2/(4\pi)$ is the fine structure constant and m_e is the electron mass. $F_{\mu\nu}$ is the electromagnetic field strength tensor and $\tilde{F}_{\mu\nu} \equiv (1/2)\epsilon_{\mu\nu\rho\sigma}F^{\rho\sigma}$ is its dual. The metric tensor of a weak gravitational wave propagating in flat space-time can be written as follows:

$$g_{\mu\nu} = \eta_{\mu\nu} + \kappa h_{\mu\nu}(\mathbf{x}, t), \tag{5.4}$$

where $\eta_{\mu\nu}$ is the flat Minkowski metric tensor and $h_{\mu\nu}$ are small perturbation around flat space-time, $|h_{\mu\nu}| \ll 1$. Considering terms up to the second order in $h_{\mu\nu}$ we rewrite gravitational action Equation 5.2 as

$$\mathcal{S}_g = -\frac{1}{4}\int \mathrm{d}^4x\,[\partial_\mu h_{\alpha\beta}\partial^\mu h^{\alpha\beta} - \partial_\mu h\partial^\mu h + 2\partial_\mu h^{\mu\nu}\partial_\nu h - 2\partial_\mu h^{\mu\nu}\partial_\rho h^\rho_\nu] \tag{5.5}$$

*In the literature another notation is often used, namely, $\kappa = 8\pi G$.

and electromagnetic part Equation 5.3 becomes:

$$\mathcal{S}_{em} = -\frac{1}{4}\int \mathrm{d}^4x\, F_{\mu\nu}F^{\mu\nu} + \frac{\kappa}{2}\int \mathrm{d}^4x\, h_{\mu\nu}T^{\mu\nu} + \frac{\alpha^2}{90m_e^4}\int \mathrm{d}^4x\,[(F_{\mu\nu}F^{\mu\nu})^2 + \frac{7}{4}(\tilde{F}_{\mu\nu}F^{\mu\nu})^2], \tag{5.6}$$

where $T_{\mu\nu}$ is the electromagnetic energy-momentum tensor, $T^{\rm em}_{\mu\nu} = F_{\mu\rho}F^{\rho}_{\nu} - \eta_{\mu\nu}F_{\alpha\beta}F^{\alpha\beta}/4$. Total Lagrangian density Equation 5.1 is given by the sum of linearized actions Equation 5.5 and Equation 5.6.

The Euler-Lagrange equation of motion for fields $h_{\mu\nu}$ and A_μ are obtained by taking the variation of the total action with respect to these fields with usually imposed the Traceless Transverse (TT) gauge condition: $h_{0\mu} = 0, \partial_j h_{ij} = 0, h^i_i = 0$. The equations of motions determined by $S_g + S_{em}$ are the coupled Einstein-Maxwell equations of motion:

$$\Box h_{\mu\nu} = -\kappa T^{\rm em}_{\mu\nu}\,, \tag{5.7}$$

$$\partial_\mu\left(F^{\mu\nu} - \frac{\alpha^2}{45m_e^4}[4F^2F^{\mu\nu} + 7(F\cdot\tilde{F})\tilde{F}^{\mu\nu}]\right) = \kappa\partial_\mu[h^{\mu\beta}F^{\nu}_{\beta} - h^{\nu\beta}F^{\mu}_{\beta}]\,, \tag{5.8}$$

where we made use of the fact that the electromagnetic field tensor is traceless and defined $F^2 \equiv F_{\mu\nu}F^{\mu\nu}$ and $\tilde{F}F \equiv \tilde{F}_{\mu\nu}F^{\mu\nu}$, the indices here are raised by flat metric tensor $\eta_{\mu\nu}$.

In Equation 5.8 the electromagnetic field tensor, $F_{\mu\nu}$, is the sum of the free field (incident wave) tensor $f_{\mu\nu}$ and the static external field tensor $F^{(e)}_{\mu\nu}$, $F_{\mu\nu} = F^{(e)}_{\mu\nu} + f_{\mu\nu}$, where $|F^{(e)}_{\mu\nu}| \gg |f_{\mu\nu}|$. At this point one can see that the second and the third terms (the Heisenberg-Euler ones) in Equation 5.8 modify the usual vacuum Maxwell equations creating refraction indexes in external magnetic field, which give rise to birefringence effects [104, 105]. For the transverse and parallel modes these indexes are equal to

$$\begin{aligned} n_1^2 - 1 &= 4\rho B_e^2\sin^2\phi\,, \qquad \text{transverse mode}\,, \\ n_2^2 - 1 &= 7\rho B_e^2\sin^2\phi\,, \qquad \text{parallel mode}, \end{aligned} \tag{5.9}$$

where B_e is the strength of the external magnetic field, e is the electron charge, ϕ is the angle between the incident wave and the direction of the external magnetic field $\mathbf{B}_e$, and ρ is defined as,

$$\rho = (\alpha/45\pi)(e/m_e^2)^2. \tag{5.10}$$

Deviation of the refraction index from unity destroy equality of the photon momentum, k, and frequency, ω, and gives rise to effective photon mass, $m_\gamma^2 = \omega^2 - k^2 \neq 0$, as one can see from the solution of the homogeneous part of Equation 5.8.

Since we are working in the TT gauge the spatial parts of Equation 5.7 and Equation 5.8 describing propagating waves now read

$$\Box h_{ij} = -\kappa T^{\rm em}_{ij}\,, \tag{5.11}$$

$$\left[\Box - m_\gamma^2\right]A^j = \kappa\partial_i[h^{ik}F^{(e)j}_{k} - h^{jk}F^{(e)i}_{k}]\,, \tag{5.12}$$

where in the r.h.s. of Equation 5.11 we took into account only terms which are bilinear in $F_{\mu\nu}$ and $f_{\mu\nu}$, see below Equation 5.14.

Let us consider now plane gravitational wave propagating through a region with magnetic field vector $\mathbf{B}_e$ assuming the latter to be homogeneous at the scale of the gravitational wave length. We expand as usually the gravitational wave tensor in its Fourier components:

$$h_{ij}(\mathbf{x},t) = \sum_{\lambda=\times,+} h_\lambda(\mathbf{x}) \mathrm{e}^{\lambda}_{ij} e^{-i\omega t}, \tag{5.13}$$

where λ denotes the GW polarization index and e_{ij} is the gravitational wave polarization tensor, Equation 1.29. The energy-momentum tensor of the electromagnetic wave generated in the process of the graviton-photon transformation is given by:

$$T^j_i = E_i E^j_e + B_i B^j_e - \frac{1}{2}\delta^j_i (E^2 + B^2), \tag{5.14}$$

where lower index e refers to the external electromagnetic field.

Let us introduce vector potential, A^j, of the electromagnetic wave:

$$A_j = i \sum_\lambda \mathrm{e}^\lambda_j(\hat{\mathbf{k}}) A_\lambda e^{-i\omega t}, \tag{5.15}$$

where e^λ_j is the photon polarization vector and the magnetic field of the propagating electromagnetic wave is given by $B_k = (\nabla \times A)_k = \epsilon_{ijk}\partial_j A_k$. Now plugging Equation 5.13 and Equation 5.15 into equations Equation 5.11 and Equation 5.12 we obtain the following system of equations:

$$(\omega^2 + \partial^2_{\mathbf{x}}) h_\lambda = -i\kappa \partial_{\mathbf{x}} A_\lambda(\mathbf{x}) B_T\,, \tag{5.16}$$

$$(\omega^2 + \partial^2_{\mathbf{x}}) A_\lambda + (k^2 - \omega^2) A_\lambda = -i\kappa \partial_{\mathbf{x}} h_\lambda(\mathbf{x}) B_T\,, \tag{5.17}$$

where B_T is the strength of the transverse external magnetic field.

The system of Equation 5.16 and Equation 5.17 is not easy to handle but one can simplify the work assuming that the coherence length of the background magnetic field λ_B is much greater than the photon wavelength λ_p: $\lambda_B \gg \lambda_p$. Under this assumption the operator $\omega^2 + \partial^2_{\mathbf{x}}$ can be expanded as $\omega^2 + \partial^2_{\mathbf{x}} = (\omega + i\partial_{\mathbf{x}})(\omega - i\partial_{\mathbf{x}}) \simeq 2\omega(\omega + i\partial_{\mathbf{x}})$ where $(-i\partial_{\mathbf{x}}) = k$ is the momentum operator and we assume that refraction index n slightly differs from unity, $|n-1| \ll 1$, and $\omega + k \simeq 2\omega$ with ω satisfying the general dispersion equation $k = \omega n$. In this case the system of Equation 5.16 and Equation 5.17 becomes

$$(\omega + i\partial_{\mathbf{x}}) h_\lambda \simeq -\frac{\kappa}{2} A_\lambda(\mathbf{x}) B_T\,, \tag{5.18}$$

$$(\omega + i\partial_{\mathbf{x}}) A_\lambda + \omega(n-1) A_\lambda \simeq -\frac{\kappa}{2} h_\lambda(\mathbf{x}) B_T\,, \tag{5.19}$$

where n is the total refraction index. It includes respectively the QED effects due to vacuum polarization, the plasma effects due to refraction of the photon in the medium and birefringence effects such as the Cotton-Mouton effect,

$$n = n_{\mathrm{QED}} + n_{\mathrm{plasma}} + n_{\mathrm{CM}}\,. \tag{5.20}$$

Here the plasma refraction index is given by

$$n_{\text{plasma}} = -\frac{\omega^2_{\text{plasma}}}{2\omega^2}\,, \tag{5.21}$$

where the plasma frequency is as usually $\omega^2_{plasma} = n_e e^2/m$ with $e^2 = 4\pi\alpha$, and n_e is the number density of free electrons.

The refraction indices for two polarizations states of photon, n_1 and n_2, are given by equation (5.9) and in the case of weak magnetic field they can be approximated as

$$\begin{aligned} n_+ &= 1 + \frac{4}{2}\rho B_e^2 \sin^2\phi\,, \qquad \text{transverse mode}\,, \\ n_\times &= 1 + \frac{7}{2}\rho B_e^2 \sin^2\phi\,, \qquad \text{parallel mode,} \end{aligned} \tag{5.22}$$

where $n_1 = n_+$ and $n_\times = n_2$. The Cotton-Mouton effect arises when the photons travel through gas-like medium and as a consequence the difference between the two refraction indices is given by

$$n^+_{\text{CM}} - n^\times_{\text{CM}} = C\lambda_p B_e^2, \tag{5.23}$$

where C is the Cotton-Mouton constant.

The system of equations Equation 5.18 and Equation 5.19 can be written in the matrix form:

$$\left[(\omega + i\partial_{\mathbf{x}}) + \begin{bmatrix} \omega(n-1)_+ & B_T/m_{Pl} & 0 & 0 \\ B_T/m_{Pl} & 0 & 0 & 0 \\ 0 & 0 & \omega(n-1)_\times & B_T/m_{Pl} \\ 0 & 0 & B_T/m_{Pl} & 0 \end{bmatrix}\right] \begin{bmatrix} A_+(\mathbf{x}) \\ h_+(\mathbf{x}) \\ A_\times(\mathbf{x}) \\ h_\times(\mathbf{x}) \end{bmatrix} = 0\,, \tag{5.24}$$

which will be the starting point of the next section.

5.2 Graviton-photon mixing

In the previous section we have derived the equations of motion for the graviton-photon system in presence of an external magnetic field. In order to solve Equation 5.24 it is necessary to make some assumption on the nature of the magnetic field. The system of Equation 5.24 was derived in the approximation of a background magnetic field with coherence length much larger than the photon or graviton wavelength. System Equation 5.24 can be further simplified by making some reasonable assumptions on the nature of the background magnetic field. In this section we assume that the background magnetic field is homogeneous on a sufficiently large coherence length λ_B.

In order to solve the system of equations Equation 5.24 notice that there is no mixing between the photon or graviton states $+$ and $\times$. Correspondingly system (5.24) of four equations decouples into two independent systems of two equations each:

$$\left[(\omega + i\partial_{\mathbf{x}}) + \begin{bmatrix} M_+ & 0 \\ 0 & M_\times \end{bmatrix}\right] \begin{bmatrix} \hat{\Psi}_+(\mathbf{x}) \\ \hat{\Psi}_\times(\mathbf{x}) \end{bmatrix} = 0, \tag{5.25}$$

where we have defined

$$\hat{\Psi}_+(\mathbf{x}) \equiv \begin{bmatrix} A_+(\mathbf{x}) \\ h_+(\mathbf{x}) \end{bmatrix}, \qquad \hat{\Psi}_\times(\mathbf{n}) \equiv \begin{bmatrix} A_\times(\mathbf{x}) \\ h_\times(\mathbf{x}) \end{bmatrix}, \tag{5.26}$$

$$M_+ \equiv \begin{bmatrix} m_+ & m_{g\gamma} \\ m_{g\gamma} & 0 \end{bmatrix}, \qquad M_\times \equiv \begin{bmatrix} m_\times & m_{g\gamma} \\ m_{g\gamma} & 0 \end{bmatrix}, \tag{5.27}$$

and

$$m_+ = \omega(n-1)_+, \quad m_\times = \omega(n-1)_\times, \quad m_{g\gamma} = B_T/m_{\rm Pl}. \tag{5.28}$$

Since there is no mixing between + and × states, we can concentrate on one of the reduced matrices, M_+, where from now we drop index +. In this case the Schrödinger-like equation of motion, to be solved, has the form

$$(\omega + i\partial_{\mathbf{x}})\hat{\Psi}(\mathbf{x}) + M\hat{\Psi}(\mathbf{x}) = 0. \tag{5.29}$$

Equation 5.29 can be solved using the unitary transformation of field $\hat{\Psi}(\mathbf{x})$:

$$\hat{\Psi}'(\mathbf{x}) = U\hat{\Psi}(\mathbf{x}), \tag{5.30}$$

where U is the unitary matrix with the entries:

$$U = \begin{bmatrix} \cos\theta & \sin\theta \\ -\sin\theta & \cos\theta \end{bmatrix}. \tag{5.31}$$

In the new basis the equation of motion reads

$$(\omega + i\partial_{\mathbf{x}})\hat{\Psi}'(\mathbf{x}) + M'\hat{\Psi}'(\mathbf{x}) = 0, \tag{5.32}$$

where M' is the diagonal matrix, $M' = \mathrm{diag}[m_1, m_2]$ and m_1 and m_2 are the eigenvalues of matrix M:

$$m_{1,2} = \frac{1}{2}[m_+ \pm \sqrt{m_+^2 + 4m_{g\gamma}^2}]. \tag{5.33}$$

The formal solution of Equation 5.32 is given by

$$\hat{\Psi}'(\mathbf{x}) = \exp\{i\int_{\mathbf{0}}^{\mathbf{x}'}(\omega + M')\mathrm{d}\mathbf{x}'\}\hat{\Psi}'(\mathbf{0})\,. \tag{5.34}$$

Now we can go back to the old basis by multiplying the left hand side of Equation 5.34 by U^T and obtain

$$\hat{\Psi}(\mathbf{x}) = \exp\{i\int_{\mathbf{0}}^{\mathbf{x}'} U^T M' U\,\mathrm{d}\mathbf{x}'\}\hat{\Psi}(\mathbf{0})\,, \tag{5.35}$$

where common phase $e^{i\omega|\mathbf{x}|}$ was absorbed in field $\hat{\Psi}$. The explicit expressions for photon field, A, and graviton field, h, are

$$A(\mathbf{x}) = (\cos^2\theta e^{im_1|\mathbf{x}|} + \sin^2\theta e^{im_2|\mathbf{x}|})A(\mathbf{0}) + \sin\theta\cos\theta(e^{im_1|\mathbf{x}|} - e^{im_2|\mathbf{x}|})h(\mathbf{0})\,, \tag{5.36}$$

$$h(\mathbf{x}) = \sin\theta\cos\theta(e^{im_1|\mathbf{x}|} - e^{im_2|\mathbf{x}|})A(\mathbf{0}) + (\sin^2\theta e^{im_1|\mathbf{x}|} + \cos^2\theta e^{im_2|\mathbf{x}|})h(\mathbf{0})\,, \tag{5.37}$$

where θ is the graviton-photon mixing angle defined as:

$$\tan 2\theta = \frac{2m_{g\gamma}}{m_+}. \tag{5.38}$$

At this point one can easily calculate the probability of the graviton conversion to photon by assuming that initially there are only gravitons and no photons, that is, $h(\mathbf{0}) = 1$ and $A(\mathbf{0}) = 0$:

$$P_{g\to\gamma} = |\langle h(\mathbf{0})|A(\mathbf{x})\rangle|^2 = \sin^2(2\theta)\sin^2(\sqrt{m_+^2/4 + m_{g\gamma}^2}\cdot|\mathbf{x}|)\,. \tag{5.39}$$

Equation 5.39 gives the oscillation probability of a graviton to convert into a photon and vice-versa. We can also notice that the expression for the oscillation probability is completely analogous to the oscillation probability between neutrinos with different flavors [106].

5.3 Mixing strength: qualitative description

In the previous section we have calculated the probability of graviton to photon transformation and in this section we study various regimes of Equation 5.39. For an order of magnitude estimate, we neglect for the moment the absorption or scattering of the photons in the surrounding medium, the expansion of the Universe, and the Cotton-Mouton effect.

In order to estimate the oscillation probability we present the numerical values of the three terms in the right hand side of Equation 5.20. The plasma effects are included in term $m_{\text{plasma}} = -\omega_{\text{plasma}}^2/2\omega$ and its numerical value is[†]:

$$m_{\text{plasma}} = -3.5\cdot 10^{-17}\left[\frac{1\text{eV}}{\omega}\right]\left[\frac{n_e}{\text{cm}^{-3}}\right] \quad \text{cm}^{-1}, \tag{5.40}$$

where n_e is the electronic number density. The QED effects are included in the term m_{QED}[‡] which reads:

$$m_{\text{QED}} = \left[\frac{\alpha}{45\pi}\right]\left[\frac{B_T}{B_c}\right]^2\omega, \tag{5.41}$$

where $B_c = m_e^2/e = 4.41\cdot 10^{13}$ Gauss and the numerical value of m_{QED} is:

$$m_{\text{QED}} = 1.33\cdot 10^{-27}\left[\frac{\omega}{1\text{eV}}\right]\left[\frac{B_T}{1\text{G}}\right]^2 \quad \text{cm}^{-1}. \tag{5.42}$$

The mixing term is $m_{g\gamma} = B_T/m_{Pl}$ and it is equal to:

$$m_{g\gamma} = 8\cdot 10^{-26}\left[\frac{B_T}{1\text{G}}\right] \quad \text{cm}^{-1}. \tag{5.43}$$

[†]From now on we omit index + in m_+

[‡]In fact the expression for m_{QED} should include the factor 2 or 7/2 depending on the mode considered in the calculations. Here we omit these factors since in the case considered below the plasma effects dominate over the QED effects and the contribution from these factors are not essential

Equation 5.39 has different limiting forms, depending on the value of mixing angle θ.
a) *Weak mixing*
In this case $\theta \ll 1$ which corresponds to $m_{g\gamma} \ll m$ (remind that m is either m_+ or $m_\times$). Equation 5.39 in this case becomes

$$P_{g\to\gamma}(|\mathbf{x}|,\theta) = 4\theta^2 \sin^2\left[\frac{m|\mathbf{x}|}{2}\right] = 4\theta^2 \sin^2\left[\frac{\pi|\mathbf{x}|}{l_{\rm osc}}\right], \tag{5.44}$$

where the oscillation length is defined as $l_{\rm osc} = 2\pi/m$. Now if the oscillation length is greater than path $|\mathbf{x}|$, the oscillation probability is given by the simple expression:

$$P_{g\to\gamma}(|\mathbf{x}|,\theta) \simeq (m_{g\gamma}|\mathbf{x}|)^2. \tag{5.45}$$

It is interesting to see when the weak mixing condition is fulfilled during the evolution of the Universe. In other words we need to check when $m_{g\gamma} \ll m$ that is:

$$8\cdot 10^{-26}\left[\frac{B_T}{1\rm G}\right] \ll \mid 1.33\cdot 10^{-27}\left[\frac{\omega}{1\rm eV}\right]\left[\frac{B_T}{1\rm G}\right]^2 - 3.5\cdot 10^{-17}\left[\frac{1\rm eV}{\omega}\right]\left[\frac{n_e}{\rm cm^{-3}}\right]\mid . \tag{5.46}$$

Evidently the l.h.s. of this relation vanishes at the frequency equal to:

$$\omega_{res} = 1.6\cdot 10^5\,{\rm eV}\left(\frac{1G}{B_T}\right)\left(\frac{n_e}{cm^{-3}}\right)^{1/2}. \tag{5.47}$$

This is the so called resonance frequency when the mixing angle is close to $\pi/4$.

Let us see whether the mixing could be weak or strong in the present day universe. To this end we need to know three parameters which are the strength of magnetic field, B_T, the frequency of gravitons, ω, and the electronic density, n_e. Large scale magnetic fields are constrained by the CMB observations since they can create an anisotropic pressure which in turn requires an anisotropic gravitational field in order to maintain equilibrium. Gravitational instabilities in the post recombination era, created by the magnetic fields generate fluctuations in the CMB spectrum due to the Sachs-Wolfe effect [107]. In [108] the authors, using the 4-year Cosmic Background Explorer (COBE) microwave background isotropy measurements infer an upper limit on large scales magnetic field strength $B(t_0)$[§]

$$B(t_0) \simeq 5\times 10^{-9} f^{1/2}(\Omega_0 h_{70}^2)^{1/2} \quad {\rm G}. \tag{5.48}$$

where f is a shape factor of the order of unity. Recent limits based on the WMAP 7 year and South Pole Telescope (SPT) data, allow to conclude that the primordial magnetic field on scales, $\lambda_B < 1$ Mpc is bounded by $B(t_0) \lesssim 3$ nG at 95% (CL) [109, 110, 111].

Primordial magnetic field also induces the Faraday rotation of the linear polarization of CMB and can induce non zero parity odd cross correlations between the CMB temperature and B-polarization anisotropies. The authors of [112] put upper limits on the amplitude of the large scale magnetic field in the range $6\cdot 10^{-8}$ G to $2\cdot 10^{-6}$ G.

[§]From now we omit index "T" in B_T, where the magnetic field strength refers to the transverse part.

More stringent constraints on large scale magnetic fields at the present day wave length $\lambda_B \sim 0.1$ Mpc come from BBN bound on gravitational waves. If primordial magnetic field was generated before BBN, it would create an anisotropic stress in the l.h.s. of the Einstein equations which in turn would create perturbations in the curvature of space-time, namely GWs. The authors of [113, 114] argued that the large scale magnetic fields, produced at the electroweak phase transition must be weaker than $B \lesssim 10^{-27}$ G and the magnetic field produced at inflation weaker than$B \lesssim 10^{-39}$ G. These results were criticized in [115]. Here we assume validity of the CMB bounds on the large scale magnetic fields, quoted above.

At the present epoch the free electron number density is not a well known quantity and just for an order of magnitude estimate we take it equal to its upper bound, assuming that almost all matter is ionized

$$n_e(t_0) \lesssim n_B(t_0) = \frac{3H_0^2\Omega_B}{8\pi G m_p} = 1.123 \cdot 10^{-5}(h_0^2\Omega_B)\,\mathrm{cm}^{-3} \simeq 2.47 \cdot 10^{-7}\,\mathrm{cm}^{-3}\,, \quad (5.49)$$

where according to WMAP 7 years measurements [33] $H_0 = 100h_0$ km/s/Mpc with $h_0 \simeq 0.7$; $h_0^2\Omega_B \simeq 0.022$ is the present day baryon density parameter and m_p is the proton mass. More accurate estimates are presented below.

According to Equation 5.46, the validity of the weak mixing condition depends upon the photon frequency. As a guiding example let us take $\omega = 10^3$ eV, $B(t_0) \simeq 5 \cdot 10^{-9}$ G and $n_e(t_0) \simeq 2.47 \cdot 10^{-7}$ cm^{-3} and obtain:

$$l_{\mathrm{osc}} = \frac{2\pi}{|m_{\mathrm{plasma}}|} \simeq 7.26 \cdot 10^{26}\mathrm{cm}, \quad (5.50)$$

where clearly the plasma effects dominates over QED effects and $m \simeq |m_{\mathrm{plasma}}|$. So for the path of the graviton of the order of the present day Hubble radius $|\mathbf{x}| = H^{-1}(t_0) \simeq 1.32 \cdot 10^{28}$ cm, the oscillation probability today would be:

$$P_{g\to\gamma} \simeq 2 \cdot 10^{-15}. \quad (5.51)$$

Here we used Equation 5.38, Equation 5.40, Equation 5.43 and Equation 5.44. Equation 5.51 shows that for the present day value of the magnetic field $B(t_0)$ equal to its upper bound Equation 5.48, $n_e(t_0)$ determined by Equation 5.49, and for the gravitons with frequencies $\omega < m_e$ the condition for the weak mixing regime is satisfied. Thus the probability of graviton transition to photon is small but not negligible, which can lead to some observable effects.

It is instructive to estimate the graviton-photon transition probability at different periods of the cosmological evolution. Before the matter-radiation decoupling at $z \simeq 1090$, one might expect that the magnetic field was larger than that at the recombination because under condition of the magnetic flux conservation the field strength evolves as the inverse scale factor squared. This would be true if the cosmological magnetic field was generated at some earlier epoch, before recombination.

If magnetic field was generated before the BBN era, its strength could be constrained by the observed abundances of light elements. In particular, an impact of magnetic field on the cosmological expansion, an increase of the decay rate of neutrons, and other phenomena, described e.g. in [116, 117], would change the abundances of light elements. In the pioneering papers [118, 119, 120] the upper limit on the field strength at BBN was derived: $B \lesssim 10^{12}$ G. In more recent studies of the effect of magnetic field on the abundances of light elements, especially of ^{4}He, somewhat weaker bound, $B \lesssim 10^{13}$ G, was inferred [121, 122, 123, 124]. So huge magnetic fields are formally allowed at BBN.

On the other hand, the electronic number density increases with decreasing scale factor as $n_e(a) \sim a^{-3} \sim T^3$. This leads to an increase of the plasma effects, so they dominate over the QED effects. Thus in this case the weak mixing condition is realized, as one can see from Equation 5.46. The very small mixing angle gives negligible transition probability of gravitons to photons with frequencies $\omega \ll m_e$.

Things start to change near recombination when the plasma temperature was $T \simeq 0.26$ eV. The electronic density (plasma density) can be parametrized as

$$n_e(t_{\rm rec}) = X_e\, n_B(t_0)(T/T_0)^3, \tag{5.52}$$

where n_B is the total baryon density, $n_B = n_p + n_H$, with n_p and n_H being respectively the free proton and neutral hydrogen densities, $X_e(z)$ is the red-shift dependent ionization fraction, defined as $X_e = n_p/n_B$. The condition of electric neutrality, $n_e = n_p = X_e n_B$, is of course assumed. Since the present day baryon number density is given by Equation 5.49, we obtain

$$n_e(t_{\rm rec}) \simeq 1.123 \cdot 10^{-5} X_e (1+z)^3 (h_0^2 \Omega_B)\,{\rm cm}^{-3}\,, \tag{5.53}$$

where $T/T_0 = 1+z$ is substituted. Ionization fraction, $X_e(z)$, can be calculated by solving the out of equilibrium Saha-like non linear differential equation. Near recombination time, the solution is well approximated by the expression [125, 126]:

$$X_e(z) = 7.2 \cdot 10^{-3} \frac{(h_0^2\Omega_M)^{1/2}}{h_0^2\Omega_B} \left(\frac{1+z}{1090}\right)^{12.75}, \quad (800 < z < 1200), \tag{5.54}$$

where $h_0^2\Omega_M$ is the present day matter density parameter. Inserting Equation 5.54 into Equation 5.53 we get

$$n_e(t_{\rm rec}) \simeq 104.71\, (\Omega_M h_0^2)^{1/2} \left(\frac{1+z}{1090}\right)^{15.75} {\rm cm}^{-3} \quad (800 < z < 1200). \tag{5.55}$$

Since according to WMAP 7 year data the redshift at recombination is $1+z = 1090$ and the matter density parameter is $\Omega_M h_0^2 \simeq 0.15$, the free electron density at recombination would be $n_e(t_{\rm rec}) \simeq 40.5\,{\rm cm}^{-3}$.

Assuming that the observed contemporary magnetic field originated from primordial magnetic field seeds without much dynamo effects, one finds that on the horizon length at the recombination time, the field strength was:

$$B(t_{\rm rec}) \simeq B(t_0)(1+z)^2 = 3\cdot 10^{-3}\,{\rm G}, \tag{5.56}$$

where we took $B(t_0) \simeq 3\cdot 10^{-9}$.

Taking $B(t_{\rm rec}) \sim 3\cdot 10^{-3}$ G and $n_e \sim 40.5\ {\rm cm}^{-3}$, we find that the ratio of the plasma term to the QED term at recombination:

$$r = \frac{|m_{\rm plasma}|}{m_{\rm QED}} = 2.63\cdot 10^{10}\left[\frac{1{\rm eV}}{\omega}\right]^2\left[\frac{1{\rm G}}{B}\right]^2\left[\frac{n_e}{{\rm cm}^{-3}}\right] \tag{5.57}$$

is larger than unity for all frequencies below $\omega \lesssim 3.4\cdot 10^8$ eV. Recall that the approximation used here is valid only for $\omega \ll m_e$.

With these values we estimate the oscillation probability at the recombination epoch when the Hubble radius was equal to:

$$H(t_{\rm rec})^{-1} = H_0^{-1}/[\Omega_\Lambda + \Omega_M(1+z)^3]^{1/2} \simeq 6.7\cdot 10^{23}{\rm cm}, \tag{5.58}$$

where $H_0^{-1} = 1.32\cdot 10^{28}$ cm, $\Omega_\Lambda \simeq 0.7$ and $\Omega_M \simeq 0.3$. The oscillation length in this case reads

$$l_{\rm osc} = \frac{2\pi}{|m_{\rm plasma}|} \sim 4.43\cdot 10^{20}\,{\rm cm}, \tag{5.59}$$

which is 3 orders of magnitude smaller than the Hubble distance at recombination. Taking $B(t_{\rm rec}) \simeq 3\cdot 10^{-3}$ G, $n_e(t_{\rm rec}) \simeq 40.5\ {\rm cm}^{-3}$, and graviton initial energy $\omega_i \simeq 10^5$ eV and using Equation 5.38, Equation 5.40, Equation 5.43 and Equation 5.44, we find that the oscillation probability is

$$P_{g\to\gamma} \simeq 10^{-15}\left(\frac{\omega_i}{10^5\,{\rm eV}}\right)^2\left(\frac{B_i}{3\cdot 10^{-3}\,{\rm G}}\right)^2\left(\frac{40.5\,{\rm cm}^{-3}}{n_e}\right)^2. \tag{5.60}$$

One can see that probability Equation 5.60 depends on the frequency of the graviton and noticeable amount of high energy photons can be produced if the original graviton spectrum is not cut-off at high frequencies [14].

b) *Resonance*

At the resonance $r = 1$, Equation 5.57, and thus $m = 0$, so the mixing angle becomes large, $\theta = \pi/4$. In this case the expression for the oscillation probability is

$$P_{g\to\gamma} = \sin^2(m_{g\gamma}\cdot|{\bf x}|). \tag{5.61}$$

If the resonance is wide the complete transition of graviton into photon is possible. Note that near the resonance the two regimes of weak mixing and maximum mixing have the same expression for probability, Equation 5.45, in the case when the oscillation length is larger than the path. However, the excitation of resonance depends upon the effects of

damping and loss of coherence and so its proper treatment demands the density matrix formalism. This is done in the next section.

Even if the resonance is not excited, as is the case when $\omega < m_e$, the density matrix formalism leads to an essential enhancement of the photon production because the photons loose coherence due to scattering on electrons and do not oscillate back. This happens if the coherence loss rate is faster than the Universe expansion rate.

5.4 Oscillations: density matrix description

In the previous section we have calculated the probability of the graviton-photon oscillations in the wave function approximation. Graviton conversion into photons in the present day universe in the wave function approximation was also considered in [127] but their results are significantly different from ours as we will see below. This approximation is sufficiently accurate if the loss of coherence due to non-forward or inelastic scattering of the participating particles (i.e. of the photons in the considered case) may be neglected. This is realized if the mean free path with respect to such scattering is greater than the oscillation length. In the opposite case the graviton-photon system becomes open (i.e. not self-contained) and the density matrix formalism should be applied. The corrections to the wave function approximation are especially important in the resonance situation when the oscillation length becomes large:

$$l_{osc} = \frac{2\pi}{\sqrt{m^2/4 + m_{g\gamma}^2}} \to \frac{2\pi}{\sqrt{m_{g\gamma}^2}}, \tag{5.62}$$

where $m = 0$ at resonance.

Generally speaking the density matrix operator the is 4×4-matrix describing transitions between photon and gravitons with different helicity states:

$$\hat{\rho} \equiv |A_+, h_+, A_\times, h_\times\rangle \otimes \langle A_+, h_+, A_\times, h_\times|, \tag{5.63}$$

where the C-valued density matrix $\hat{\rho}_{ij}$ is obtained by averaging the matrix elements over medium, $\rho = \langle\hat{\rho}\rangle$. However, since there is no mixing between states $|+\rangle$ and $|\times\rangle$ the density matrix is reduced to two independent 2×2-matrices separately for $|+\rangle$ and $|\times\rangle$ states having the form

$$\hat{\rho} = \hat{\Psi}\hat{\Psi}^\dagger, \tag{5.64}$$

where $\hat{\Psi}$ is two-dimensional column describing the graviton and photon states $\Psi = [\Psi_g, \Psi_\gamma]^T$ of either polarization $|+\rangle$ or $|\times\rangle$. Here upper index "T" means transposition.

The density matrix operator satisfies the Liouville-von Neumann equation:

$$i\frac{d\hat{\rho}}{dt} = [\hat{\mathcal{H}}, \hat{\rho}] \tag{5.65}$$

where $\mathcal{H}$ is the total Hamiltonian of the system. If the system is open the total Hamiltonian is not Hermitian and the anti-Hermitian part of the Hamiltonian describes coherence breaking due to scattering and absorption. In general case it is expressed through

the collision integral modified to include the matrix structure of the process. For the case of neutrino oscillations the equation for the density matrix was derived in [128], see also [129, 130]. It is a non-linear integro-differential equation due to presence of complicated collision integrals. However, for an an order of magnitude estimate the equation can be linearized in the usual way[¶]:

$$i\frac{d\rho}{dx} = [M,\rho] - i\{\Gamma,(\rho-\rho_{ext})\}, \tag{5.66}$$

where M is given by Equation 5.27, ρ_{ext} is the density matrix of the corresponding particles in the medium, the time derivative has been replaced with derivative respect to position in space, $d/dt = d/dx$ for $c = 1$ and Γ is the damping factor which in our case has the form:

$$\Gamma = \begin{bmatrix} \Gamma_\gamma & 0 \\ 0 & 0 \end{bmatrix} \tag{5.67}$$

where Γ_γ is the inverse mean free path due to Thompson scattering[‖] of photons on electrons $\Gamma_\gamma = \sigma_T n_e$ with $\sigma_T = 6.65 \cdot 10^{-25}$ cm^{-2} being the Thompson cross section. The damping of gravitons is neglected due to weakness of their interactions. We also neglect ρ_{ext}, assuming that the medium is not populated by photons. The latter can be easily taken into account.

In the previous section we estimated the oscillation probability at various stages during the evolution of the Universe, namely at the present time and at the recombination but the universe expansion was not explicitly accounted for. To do that in the cosmological FRW metric we notice that for a given function $f(p,t)$ the total derivative is given by:

$$\frac{df}{dt} = \frac{\partial f}{\partial t} + \dot{p}\frac{\partial f}{\partial p} = \frac{\partial f}{\partial t} - Hp\frac{\partial f}{\partial p}\,. \tag{5.68}$$

Here we have taken into account the redshift, $\dot{p} = -Hp$, where $H = \dot{a}/a$ is the Hubble parameter and a is the cosmological scale factor. Hence Equation 5.66 can be rewritten as

$$iHa\frac{\partial\rho}{\partial a} = [M,\rho] - i\{\Gamma,\rho\}, \tag{5.69}$$

where we made use of the fact that in the FRW metric $\partial_x = Ha\partial_a$.

Let us write the off-diagonal density matrix elements as: $\rho_{\gamma g} = \rho^*_{g\gamma} = R + iI$, where R is the real part and I is the imaginary part. The diagonal components ρ_{gg} and $\rho_{\gamma\gamma}$ are the number densities of gravitons and photons, respectively, so they are real and non-negative. Thus after the split between the real and imaginary parts we obtain the

[¶]As usually $[,]$ denotes the commutator between two operators a and b and $\{,\}$ denotes the anti-commutator.

[‖]The photoelectric effect on the neutral matter is another damping effect which reduce the number of produced photons. However, for the frequencies considered in this chapter this effect is not too large and we neglect it.

following system of differential equations:

$$\rho'_{\gamma\gamma} = \frac{-2m_{g\gamma}I - \Gamma_\gamma \rho_{\gamma\gamma}}{Ha}, \tag{5.70}$$

$$\rho'_{gg} = \frac{2m_{g\gamma}I}{Ha}, \tag{5.71}$$

$$R' = \frac{mI - \Gamma_\gamma R/2}{Ha}, \tag{5.72}$$

$$I' = \frac{-mR - \Gamma_\gamma I/2 - m_{g\gamma}(\rho_{gg} - \rho_{\gamma\gamma})}{Ha}, \tag{5.73}$$

where prime means derivative with respect to a and the initial conditions are taken at the initial value of the scale factor $a = a_i$ as: $\rho_g(a_i) = 1, \rho_\gamma(a_i) = 0, I(a_i) = 0$, and $R(a_i) = 0$. To solve this system of equations we need to know how parameters $m, m_{\gamma g}$, and Γ_γ (in units cm^{-1}) depend on the scale factor:

$$m_{\gamma g}(a) = 8 \cdot 10^{-26} \left[\frac{B_i}{1\mathrm{G}}\right] \left[\frac{a_i}{a}\right]^2, \tag{5.74}$$

$$\Gamma_\gamma(a) = 2.12 \cdot 10^{-22} X_e(a) \left[\frac{a_i}{a}\right]^3, \tag{5.75}$$

$$m(a) = 1.33 \cdot 10^{-27} \left(\frac{B_i}{1\mathrm{G}}\right)^2 \left(\frac{\omega_i}{1\mathrm{eV}}\right) \left(\frac{a_i}{a}\right)^5 - 1.12 \cdot 10^{-14} X_e(a) \left(\frac{1\mathrm{eV}}{\omega_i}\right) \left(\frac{a_i}{a}\right)^2,$$

where initial values B_i and ω_i are taken at the cosmological recombination time, $t_i = t_{\mathrm{rec}}$ and we expressed $n_e(a) = X_e(a) n_B(t_{\mathrm{rec}})$ with $n_B(t_{\mathrm{rec}}) = n_B(t_0)(1+z)^3 \simeq 320\ \mathrm{cm}^{-3}$. The ionization fraction is governed by the following differential equation [34]:

$$\frac{\mathrm{d}X_e}{\mathrm{d}a} = -\frac{\alpha n_B}{Ha} \left(1 + \frac{\beta}{\Gamma_{2s} + 8\pi/\lambda_\alpha^3 n_B (1 - X_e)}\right)^{-1} \left(\frac{S X_e^2 + X_e - 1}{S}\right), \tag{5.76}$$

where H is the Hubble parameter, $\Gamma_{2s} = 8.22458\ \mathrm{s}^{-1}$ is the two-photon decay rate of $2s$ hydrogen state, $\lambda_\alpha = 1215.682 \cdot 10^{-8}$ cm is the wavelength of Lyman α photons, $\alpha(T)$ is the case B recombination coefficient and $S(T)$ is the coefficient in the Saha equation, $X(1 + SX) = 1$. Both α and S depend on temperature T which can be expressed in terms of scale factor a as follows:

$$T = \left(\frac{g_{*S}(T_i)}{g_{*S}(T)}\right)^{1/3} \left(\frac{a_i}{a}\right) T_i \tag{5.77}$$

where $g_{*S}(T)$ is number of the entropy degrees of freedom. Generally it depends on temperature but after recombination the only effective massless particles in the standard model are 3 neutrino species and the photon. Thus the number of the degrees of freedom is constant which is equal to $g_{*S}(T) = 3.91$. In this case the temperature drops down as $T = T_i/a$ where $T_i = (1 + z_{\mathrm{rec}}) T_{0\gamma} = 2970.25$ K. In what follows we take $a_i = 1$ corresponding to recombination time, $t_i = t_{\mathrm{rec}}$. Coefficient α depends on the scale factor as [131, 132]:

$$\alpha(a) = \frac{1.038 \cdot 10^{-12} a^{0.6166}}{1 + 0.352 a^{-0.53}}, \tag{5.78}$$

while $S(a)$ is equal to

$$S(a) = 6.221 \cdot 10^{-19} e^{53.158a} a^{-3/2}. \tag{5.79}$$

Coefficient β which is also a function of temperature can be expressed through α as follows

$$\beta(a) = 3.9 \cdot 10^{20} a^{-3/2} e^{-13.289a} \alpha. \tag{5.80}$$

With the these parameters Equation 5.76 was solved numerically. Some values of the ionization fraction $X_e(a)$ as a function of the scale factor are presented in Table 5.1 and plots of $X_e(a)$ and $X_e(T)$ are shown in Figure 5.1 and Figure 5.2. Below we solve numerically equations describing evolution of the mixed graviton-photon density matrix together with Equation 5.76 introducing into them a factor describing reionization of the cosmic plasma.

a	$X_e(a)$
1	0.13
1.04	0.0813
1.18	0.0160
1.23	0.00947
1.5	0.00171
2	0.000731
4	0.000373
10	0.000278
30	0.000246
51.9	0.000239
136.25	1
1090	1

Table 5.1: Ionization fraction X_e as a function of the scale factor for $h_0^2\Omega_M \simeq 0.15$ and $h_0^2\Omega_B \simeq 0.022$ calculated from eq. (5.76). We have also presented two additional pieces of data for $a = 136.3$, which correspond to the period of reionization, and to the present day $a = 1090$ where the intergalactic medium is almost fully ionized with constant ionization fraction, $X_e \simeq 1$

The resonance condition, $m(a) = 0$, is fulfilled at

$$\omega = 2.9\,\mathrm{MeV}\, X_e^{1/2}(a) \left(\frac{1\mathrm{G}}{B_i}\right) a^{3/2}. \tag{5.81}$$

The ratio of the oscillation length to the mean free path in this case is

$$\frac{l_{osc}^{(res)}}{l_{free}} = \frac{2\pi \cdot \Gamma_\gamma}{m_{g\gamma}} = 1.66 \cdot 10^4 \left[\frac{1\,\mathrm{G}}{B_i}\right]. \tag{5.82}$$

In this case the resonance frequency at recombination would be about 10 MeV for $B_i \simeq 10^{-1}$ G. For possibly larger B_i resonance shifts to smaller ω. Even out of the

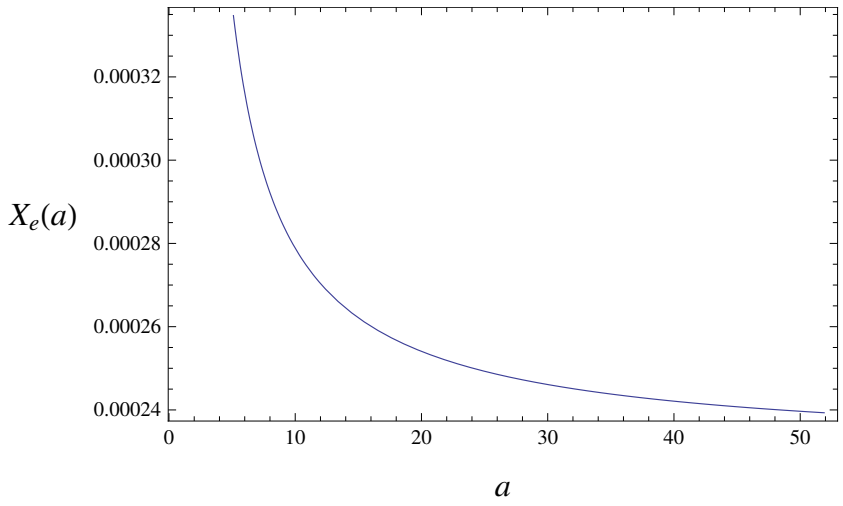

Figure 5.1: Ionization fraction X_e as a function of cosmological scale factor a. The plot is shown in the interval starting from recombination, $a = 1$, till $a = 51.9$ corresponding to the beginning of re-ionization.

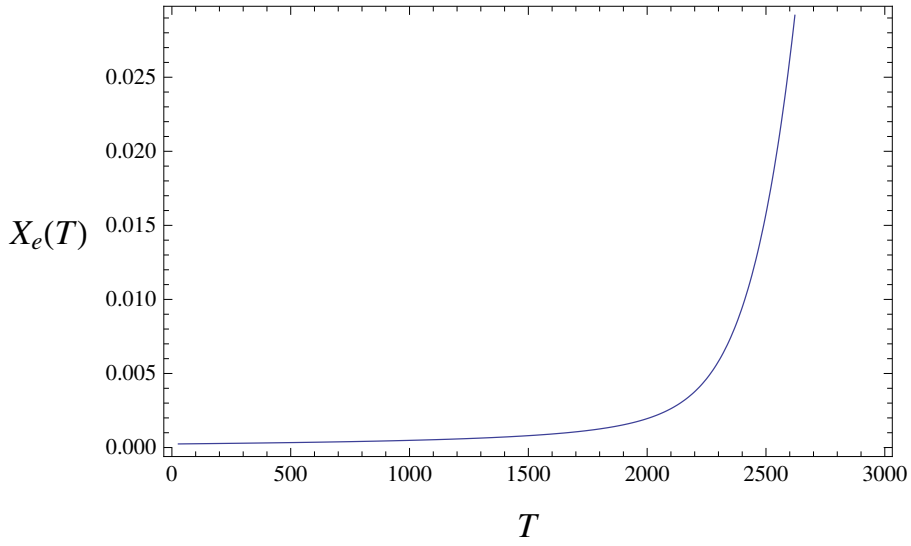

Figure 5.2: Ionization fraction X_e as a function of temperature T in Kelvin. The temperature T changes in the interval $T = 2970.25$ K corresponding to recombination time to $T = 57.22$ K corresponding to onset of of re-ionization.

resonance inequality $l_{osc} \geqslant l_{free}$ may remain true and use of the density matrix formalism is obligatory.

We need to mention however, that very energetic gravitational waves with energy $\omega \gg m_e$ would create photons whose scattering on electrons is weaker than the Thompson one, roughly speaking, by $(m_e/E)^2$. This effect would diminish the damping factor Γ_γ by the same amount and can be easily taken into account. However, in this chapter we consider graviton energies smaller than the electron rest mass, $\omega < m_e$. In the process of the cosmological expansion the graviton-photon transition could pass through resonance if their frequency satisfies resonance condition, Equation 5.81. However, since we consider graviton energies, $\omega < m_e$, the resonance condition Equation 5.81 is not satisfied in the post-recombination epoch.

Next we need to evaluate factor Ha. Since, we are interested in the cosmological epoch just after recombination till the present time, when the Universe is dominated by nonrelativistic matter, the Hubble constant as a function of the redshift is given by Equation 5.58. In terms of the scale factor, the product Ha is given by

$$Ha = H(t_i)\,[\Omega_M/a + \Omega_\Lambda a^2]^{1/2}. \tag{5.83}$$

For redshift $z > 1$ we can neglect the contribution of the cosmological constant into the energy density of the Universe since it becomes important only for $z \lesssim 1$. We take $\Omega_M \simeq 1$ and $1/Ha = 6.7 \cdot 10^{23} a^{1/2}$ cm for the former case and $1/Ha = 6.7 \cdot 10^{23}[0.3/a + 0.7a^2]^{-1/2}$ cm for the latter case. According to our notations the redshift $z = 1$ corresponds to the scale factor $a = 545$ with respect to the recombination time.

For $7 < z < 11$ the universe is re-ionized by the first generation stars. According to [133] if the universe went into a sudden complete ionization, the re-ionization redshift $z_{\rm reion} = 6$ is excluded at 99% (CL) in favor of $z_{\rm reion} = 11$. Using the WMAP 5 year data the authors of [133] suggest that the universe underwent an extended period of partial re-ionization starting at $z \sim 20$ and ending with a complete ionization for $z \sim 7$ instead of a sudden re-ionization. For $z \sim 20$ the value of the scale factor with respect to recombination is $a = 51.9$ and for $z = 7$, $a = 136.25$.

In Figure 5.3, Figure 5.4, Figure 5.5, Figure 5.6, Figure 5.19 and in Figure 5.8 the probability of photon creation, $\rho_{\gamma\gamma}$ is presented as a function of the cosmological scale factor for various values of the initial background magnetic field and for graviton energy $\omega_i = 10^5$ eV. For such ω, the resonance does not occur but still the probability is much higher than the simple estimate in the wave function formalism. We can see that in all Figure 5.3, Figure 5.4, Figure 5.5, Figure 5.6, Figure 5.19 and in Figure 5.8 the oscillation probability rapidly increases for $a < 20$ and remains almost constant for $a > 20$ until onset of the period of re-ionization at $a \simeq 52$. The rapid increase of $\rho_{\gamma\gamma}$ for $a < 20$ is due to two reasons: a quick drop of the ionization fraction from its value at recombination and sharp decrease of the oscillation frequency. For $20 < a < 52$ the ionization fraction practically remains constant with $\rho_{\gamma\gamma}$ slowly rising. From beginning of the reionization period at $a \simeq 52$ till $a \simeq 545$ or $z \simeq 1$, $\rho_{\gamma\gamma}$ slowly

decreases with superimposed oscillations of decreasing amplitude. For $a > 545$ the vacuum energy density dominates over the matter energy density. At this period the photon creation probability remains almost constant. The oscillation probability drops from $a \simeq 100$ up to $a = 1090$ roughly speaking by 20-30 %. The value of the magnetic field at recombination has been evaluated by the anti-redshift of the present day large scale magnetic field as given in [109, 112].

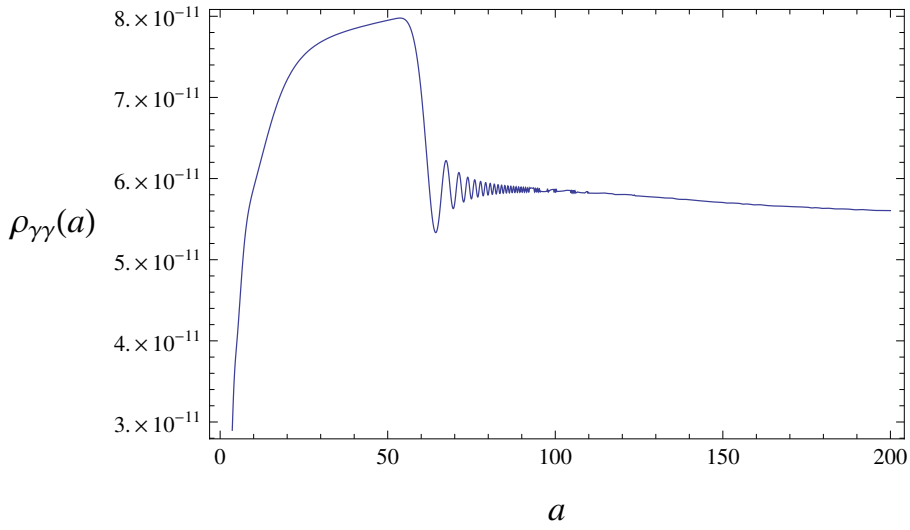

Figure 5.3: Probability $P_{g\gamma} = \rho_{\gamma\gamma}$ of photon production by graviton as a function of cosmological scale factor a in the interval $1 \leqslant a \leqslant 200$ for graviton initial energy $\omega_i = 10^5$ eV and background magnetic filed $B_i \simeq 3 \cdot 10^{-3}$ G .

5.5 Models of an early production of high frequency gravitons.

In section 5.5 we calculated the probability of graviton-to-photon transition taking into account both redshift and coherence breaking in plasma and found that for graviton energy of the order of $\omega \simeq 0.1$ MeV the oscillation probability is quite large, $P_{g\gamma} \simeq 10^{-11}$ for $B \simeq 10^{-3}$ G up to 10^{-5} for $B \simeq 1.2$ G. The number density of the produced photons, which could be directly observed as X-ray background, is proportional to the initial density of the gravitons. The amount of GWs at present time is usually expressed through the density parameter in gravitational waves which is defined in Equation 3.10. Since we are interested in GWs of cosmological origin, we consider here only those emitted before BBN.

The abundances of light elements produced at BBN depend upon the energy density of relativistic species at $t \sim 1 - 100$ sec, see e.g. book [41]. According to the recent data [134] an additional energy density at BBN, equal to that of one massless neutrino is

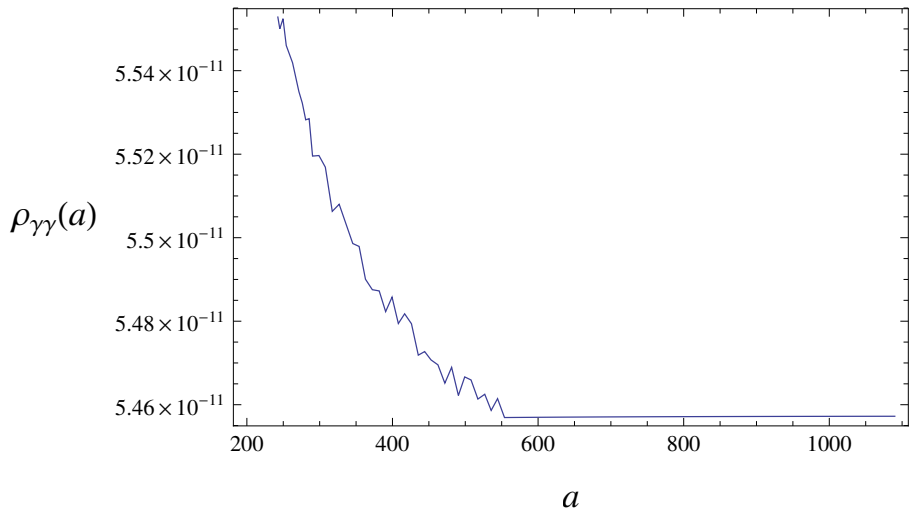

Figure 5.4: Probability $P_{g\gamma} = \rho_{\gamma\gamma}$ of photon production by graviton as a function of cosmological scale factor a in the interval $200 \leqslant a \leqslant 1090$ for graviton initial energy $\omega_i = 10^5$ eV and background magnetic filed $B_i \simeq 3 \cdot 10^{-3}$ G . For $a > 200$, the production probability remains almost constant.

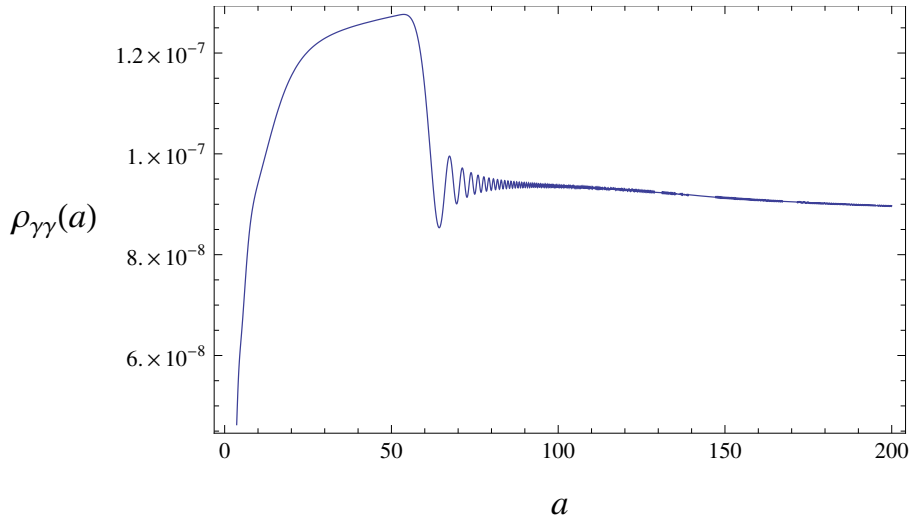

Figure 5.5: The same interval for the scale factor as in Figure 5.3 and for graviton initial energy $\omega_i = 10^5$ eV and for background magnetic field $B_i \simeq 1.2 \cdot 10^{-1}$

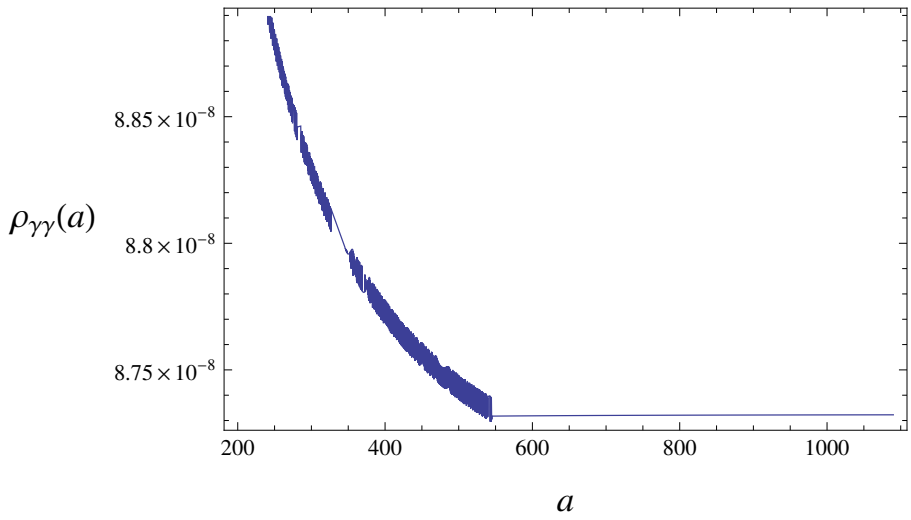

Figure 5.6: The same interval for the scale factor as in Figure 5.4 and for graviton initial energy $\omega_i = 10^5$ eV and for background magnetic field $B_i \simeq 1.2 \cdot 10^{-1}$

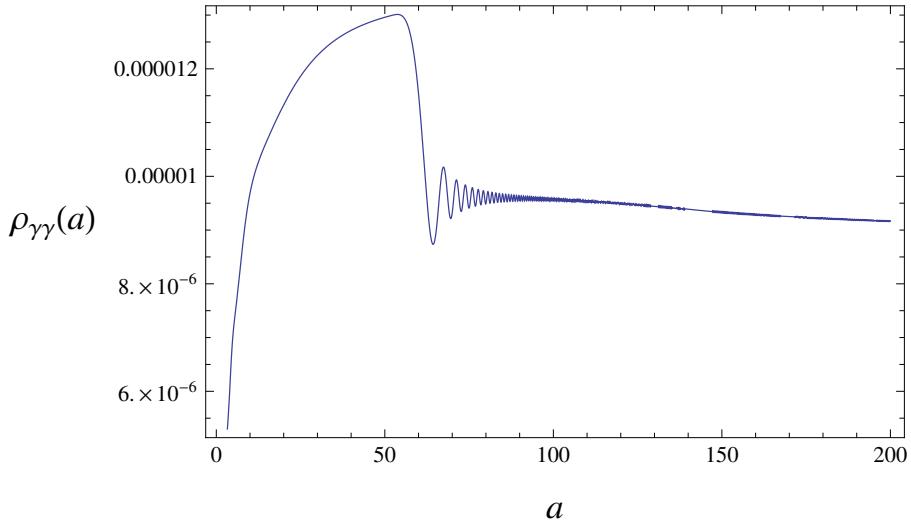

Figure 5.7: Probability $P_{g\gamma} = \rho_{\gamma\gamma}$ of photon production by graviton as a function of cosmological scale factor $a \lesssim 200$ for initial magnetic field $B_i \simeq 1.2$ G and graviton energy $\omega_i = 10^5$ eV.

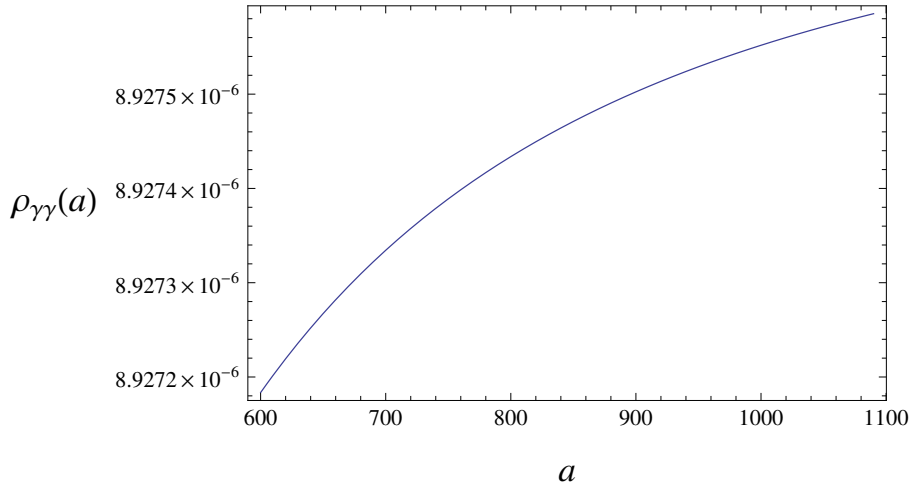

Figure 5.8: Probability $P_{g\gamma} = \rho_{\gamma\gamma}$ of photon production by graviton as a function of cosmological scale factor $a > 545$ for initial magnetic field $B_i \simeq 1.2$ G and graviton energy $\omega_i = 10^5$ eV. We can clearly see an almost constant $\rho_{\gamma\gamma}$ with a slowly variation with the scale factor

allowed and even desirable, $N - N_\nu \leqslant 1$. The particles which carry this additional energy are not known. They are called generically dark radiation. At BBN the energy density of one neutrino species (that is of neutrino plus antineutrino with vanishing chemical potential) is approximately equal to that of photons. However after e^+e^--annihilation the ratio of neutrino to photons energy densities dropped down approximately by factor four. The density parameter of additional degrees of freedom at BBN is bounded above by Equation 3.40 and it would be interesting if $N - N_\nu \approx 1$ is explained by primordial GWs.

The oscillation probability strongly depends on the graviton frequency and spectrum. The models of primordial GW production mostly predict low frequency of stochastic background of GWs, mainly concentrated at the present day frequencies of GWs near $f \lesssim 1$ Hz. For example, as we saw in chapter 3 inflationary models predict an almost scale invariant spectrum at large wavelengths, and their density parameter depends mainly on two factors, the GW frequency and the Hubble parameter H at inflation. In the frequency range $f = 10^{-15}$ Hz up to $f \simeq$ GHz the density parameter is very low, $h_0^2\Omega_{\rm gw}(t_0) \sim 10^{-15}$. Other post inflationary models such as pre-heating phase [47, 48], first order phase transitions [54], and topological defects [59], in particular, cosmic strings [57, 58] predict in the high frequency range $f \sim$ GHz the density parameter of the order $h_0^2\Omega_{\rm gw}(t_0) \lesssim 10^{-8}$.

All the above mentioned GWs production models, though predict a substantial density parameter, have maximum frequency today not more than 10^{-5} eV. We calculated numerically the graviton-photon oscillation probability for frequencies $f \sim 10^{-5}$ eV and found that it is of the order, 10^{-30}. With this low value of the probability the total

density parameter in photons of most of post-inflationary GWs models at the maximum frequency $f \sim$ GHz would be

$$h_0^2\Omega_\gamma(t_0) = h_0^2\Omega_{\rm gw}(t_0)\cdot\rho_{\gamma\gamma} \simeq 10^{-38}. \tag{5.84}$$

Such a small value of the density parameter makes improbable observations of photons from these GWs. However, as we saw in chapter 4 the GW emission could exceed that produced by other mechanisms. Among the mechanisms considered there, we single out the graviton evaporation, where the emitted peak frequency of quasi-thermal gravitons would be in the range from $f \sim$ keV up to $f \sim$ MeV today. The peak frequency in this model depends on the BH mass which turns out to be in the interval from the Planck mass, up to $\lesssim 10^8$ g.

Let us consider, for example, gravitons with the initial energy $\omega_i = \omega(t_{\rm rec}) = 10^5$ eV. Their frequency today would be $\omega = \omega_i/(1+z_{\rm rec}) = \omega_i/1090 = 91.7$ eV and they would produce photons with the same frequency. The value of the graviton density parameter at this frequency according to the above quoted scenario, could be $h_0^2\Omega_{\rm gw}(t_0) \simeq 5\cdot 10^{-8}$. And so the corresponding density parameter of the produced photons could be in the interval(or even two orders of magnitude higher):

$$h_0^2\Omega_\gamma(t_0) = h_0^2\Omega_{\rm gw}(t_0)\cdot P_{g\gamma} \simeq 3\cdot 10^{-18} - 4\cdot 10^{-13}, \tag{5.85}$$

where $P_{g\gamma} \simeq 5.5\cdot 10^{-11} - 9\cdot 10^{-6}$ is the probability of graviton to photon conversion. The energy flux of such photon background at the present time would be

$$F_\gamma = \left(\frac{{\rm d}E_{\rm gw}}{{\rm d}A\,{\rm d}t}\right)\cdot P_{g\gamma} = c\,T_{00}^{\rm gw}\cdot P_{g\gamma} = c\,h_0^2\Omega_{\rm gw}\,\rho_c\cdot P_{g\gamma}, \tag{5.86}$$

where $T_{00}^{\rm gw} = \rho_{\rm gw}$ is the 00 component of the GW energy-momentum tensor and we restored the light velocity in order to express the photon flux in the standard units (erg/cm^2 s). Taking the present day photon energy $\omega_{\rm ph} \sim 0.1$ keV, $c = 3\cdot 10^{10}$ cm/s and $\rho_c = 1.878\cdot 10^{-29}$ gr/cm^{-3} we obtain the energy flux

$$F_\gamma \simeq 1.5\cdot 10^{-15} - 2\cdot 10^{-10}\,[{\rm erg/cm^2\,s}], \tag{5.87}$$

which is comparable to the energy flux of most AGNs in the soft X-ray spectrum [135, 136] and even higher.

5.6 Resonant mixing at higher energies

In the previous sections we limited our considerations to the case of gravitons with energy smaller than the electron rest mass, $\omega \ll m_e$. In this section we abandon this restriction and consider resonance graviton-photon transformation. In the resonance case it is possible for the gravitons to reach an analogue of the MSW resonance in complete analogy with neutrino oscillation in matter. As we saw at the beginning of this chapter the

Euler-Heisenberg effective Lagrangian is valid in the limit of low photon energy, when the kinematic variables $s = (k_1 + k_2)^2$ and $|t| = |(k_1 - k_3)^2|$ are much smaller than m_e^2. Here k_1 and k_2 are 4-momenta of the initial photons and k_3 and k_4 are the final ones. It is essentially means that the Euler-Heisenberg approximation is valid for sufficiently low photon energy, $\omega \ll m_e$ in the center of mass. For the photon scattering in external (magnetic) field, which we consider in what follows, the restriction is much milder, ω may be much larger than m_e in the laboratory frame.The amplitude of the graviton-photon transformation depends upon the photon refraction index which in turn is proportional to the amplitude of the forward scattering of photons in the medium. We assume that the external magnetic field is homogeneous at macroscopically large scale λ_B and slowly varying in with characteristic time t_B. It means that the energy and momentum of the external field can be estimated as $1/t_B$ and $1/\lambda_B$. The momentum and energy transfer to the incoming photon are respectively $1/\lambda_B$ and $1/t_B$. Correspondingly the characteristic value of effective kinematical variable s is of the order of $s \sim (\omega/\lambda_B + \omega/t_B)$, so even for $\omega \gg m_e$ the Euler-Heisenberg effective Lagrangian would be valid. Thus for the calculations of the graviton-photon transformation we can apply equations used in section 5.2 in the Euler-Heisenberg approximation. This approximation is valid for a wide range of frequencies as far as $\omega \ll (2m_e/3)(B_c/B)$ [137, 138, 139] and depends essentially on the strength of the background magnetic field. In fact, if the strength of the magnetic field is a few $\cdot 10^{-9}$ G we have that Equation 5.9 is valid for present day graviton energies of $\omega \ll m_{\rm Pl}$. This emphasize the fact that the Euler-Heisenberg Lagrangian and vacuum refraction indexes Equation 5.9 are valid for almost desired graviton energies as far as we deal with large scale cosmological magnetic fields.

The relevant terms contributing to the damping depend essentially on the energy of the formed photon through the mechanism of graviton to photon oscillation. The most important interactions of photons with matter in the energy range from few eV up to 100 GeV are the photoelectric effect, Compton scattering on electrons and pair production in the field of atomic nuclei. The photoelectric effect is the most important effect of absorption of photons from atoms in the energy range from few eV up to few keV. In the energy range from few keV up to few MeV the Compton scattering is the dominant process of photon interaction with matter. For higher energies it turns that pair production on atomic nuclei is the dominant process starting from few MeV up to 100 GeV. However, as we shall see in the next section we limit our consideration for present day energy range of from keV up to 100 keV. At the recombination time which is our starting point on studying the graviton to photon oscillations, the interval 1-100 keV correspond to an energy range at recombination (roughly) 1-100 MeV, where $1 + z_{\rm rec} = 1090$. Evidently in this case the photoelectric effect is completely irrelevant because we consider an energy range on which this effect is completely negligible [140] for present day energies $\omega \sim 1 - 100$ keV and for higher energies this effect is completely negligible in comparison to Compton scattering. The absorption of γ-rays by heavy elements at later stage due to photoelectric effect might be important but the cosmological density

of heavy elements is low, so for this reason we neglect it [141]

Expression for the differential cross section due to Compton scattering is given by the Klein-Nishina formula [142]

$$\left(\frac{d\sigma}{d\Omega}\right)_{\text{lab}} = \frac{r_e^2}{2}\left(\frac{\omega'}{\omega}\right)^2\left[\frac{\omega}{\omega'} + \frac{\omega'}{\omega} - \sin^2\theta\right], \tag{5.88}$$

where r_e is the classical electron radius, ω' is the photon energy after scattering and $\omega'/\omega = m_e/[m_e + \omega(1-\cos\theta)]$ with θ being the scattering angle. The total cross section due to Compton scattering is given by integrating Equation 5.88 over all angles and it reads

$$\sigma_{KN} = \frac{3}{4}\sigma_T\left[\frac{2 + x(1+x)(8+x)}{x^2(1+2x)^2} + \frac{(x^2 - 2x - 2)\log(1+2x)}{2x^3}\right], \tag{5.89}$$

where x is the ratio of the photon energy to the electron rest mass energy, $x = \omega/m_e$. The total cross section due to pair production is not an easy task to find for almost all elements, however, for photon energies in the range $1 \ll x \ll 1/\alpha Z^{1/3}$ there is an approximate expression which reads [140]

$$\sigma_{pp} = \frac{\alpha Z(Z+1)}{\pi}\sigma_T\left[\frac{28}{24}\ln(2x) - \frac{218}{72}\right]. \tag{5.90}$$

In the case of ultra-relativistic energies of all particles participating in the process and complete screening by atomic electrons, $x \gg 1/\alpha Z^{1/3}$ the total cross section due to pair production is

$$\sigma_{pp} = \frac{\alpha Z(Z+1)}{\pi}\sigma_T\left[\frac{28}{24}\ln(183/Z^{1/3}) - \frac{1}{36}\right]. \tag{5.91}$$

In the case of ultra-relativistic energies we can clearly see that the total cross section is independent of the photon energy but it depends essentially on the atomic number Z. Both Equation 5.90 and Equation 5.91 take into account the cross section of pair production in the nuclei field and in the electron field. Contribution from only atomic nuclei is proportional to $\propto Z^2$ while if we take into account also pair production in the electron field one has to replace $Z^2 \to Z(Z+1)$.

Taking into account all damping terms due to interactions of photons with the medium, the damping matrix Γ with elements, $\Gamma_{\lambda\lambda'} = \langle\Psi_\lambda|\hat{\Gamma}|\Psi_{\lambda'}\rangle\delta_{\lambda\lambda'}$ which enters Liouville-von Neumann equations is given by $\Gamma = \text{diag}[\Gamma_\gamma, 0]$. The damping term for photons, Γ_γ is given by

$$\Gamma_\gamma = n_e\sigma_{KN} + \sum_i n_i\sigma_{pp}^i, \tag{5.92}$$

where n_e is the free electron number density, n_i is the number density of the i-th atomic specie, σ_{KN} is the total cross section due to Compton scattering and σ_{pp} is the total absorption cross section due to pair production. The damping term due to Compton scattering is given by (in units of cm^{-1})

$$\Gamma_\gamma^C(a) = 1.6\cdot 10^{-22}X_e(a)F(a;\omega_i)\left[\frac{a_i}{a}\right]^3, \tag{5.93}$$

where $F(a;\omega_i) = F(x)$ with $F(x)$ being the expression within the square brackets in Equation 5.89. However, in what follow we take $X_e(a) = 1$ in the case of Compton scattering. In fact, in the energy range $\omega > m_e$, the energy of the formed γ-photons is very high so they are very penetrating and as a result these photons will scatter not only the free electrons in the plasma but even the atomic electrons of the hydrogen and helium. The total damping term which arises due to pair production is the sum of damping on hydrogen and helium nuclei. By noting that for hydrogen the atomic number is $Z = 1$ and for helium $Z = 2$ we can easily see that $\sigma_{pp}^{(He)} = 3\sigma_{pp}^{(H)}$. The total number density per co-moving volume of hydrogen atoms is $n_H \simeq n_B$ and the total number density of primordial atomic helium is $n_{He} \simeq Y_p n_B/4(1-Y_p)$ where $Y_p = 4n_{He}/(4n_{He}+n_H)$ is the fractional abundance by weight of primordial helium. Taking this into account, the damping term due to pair production on hydrogen and helium atoms is given by (in units of cm^{-1})

$$\Gamma_\gamma^{pp} \simeq 9.85\cdot 10^{-25}\left(1+\frac{3}{4}\frac{Y_p}{Y_p-1}\right)G(a;\omega_i)\left[\frac{a_i}{a}\right]^3, \tag{5.94}$$

where $G(a;\omega_i) = G(x)$ is the function within square brackets in Equation 5.90. In Figure 5.9 are shown Γ_γ^C and Γ_γ^{pp} due to Compton scattering and pair production. We can see that for initial graviton energy $\omega_i = 10^9$ eV, Γ_γ^{pp} (red dashed color) is larger than Γ_γ^C (red color) for $a < 10$, here we use the normalization $a_i = 1$ at recombination time and $Y_p \simeq 0.24$. For $a > 10$ Γ_γ^C takes over Γ_γ^{pp} which goes to zero at the beginning of re-ionization epoch. In the case of graviton initial energy $\omega_i = 10^8$ eV, $\Gamma_\gamma^{pp} \sim \Gamma_\gamma^C$ for $a < 5$ and for $a > 5$, Γ_γ^{pp} rapidly decreases to zero when the photon energy is below the threshold of pair production $\omega(a) < 2m_e$. Therefore, Γ_γ^{pp} due pair production is important only for photon energies above 10^8 eV and completely negligible for lower photon energies.

As in section 5.5, here we solve equations of motions for the elements of the density matrix ρ in the case of $\omega > m_e$ in the post-recombination epoch. In the energy range $\omega > m_e$ and for some particular value of the graviton energy the oscillation of gravitons into photons is in resonance and an enhancement of the oscillation probability occurs. The resonance is reached when there is a level crossing between the QED effects due to vacuum polarization and plasma effects. In this case there is a maximum mixing between the graviton and the photon. Level crossing occurs, when $m(a) = 0$ and in this case the resonance energy as a function of the scale factor is given by Equation 5.81. Given a graviton with energy as a function of the scale factor $\omega(a) = \omega_i/a$, its energy would eventually cross the resonance energy when $\omega_{\rm res}(a) = \omega(a)$. Since the resonance energy depends on the ionization fraction and due to the fact that an analytical form of the last is unknown, in Figure 5.10 we present a graphical solution of $\omega_{\rm res}(a) = \omega(a)$. We can clearly see that the resonance is crossed in general relatively early respect to the recombination epoch and in some cases it is crossed twice as in the case of gravitons with initial energy $\omega_i = 10^7$ eV and initial value of magnetic field $B_i = 3\cdot 10^{-3}$ G.

The background of GWs at recombination epoch is assumed to be unpolarized and isotropic and therefore the following initial conditions $\rho_{\gamma\gamma}(a_i) = 0, \rho_{gg}(a_i) = 1/2, R(a_i) =$

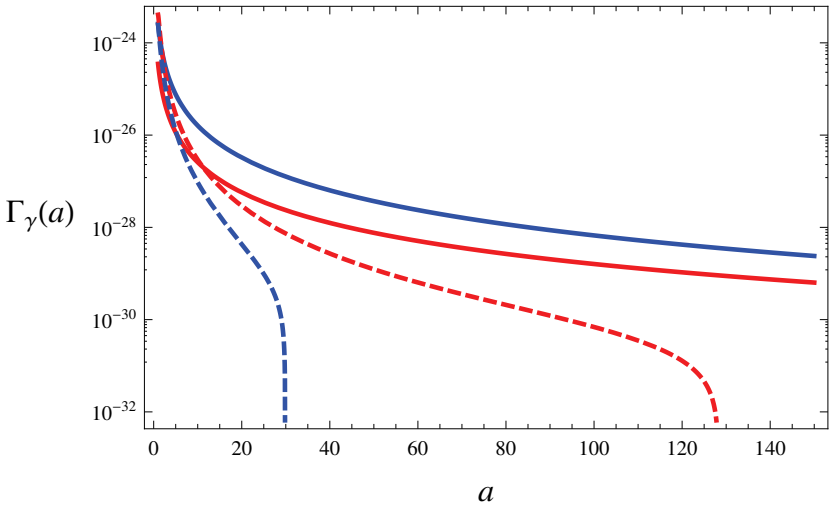

Figure 5.9: Plot of Γ_γ^C and Γ_γ^{pp} as a function of the scale factor a. For initial graviton energy $\omega_i = 10^9$ eV it is shown Γ_γ^C (in red color) and Γ_γ^{pp} (in red dashed color). For initial graviton energy $\omega_i = 10^8$ eV it is shown Γ_γ^C (in blue color) and Γ_γ^{pp} (in blue dashed color).

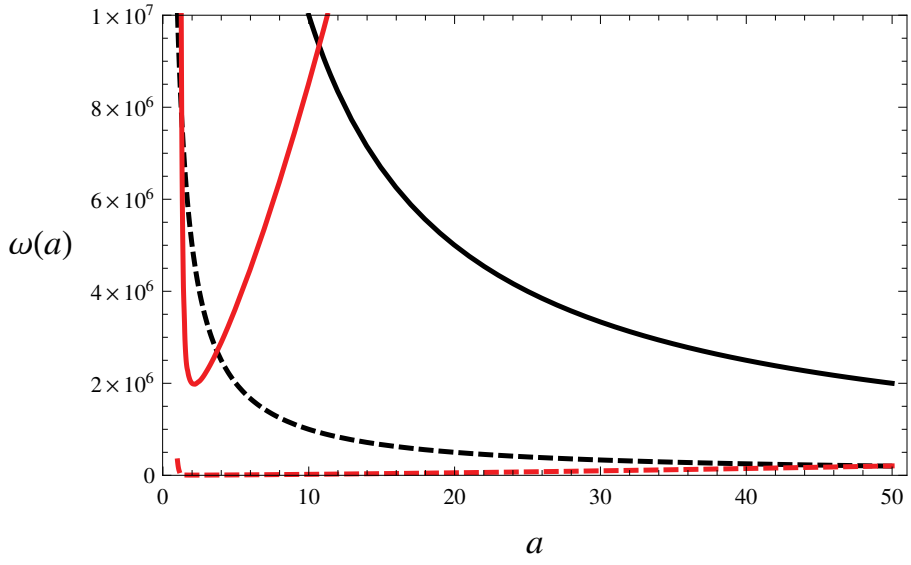

Figure 5.10: Plot of the resonance frequency $\omega_{\rm res}$ and graviton frequency ω as a function of the scale factor a. In black color and in black dashed color are presented respectively the the graviton energies as a function of a for initial graviton energies $\omega_i = 10^8$ eV and $\omega_i = 10^7$ eV. In red color and in red dashed color are presented the resonance energies respectively for initial value of magnetic field $B_i = 3 \cdot 10^{-3}$ G and $B_i = 1.2$ G.

0 and $I(a_i) = 0$ are imposed on solutions of Equation 5.70. The factor $1/2$ in the initial conditions for the graviton probability takes into account the statistical weight of the polarization state λ. However, since we are working on the reduced density matrix of the system, namely we solve its equation of motion for a given polarization state λ, at the end we should multiply $\rho_{\gamma\gamma}$ by a factor two in order to take into account that the initial background of GWs is composed by two independent polarization states. In Figure 5.11 and Figure 5.12 it is shown the photon survival probability as a function of the scale factor a starting from recombination epoch until the present epoch. In deriving our results we took into account the universe re-ionization. In Figure 5.11 and Figure 5.12 it can be clearly seen that once the onset of re-ionization starts $a \sim 52$ the photon survival probability starts contemporarily oscillating and decreasing until the universe start being dominated by the vacuum energy at $a \sim 545$ where afterwards the probability remains practically constant.

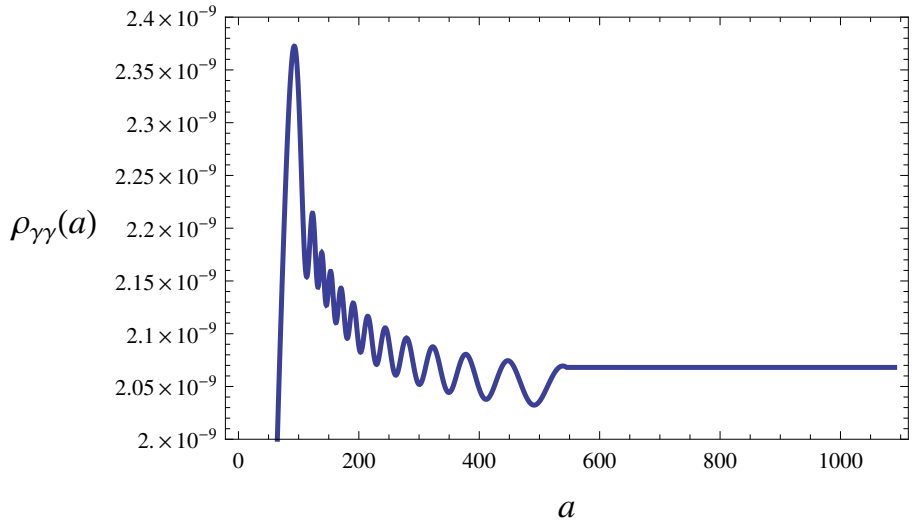

Figure 5.11: Plot of photon survival probability as a function of the scale factor for initial graviton energy $\omega_i = 10^7$ eV and initial value of magnetic field $B_i = 3 \cdot 10^{-3}$ G.

The photon production probability depends on several factors such as the energy of initial gravitons and the matter content in the post recombination epoch. In fact we can see in Figure 5.11 and Figure 5.12 a rapid increase on the oscillation or survival probability starting from relatively early $a < 10$ in the case of initial value of magnetic field $B_i = 3 \cdot 10^{-3}$ G where the resonance is crossed twice and an increase that starts from $a \sim 50$ in the case of $B_i = 1.2$ G. Such rise is partly explained by a rapid decrease of the ionization fraction which starts to grow at $a \simeq 1$ and approaches asymptotically a constant value at $a \simeq 20$. Another factor leading to an increase of the production probability is the resonance effect due to a decrease of the graviton energy. In Figure 5.13, Figure 5.14, Figure 5.15, Figure 5.16 are shown the photon production probabilities at

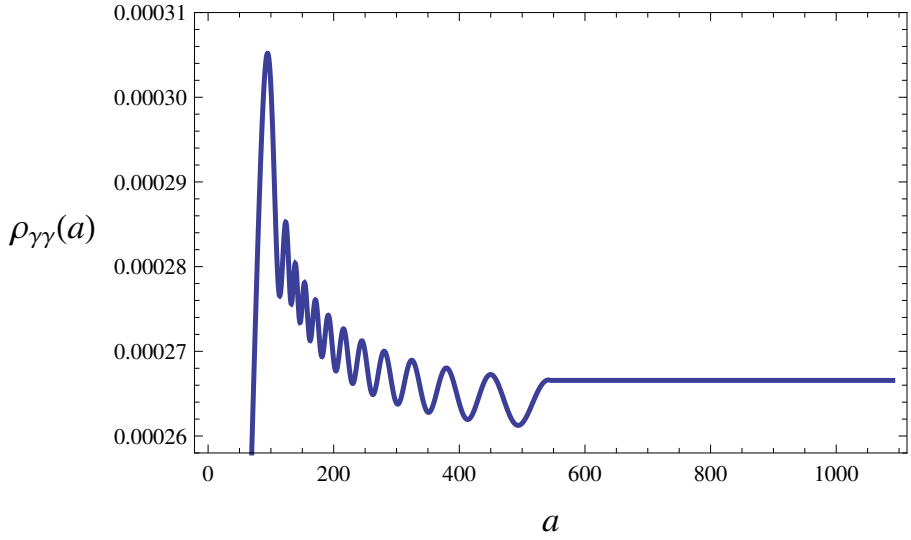

Figure 5.12: Plot of photon survival probability as a function of the scale factor for initial graviton energy $\omega_i = 10^7$ eV and initial value of magnetic field $B_i = 1.2$ G.

present epoch as a function of photon energy. We can clearly observe that the probability is quite high in comparison with the non resonant case with a difference of three orders of magnitude. The peak of the production probability depends essentially on the initial value of magnetic field at recombination. For $B_i > 1$ G the peak probability is reached in the frequency range $1 - 10$ keV and for $B_1 < 1$ G it is reached approximately for energies of 100 keV.

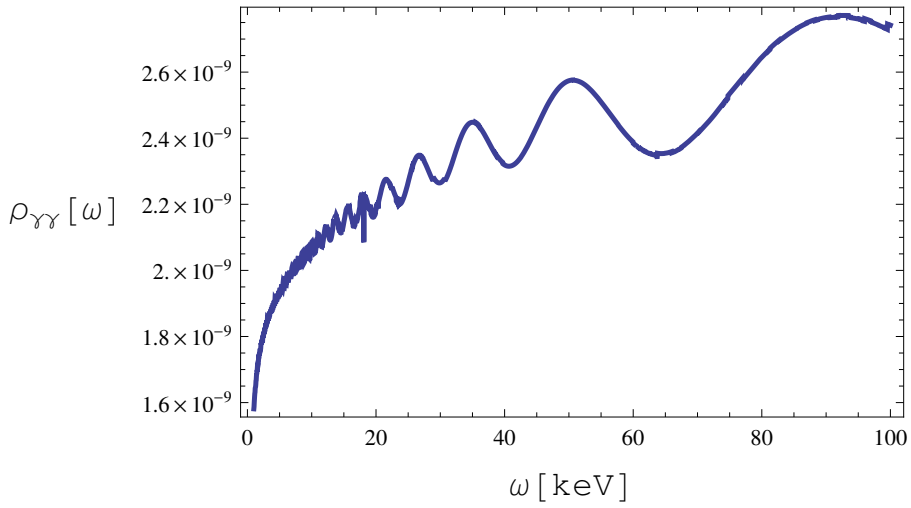

Figure 5.13: Probability $P_{g\gamma} = \rho_{\gamma\gamma}$ of photon production by graviton as a function of photon energy at present $a = 1090$ for initial value of magnetic field $B_i \simeq 3 \cdot 10^{-3}$ G.

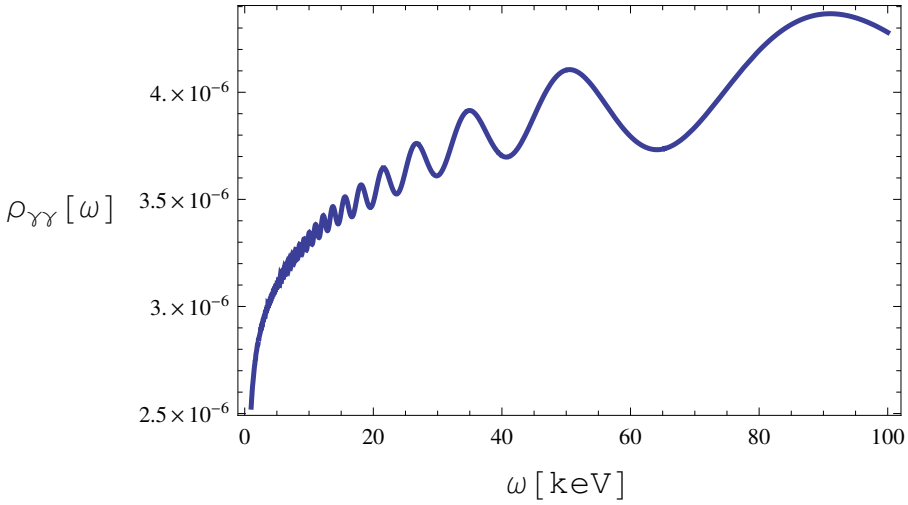

Figure 5.14: Probability $P_{g\gamma} = \rho_{\gamma\gamma}$ of photon production by graviton as a function of photon energy at present $a = 1090$ for initial value of magnetic field $B_i \simeq 0.12$ G.

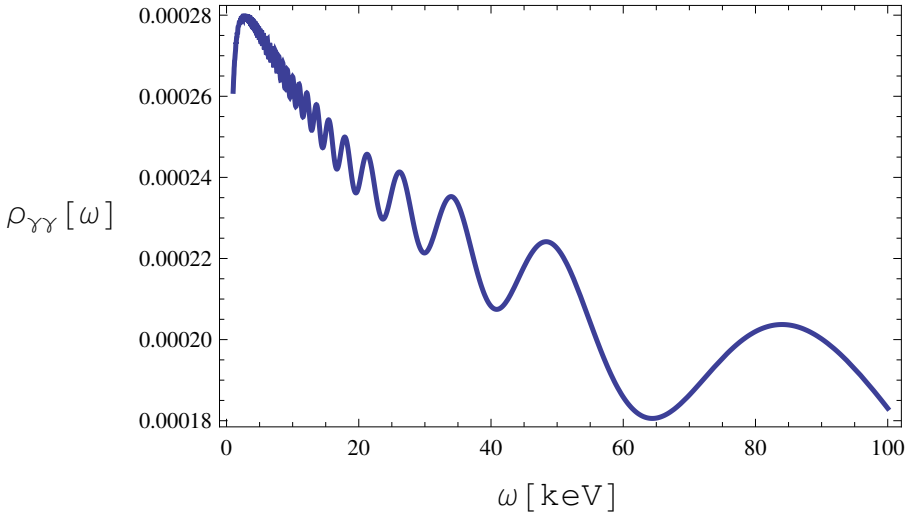

Figure 5.15: Probability $P_{g\gamma} = \rho_{\gamma\gamma}$ of photon production by graviton as a function of photon energy at present $a = 1090$ for initial value of magnetic field $B_i \simeq 1.2$ G.

In section 5.6 we discussed several mechanisms of GWs production in the early universe and calculated probability of the graviton-photon transformation in the high energy part of the graviton spectrum. The production probability of photons as a consequence of transformation of gravitons into photons resulted completely negligible for most of models apart from the model proposed in [14] where the amount of GWs produced by PBHs is substantial and concentrated in frequency range of eV or keV. Here we present

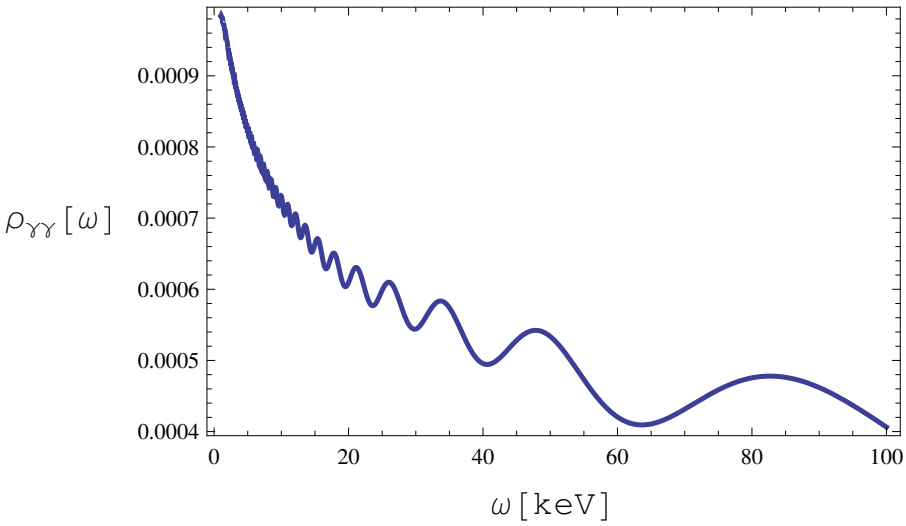

Figure 5.16: Probability $P_{g\gamma} = \rho_{\gamma\gamma}$ of photon production by graviton as a function of photon energy at present $a = 1090$ for initial value of magnetic field $B_i \simeq 2.37$ G.

detailed calculations about the spectrum of formed photons for higher energies, namely in the energy range of few keV. As discussed in chapter 4 a black hole emits a wide spectrum of particles with mass $m < T_{BH}$ and reduces its total energy E according to Equation 4.113. Taking into that the emitted gravitons as a result of BH evaporation accounts for roughly 1% of the total energy, the flux of GWs emitted by a BH with mass M_{BH} at present is given by using Equation 4.121

$$F_{\rm gw}(\omega;t_0) = 8.35\cdot 10^{10}\left(\frac{\omega}{1{\rm keV}}\right)^4\left(\frac{10^5{\rm gr}}{M}\right)^2\left(\frac{N_{eff}}{100}\right)^2 I\left(\frac{\omega}{T_{\rm BH0}}\right)\left[\frac{\rm keV}{{\rm cm}^2\ {\rm s}}\right], \quad (5.95)$$

where $T_{\rm BH0}$ is the present day temperature of an evaporating BH in the instant decay approximation and we use the fact that for a stochastic background of GWs the energy flux is given by $F_{\rm gw} = cT_{00}^{\rm gw} = c\rho_c\Omega_{\rm gw}$ with $T_{00}^{\rm gw}$ being the energy momentum tensor of GWs and $\rho_c \simeq 5.27$ keV/cm^3 is the critical energy density. In Figure 5.17 and Figure 5.18 it is shown the energy flux in photons at present epoch $F_\gamma(\omega) = \rho_{\gamma\gamma}(\omega)\cdot F_{\rm gw}(\omega)$ as a result of graviton to photon oscillation in the case of PBHs with mass $M_{BH} \simeq 10^8$ g, $N_{eff} \sim 100$ and $\Omega_p = 10^{-3}$. We can clearly see a substantial contribution to the CXB in the case of initial value of magnetic field $B_i \simeq 2.37$ G which corresponds to present day field of $B(t_0) \simeq 2\cdot 10^{-6}$ G. The maximum of the spectrum is approximately $\omega_{max} \simeq 2.8\,T_{\rm BH0}$ and correspond to the photon energy $\omega_{max} \simeq 2.25$ keV and a flux of $F_\gamma \simeq 18$ keV/cm^2 s^{-1}. In the case of $B_i = 3\cdot 10^{-3}$ G the peak of the flux is several orders of magnitude smaller and has a value of approximately $F_\gamma \simeq 3\cdot 10^{-5}$ keV/cm^2 s^{-1}.

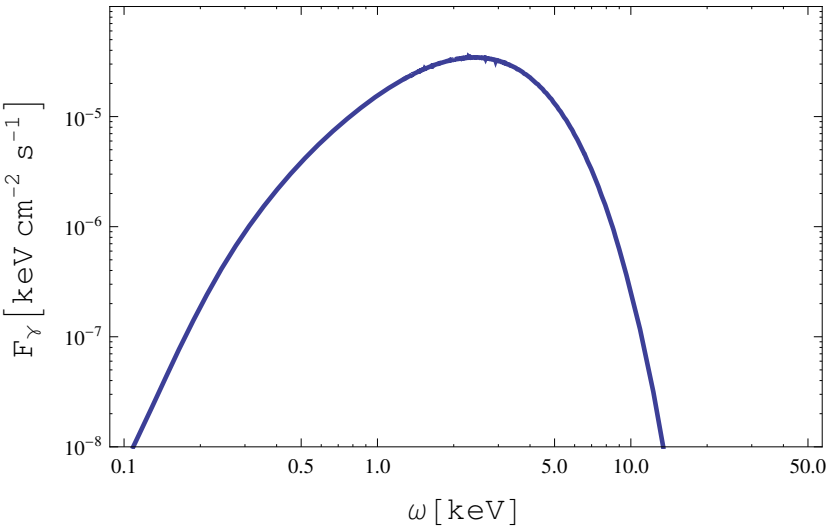

Figure 5.17: Plot of photon energy flux F_γ by transformations of gravitons into photons as a function of photon energy ω at present $a = 1090$ for initial value of magnetic field $B_i \simeq 3 \cdot 10^{-3}$ G

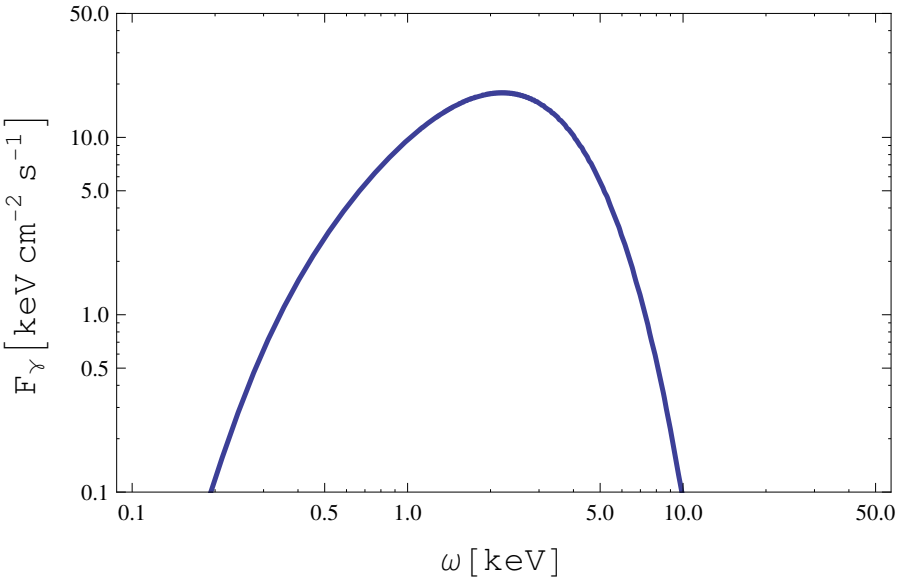

Figure 5.18: Plot of photon energy flux F_γ by transformations of gravitons into photons as a function of photon energy ω at present $a = 1090$ for initial value of magnetic field $B_i \simeq 2.37$ G.

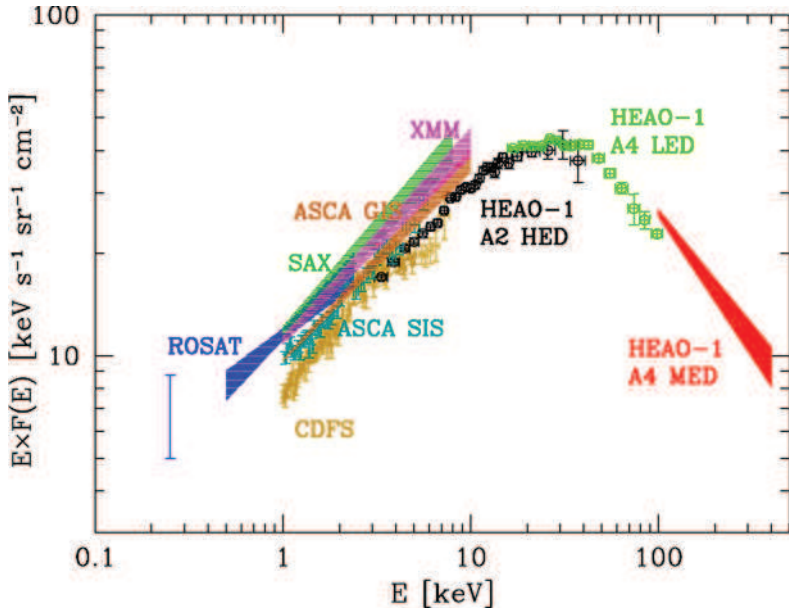

Figure 5.19: Energy flux of the extragalactic X-ray background spectrum from 0.2 to 400 keV as given in [143]. Most of the energy flux is concentrated in the energy band of 10-100 keV where the spectrum presents a peak at 30 keV with flux of approximately of 40 keV/cm^2 s^{-1}.

Results

In this thesis we have analyzed the formation and evolution of light primordial black holes in the early Universe which created a transient matter domination regime in contrast to the present standard cosmology, where the early Universe after inflation was normally radiation dominated. PBHs with masses less than $M \sim 10^8$ g evaporated before primordial nucleosynthesis leaving no trace. Thus the fraction of the energy density of such PBHs, Ω_p, in this case is a free parameter of the model, not constrained by any existing observations.

At MD stage the PBHs could form high density clusters which would be efficient sources of the primordial GWs. PBHs could have dominated the Universe for a short time of the order of their lifetime, τ_{BH}, generating relic gravitational waves by various mechanisms of their mutual interactions as well as due to their evaporation. In the former case we have shown that production of GWs is most efficient after BH density started to dominate over radiation. After that moment, high density clusters of PBHs could have been formed, leading to an efficient production of GWs. To survive till cluster formation the PBH mass at production must be bounded from below by $M \sim 4 \cdot 10^{-5}$ g $\Omega_p^{-1}\Delta_{in}^{-3/4}N_{eff}^{1/2}$, Equation 4.16, which leads to a lower bound $\Omega_p > 10^{-14}\Delta_{in}^{-3/4}N_{eff}^{1/2}$. According to the standard cosmology the amplitude of primordial density perturbations is of order of $\sim 10^{-4}$, which in our case leads to a lower bound on the density parameter of PBHs, $\Omega_p \gtrsim 10^{-11}$.

In this context we have calculated the density parameter of GWs today from scattering of PBHs in both classical and quantum regime, GWs emission from binaries, and from black hole evaporation. We have shown that a substantial amount of gravitational waves has been emitted by all mechanisms considered here. In the case of scattering of PBHs we considered *only* scattering between them neglecting the possibility of PBHs merging, which results in an underestimate on $h_0^2\Omega_{GW}$. Even in this case the density parameter is substantial at high frequencies reaching values of the order of $h_0^2\Omega_{GW} \sim 10^{-9}$ at $f \sim$ GHz for classical scattering, Equation 4.66 and the total density parameter $h_0^2\Omega_{GW} \sim 10^{-10}$ for very light primordial black holes. In the low frequency limit the density parameter in the classical case is of the order of $h_0^2\Omega_{GW} \sim 10^{-17}-10^{-20}$ in the frequency range $f \sim 10^{-1} - 10^2$ Hz which falls into the detection band of DECIGO/BBO.

The number of PBHs that form binaries after cluster formation is subjected to uncertainties and in this paper we parametrized it through factor ϵ. The exact value of this parameter could be calculated elsewhere by numerical calculations. Since the density in such clusters is very high we expect that ϵ is not very small in comparison with unity. In Figure 4.2 the expected value of the density parameter of gravitational waves today is presented. We can see that a large amount of gravitational waves has been emitted in the high frequency regime with $h_0^2\Omega_{GW} \sim 10^{-14} - 10^{-12}$ at frequency $f \sim 10^{10}$ Hz, Equation 4.104, on the BH initial mass.

In the low frequency part of the spectrum the spectral density parameter is utterly negligible making it impossible to detect GWs produced by this mechanism at present and probably in the near future. In our derivation we have considered both stationary and inspiral phases of binaries leading to a wide range of the frequencies emitted. We have considered only binaries in circular orbits and the problem with elliptical orbits will be treated later. If elliptical orbits were frequent, the amount of GWs will be presumably higher over a wide range of frequencies. We assumed that all binaries are formed with initial radius less than the average distance between PBHs and greater than the gravitational radius r_g. In this case the frequency spectrum has a cutoff in both low and high frequency bands of the spectrum.

Another mechanism of graviton productions considered here is the PBHs evaporation. This mechanism is independent on the structure formation during the PBH domination. In Figure 4.3 we show the density parameter as a function of frequency for BH masses 1 g and 10^5 g. Having a near blackbody spectrum, the frequency of the emitted gravitons can have any value, but unfortunately the GWs spectrum has a peak in the high frequency region which today make a substantial contribution into the cosmological energy density of the order of $h_0^2\Omega_{GW}(f_{peak}) \sim 10^{-7}$, Equation 4.121.

The mechanisms considered in this paper could create a rather high cosmological fraction of the energy density of the relic gravitational waves at very high frequencies and gives an opportunity on investigating the high GWs spectrum by present and future detectors. Unfortunately at the lower part of the spectrum Ω_{GW} significantly drops down. Still the planned interferometers DECIGO/BBO could be sensitive to the predicted GWs. It is noteworthy that the mechanism of GWs generation suggested here kills or noticeably diminishes GWs from inflation by the redshift of the earlier generated GWs at the PBH (MD) stage.

In connection with the high frequency part of the GW spectrum emitted by PBHs as thermal gravitons, we have shown that the non-resonant probability of the graviton-to-photon transition in large scale cosmological magnetic field after recombination epoch could be in the range $P_{g\gamma} \sim 10^{-10} - 10^{-5}$ at frequencies in 0.1 keV range (in the present day values). An efficient oscillations between graviton and photon could exist at higher frequencies too, but here we limit only at energies below the electron mass. For smaller frequencies, e.g. 1 eV, the transition probability would be smaller, by about 2-3 orders of magnitude. The oscillation probability strongly depends on the external

magnetic field and the graviton energy. For higher values of these parameters, as our numerical calculations show, the oscillation probability can increase by several orders of magnitude.

The photons produced by such mechanism could make considerable contribution to cosmic electromagnetic background if the density of the original gravitational waves, $h_0^2\Omega_{\rm gw}$, is sufficiently high. We have estimated efficiency of the photon production in various models of primordial GW generation discussed in the literature. Mostly, in the considered inflationary and post-inflationary models the density of photons produced by the GWs is quite low and is not observable at the present time.

The mechanism discussed here gives a large number of photons (for fixed values of the magnetic field) only for high frequency gravitons. We think that given the present GWs production models the only mechanism before BBN that could generate a measurable flux of photons is the graviton production by primordial black holes. Since PBH emit thermal gravitons (if one neglects gray body corrections) the spectrum of the GWs today would be rather close to the original one with some distortion induced by the different cosmological moments of GW creation.

After hydrogen recombination the plasma density drops down and the interaction of the photons, created by the graviton-photon transition, with electrons becomes much weaker in complete analogy with the CMB photons. Such photons could make observable contributions to the cosmological electromagnetic background, in particular, to X-rays or extragalactic light. If we consider a conservative present day density parameter $h_0^2\Omega_{\rm gw}(t_0) \simeq 10^{-7} - 10^{-8}$, the energy flux in X-rays by the proposed mechanism would be of the order $F_\gamma \simeq 10^{-10} - 10^{-15}$ erg/cm^2/s, Equation 5.87, where the flux upper limit is 10 percent less than the observed energy flux in the soft X-rays [144, 145, 146]. If we assume that the total density of the gravitational waves reaches its upper bound allowed by BBN (and explains the possibly observed dark radiation), $h_0^2\Omega_{\rm gw}(t_0) \lesssim 10^{-5}$, and that their frequency is close to 0.1 keV, the energy flux today would be in the range, $F_\gamma \simeq 10^{-8} - 10^{-13}$ erg/cm^2/ s. This energy flux could a possible explanation of the low part spectrum of the cosmic X-ray background being its dominant part without requiring any obscured AGN.

In the case of gravitons with energy $\omega_i \gg m_e$ the calculated photon production probability is quite high in comparison with the non-resonant case where the conversion probability is by several orders of magnitude smaller. Even in this case the effective Lagrangian which takes into account non linear terms of QED reduces to the well known Euler-Heisenberg Lagrangian where the energy of gravitons can be several orders of magnitude higher than the electron mass. In this limit the resonance oscillation is possible whenever the term $m = 0$ Equation 5.70 is zero which corresponds to the resonance energy given by Equation 5.81. Once the resonance is crossed the graviton-photon mixing is maximum with a mixing angle $\theta = \pi/4$ and a complete transition is possible. A clear evidence of resonance transition can be seen in Figure 5.11 and Figure 5.12 where a rapid increase occurs relatively early after recombination where the increase in the

transition probability is also due to a rapid decrease of the ionization plasma. The probability of photon production apart on depending on the factors mentioned above it also depends on the mechanism of produced gravitons before recombination time, namely graviton production by PBH evaporation. In Figure 5.13, Figure 5.14, Figure 5.15 and Figure 5.14 we show photon production probability by graviton to photon oscillation as a function of photon energy at present time where the probability reaches high values such as $\rho_{\gamma\gamma} \sim 10^{-3}$. In Figure 5.17 and Figure 5.18 we show the spectrum of produced photons in the case of PBHs with mass of $M_{BH} \sim 10^8$ g.

Depending on the value of the magnetic field at recombination and on the PBH mass, the produced photons in the resonant case could also make an important contribution to the extragalactic background light as in the non-resonant case. In fact, if the PBH mass is about $M_{BH} \sim 10^8$ g and $B_i \sim$ few $\cdot$ G the produced spectrum of electromagnetic radiation is the dominant component of the CXB in the the energy band of $0.1 - 10$ keV, Figure 5.17, Figure 5.18 and Fig. 5.19. In the case of $B_i \sim$ few $\cdot 10^{-3}$ and $M_{BH} \sim 10^8$ g the contribution to the CXB is smaller but still comparable with the flux of some AGN averaged over all sky. In the case of lower PBH mass (for example $M_{BH} \sim 10^5 - 10^7$ g) the spectrum is shifted to the lower part of CXB and in the ultraviolet and the oscillation probability in this energy range is several orders of magnitude smaller than the resonant case. In fact, the peak energy is proportional to the PBH temperature essentially through the combination $\omega_{max} \propto T_{BH} \propto (M/N_{eff})^{1/2}$ keV$^{1/2}$ due to the redshift of the graviton energy from the evaporation moment to the present time. So in principle heavier is the BH the greater is the peak energy where the energy flux is maximal. If one assume that the contribution to N_{eff} comes only from the standard model with $N_{eff} \sim O(10^2)$ and requiring that PBHs evaporate before BBN, the maximum mass of PBH allowed is about 10^8 g with a spectrum of produced photons given in Figure 5.17 and Figure 5.18. On the other hand if extra contribution beyond the standard model are taken into account with $N_{eff} \geqslant 10^3$ the allowed PBH maximum mass by BBN can be higher than 10^8 g. Since the redshifted PBH temperature is $T_{BH} \simeq 0.2 (M_{BH}/10^5 \text{g})^{1/2} N_{eff}^{-1/2}$ keV and knowing that the PBH mass is bounded from above $M_{BH} \lesssim 3.88 \cdot 10^7 N_{eff}^{1/3}$ g and that $T_{BH} \lesssim 4\, N_{eff}^{-1/3}$ keV, one can conclude that higher is the effective number of particle species the smaller should be the PBH temperature in order to evaporate before BBN. Consequently higher is the number of particle species, smaller is the redshifted PBH temperature at present T_{BH0}. So, if we assume for example that, $N_{eff} \sim 10^5$ the maximum value of the PBH mass from BBN is about $M \sim 10^9$ g and the ratio of M_{BH}/N_{eff} is smaller in comparison with the case of a PBH with a mass of $M \sim 10^8$ g and $N_{eff} \sim 100$. This would imply that for a BH with a mass of $M_{BH} \sim 10^9$ g the spectrum of produced photons is shifted to the lower part of CXB and ultraviolet. This is a consequence of the BBN bound on the maximum PBHs mass.

Thus what we have been discussing so far can be also used to constrain several parameters if others are known. In fact from observation of CXB, observation of other energy bands where the graviton to photon conversion is efficient and based on the pre-

dicted energy flux of this mechanism, it is possible to constrain either the magnitude of cosmological magnetic field B or the PBH mass and its density parameter production Ω_p.

Bibliography

[1] A. Einstein. Über Gravitationswellen. *Sitzungsberichte der Königlich Preußischen Akademie der Wissenschaften (Berlin), Seite 154-167.*, pages 154–167, 1918.

[2] Thibault Damour. An introduction to the theory of gravitational radiation . 1986.

[3] P. Havas. Equations of motion and radiation reaction in the special and general theory of relativity. In J. Ehlers, editor, *Isolated Gravitating Systems in General Relativity*, pages 74–155, 1979.

[4] M.H. Poincaré. Sur la dynamique de llectron. *Rendiconti del Circolo matematico di Palermo*, 21:129–175, 1906.

[5] Albert Einstein and N. Rosen. On Gravitational waves. *J.Franklin Inst.*, 223:43–54, 1937.

[6] Arthur Stanley Eddington. The propagation of gravitational waves. *Proc.Roy.Soc.Lond.*, A102:268–282, 1922.

[7] R.A. Hulse and J.H. Taylor. Discovery of a pulsar in a binary system. *Astrophys.J.*, **195**:L51–L53, 1975.

[8] T. Damour and R. Ruffini. Certain new verifications of general relativity made possible by the discovery of a pulsar belonging to a binary system. *Academie des Sciences Paris Comptes Rendus Serie Sciences Mathematiques*, 279:971–973, December 1974.

[9] J. H. Taylor and P. M. McCulloch. Evidence for the existence of gravitational radiation from measurements of the binary pulsar PSR 1913+16. In J. Ehlers, J. J. Perry, and M. Walker, editors, *Ninth Texas Symposium on Relativistic Astrophysics*, volume 336 of *Annals of the New York Academy of Sciences*, pages 442–446, February 1980.

[10] K.S. Thorne. Multipole Expansions of Gravitational Radiation. *Rev.Mod.Phys.*, 52:299–339, 1980.

[11] T. Damour. Gravitational radiation reaction in the binary pulser and the quadrupole formula controversy. *Phys.Rev.Lett.*, 51:1019–1021, 1983.

[12] L.P. Grishchuk. Amplification of gravitational waves in an istropic universe. *Sov.Phys.JETP*, 40:409–415, 1975.

[13] Alexei A. Starobinsky. Relict Gravitation Radiation Spectrum and Initial State of the Universe. (In Russian). *JETP Lett.*, 30:682–685, 1979.

[14] Alexander D. Dolgov and Damian Ejlli. Relic gravitational waves from light primordial black holes. *Phys.Rev.*, D84:024028, 2011.

[15] Alexander D. Dolgov and Damian Ejlli. Conversion of relic gravitational waves into photons in cosmological magnetic fields. *JCAP*, 1212:003, 2012.

[16] Charles W. Misner, K.S. Thorne, and J.A. Wheeler. Gravitation. 1974.

[17] L.D. Landau, E.M. Lifshitz, (Ed.) Schopf, H.G., and (Ed.) Ziesche, P. TEXTBOOK ON THEORETICAL PHYSICS. VOL. 2: CLASSICAL FIELD THEORY. (IN GERMAN). 1987.

[18] Michele Maggiore. Gravitational Waves. Vol. 1: Theory and Experiments. 2007.

[19] Richard A. Isaacson. Gravitational Radiation in the Limit of High Frequency. I. The Linear Approximation and Geometrical Optics. *Phys.Rev.*, 166:1263–1271, 1967.

[20] Richard A. Isaacson. Gravitational Radiation in the Limit of High Frequency. II. Nonlinear Terms and the Ef fective Stress Tensor. *Phys.Rev.*, 166:1272–1279, 1968.

[21] J. Weber. Evidence for discovery of gravitational radiation. *Phys.Rev.Lett.*, 22:1320–1324, 1969.

[22] J. Weber. Anisotropy and polarization in the gravitational-radiation experiments. *Phys.Rev.Lett.*, 25:180–184, 1970.

[23] M. E. Gertsenshteĭn and V. I. Pustovoĭt. On the Detection of Low-Frequency Gravitational Waves. *Soviet Journal of Experimental and Theoretical Physics*, 16:433, 1963.

[24] R. L. Forward. Wideband laser-interferometer gravitational-radiation experiment. *Phys. Rev. D*, 17:379–390, Jan 1978.

[25] V. B. Braginsky and A. B. Manukin. *Measurement of weak forces in physics experiments*. 1977.

[26] C. M. Caves, K. S. Thorne, R. W. P. Drever, V. D. Sandberg, and M. Zimmermann. On the measurement of a weak classical force coupled to a quantum-mechanical oscillator. I. Issues of principle. *Reviews of Modern Physics*, 52:341–392, April 1980.

[27] Pau Amaro-Seoane, Sofiane Aoudia, Stanislav Babak, Pierre Binetruy, Emanuele Berti, et al. eLISA: Astrophysics and cosmology in the millihertz regime. 2012.

[28] Naoki Seto, Seiji Kawamura, and Takashi Nakamura. Possibility of direct measurement of the acceleration of the universe using 0.1-Hz band laser interferometer gravitational wave antenna in space. *Phys.Rev.Lett.*, 87:221103, 2001.

[29] S. Kawamura, T. Nakamura, M. Ando, N. Seto, K. Tsubono, et al. The Japanese space gravitational wave antenna DECIGO. *Class.Quant.Grav.*, 23:S125–S132, 2006.

[30] Seiji Kawamura, Masaki Ando, Takashi Nakamura, Kimio Tsubono, Takahiro Tanaka, et al. The Japanese space gravitational wave antenna: DECIGO. *J.Phys.Conf.Ser.*, 120:032004, 2008.

[31] G.M. Harry, P. Fritschel, D.A. Shaddock, W. Folkner, and E.S. Phinney. Laser interferometry for the big bang observer. *Class.Quant.Grav.*, 23:4887–4894, 2006.

[32] Jeff Crowder and Neil J. Cornish. Beyond LISA: Exploring future gravitational wave missions. *Phys.Rev.*, D72:083005, 2005.

[33] E. Komatsu et al. Seven-Year Wilkinson Microwave Anisotropy Probe (WMAP) Observations: Cosmological Interpretation. *Astrophys.J.Suppl.*, 192:18, 2011.

[34] Steven Weinberg. Cosmology. 2008.

[35] Bruce Allen. The Stochastic gravity wave background: Sources and detection. 1996.

[36] Michele Maggiore. Gravitational wave experiments and early universe cosmology. *Phys.Rept.*, 331:283–367, 2000.

[37] L.P. Grishchuk. Discovering Relic Gravitational Waves in Cosmic Microwave Background Radiation. 2007.

[38] Alan H. Guth and So-Young Pi. The Quantum Mechanics of the Scalar Field in the New Inflationary Universe. *Phys.Rev.*, D32:1899–1920, 1985.

[39] L.F. Abbott and D.D. Harari. GRAVITON PRODUCTION IN INFLATIONARY COSMOLOGY. *Nucl.Phys.*, B264:487, 1986.

[40] E. Lifshitz. On the Gravitational stability of the expanding universe. *J.Phys.(USSR)*, 10:116, 1946.

[41] Edward W. Kolb and Michael S. Turner. The Early universe. *Front.Phys.*, 69:1–547, 1990.

[42] R. Fabbri and M.d. Pollock. The Effect of Primordially Produced Gravitons upon the Anisotropy of the Cosmological Microwave Background Radiation. *Phys.Lett.*, B125:445–448, 1983.

[43] L.F. Abbott and Mark B. Wise. Constraints on Generalized Inflationary Cosmologies. *Nucl.Phys.*, B244:541–548, 1984.

[44] E. Komatsu et al. Five-Year Wilkinson Microwave Anisotropy Probe (WMAP) Observations: Cosmological Interpretation. *Astrophys.J.Suppl.*, 180:330–376, 2009.

[45] Hiranya Peiris and Richard Easther. Slow Roll Reconstruction: Constraints on Inflation from the 3 Year WMAP Dataset. *JCAP*, 0610:017, 2006.

[46] S.Y. Khlebnikov and I.I. Tkachev. Relic gravitational waves produced after preheating. *Phys.Rev.*, D56:653–660, 1997.

[47] Richard Easther and Eugene A. Lim. Stochastic gravitational wave production after inflation. *JCAP*, 0604:010, 2006.

[48] Richard Easther, John T. Giblin, and Eugene A. Lim. Gravitational Waves From the End of Inflation: Computational Strategies. *Phys.Rev.*, D77:103519, 2008.

[49] Michael S. Turner and Frank Wilczek. Relic gravitational waves and extended inflation. *Phys.Rev.Lett.*, 65:3080–3083, 1990.

[50] Arthur Kosowsky, Michael S. Turner, and Richard Watkins. Gravitational radiation from colliding vacuum bubbles. *Phys.Rev.*, D45:4514–4535, 1992.

[51] Arthur Kosowsky and Michael S. Turner. Gravitational radiation from colliding vacuum bubbles: envelope approximation to many bubble collisions. *Phys.Rev.*, D47:4372–4391, 1993.

[52] Marc Kamionkowski, Arthur Kosowsky, and Michael S. Turner. Gravitational radiation from first order phase transitions. *Phys.Rev.*, D49:2837–2851, 1994.

[53] K. Kajantie, M. Laine, K. Rummukainen, and Mikhail E. Shaposhnikov. The Electroweak phase transition: A Nonperturbative analysis. *Nucl.Phys.*, B466:189–258, 1996.

[54] Christophe Grojean and Geraldine Servant. Gravitational Waves from Phase Transitions at the Electroweak Scale and Beyond. *Phys.Rev.*, D75:043507, 2007.

[55] Alexander Vilenkin. Cosmic Strings and Domain Walls. *Phys.Rept.*, 121:263, 1985.

[56] A. Vilenkin. COSMIC STRINGS AND OTHER TOPOLOGICAL DEFECTS. 1986.

[57] Craig J. Hogan. Gravitational Waves from Light Cosmic Strings: Backgrounds and Bursts with Large Loops. *Phys.Rev.*, D74:043526, 2006.

[58] Matthew R. DePies and Craig J. Hogan. Stochastic Gravitational Wave Background from Light Cosmic Strings. *Phys.Rev.*, D75:125006, 2007.

[59] Anupam Mazumdar and Ian M. Shoemaker. Extreme gravitational waves from inflaton fragmentation. 2010.

[60] B.P. Abbott et al. An Upper Limit on the Stochastic Gravitational-Wave Background of Cosmological Origin. *Nature*, 460:990, 2009.

[61] A.D. Dolgov, P.D. Naselsky, and I.D. Novikov. Gravitational waves, baryogenesis, and dark matter from primordial black holes. *Phys.Rev.D*, 2000.

[62] S.W. Hawking. Black Holes and Thermodynamics. *Phys.Rev.*, D13:191–197, 1976.

[63] Don N. Page. Particle Emission Rates from a Black Hole: Massless Particles from an Uncharged, Nonrotating Hole. *Phys.Rev.*, D13:198–206, 1976.

[64] B.J. Carr, Kazunori Kohri, Yuuiti Sendouda, and Jun'ichi Yokoyama. New cosmological constraints on primordial black holes. *Phys.Rev.*, D81:104019, 2010.

[65] Amandeep S. Josan, Anne M. Green, and Karim A. Malik. Generalised constraints on the curvature perturbation from primordial black holes. *Phys.Rev.*, D79:103520, 2009.

[66] Y. B. Zel'dovich and I. D. Novikov. The Hypothesis of Cores Retarded during Expansion and the Hot Cosmological Model. *azh*, 43:758, 1966.

[67] Stephen Hawking. Gravitationally collapsed objects of very low mass. *Mon.Not.Roy.Astron.Soc.*, 152:75, 1971.

[68] Bernard J. Carr and S.W. Hawking. Black holes in the early Universe. *Mon.Not.Roy.Astron.Soc.*, 168:399–415, 1974.

[69] Alexandre Dolgov and Joseph Silk. Baryon isocurvature fluctuations at small scales and baryonic dark matter. *Phys.Rev.*, D47:4244–4255, 1993.

[70] A.D. Dolgov, M. Kawasaki, and N. Kevlishvili. Inhomogeneous baryogenesis, cosmic antimatter, and dark matter. *Nucl.Phys.*, B807:229–250, 2009.

[71] Bernard J. Carr. Primordial black holes: Do they exist and are they useful? 2005.

[72] M. Yu. Khlopov. Primordial Black Holes. *Res.Astron.Astrophys.*, 10:495–528, 2010.

[73] J. D. Barrow, E. J. Copeland, and A. R. Liddle. The evolution of black holes in an expanding universe. *mnras*, 253:675–682, December 1991.

[74] Y. B. Zel'dovich and A. A. Starobinskii. Possibility of a cold cosmological singularity in the spectrum of primordial black holes. *Soviet Journal of Experimental and Theoretical Physics Letters*, 24:571–573, December 1976.

[75] A. D. Dolgov. The quantum evaporation of black holes and the baryon asymmetry of the universe. *Zhurnal Eksperimental noi i Teoreticheskoi Fiziki*, 79:337–349, August 1980.

[76] A. D. Dolgov. Hiding of the conserved (anti)baryonic charge into black holes. *Phys. Rev. D*, 24:1042–1044, Aug 1981.

[77] J. D. Barrow. Primordial baryon generation by black holes. *mnras*, 192:427–438, August 1980.

[78] J. D. Barrow and G. G. Ross. Cosmological constraints on the scale of grand unification. *Nuclear Physics B*, 181:461–486, April 1981.

[79] J. D. Barrow, E. J. Copeland, E. W. Kolb, and A. R. Liddle. Baryogenesis in extended inflation. II. Baryogenesis via primordial black holes. *prd*, 43:984–994, February 1991.

[80] Daniel Baumann, Paul J. Steinhardt, and Neil Turok. Primordial Black Hole Baryogenesis. 2007.

[81] D.J. Fixsen. The Temperature of the Cosmic Microwave Background. *Astrophys.J.*, 707:916–920, 2009.

[82] B.M. Barker, S.N. Gupta, and J. Kaskas. Graviton bremsstrahlung and infrared divergence. *Phys.Rev.*, 182:1391–1396, 1969.

[83] A. Sommerfeld. Über die Beugung und Bremsung der Elektronen. *Annalen der Physik*, 403:257–330, 1931.

[84] A.D. Sakharov. INTERACTION OF AN ELECTRON AND POSITRON IN PAIR PRODUCTION. *Zh.Eksp.Teor.Fiz.*, 18:631–635, 1948.

[85] K. Nakamura et al. Review of particle physics. *J.Phys.*, G37:075021, 2010.

[86] Bernard F. Schutz. A FIRST COURSE IN GENERAL RELATIVITY. 1985.

[87] P.C. Peters. Relativistic gravitational bremsstrahlung. *Phys.Rev.*, D1:1559–1571, 1970.

[88] J. Binney and S. Tremaine. *Galactic Dynamics: Second Edition*. Princeton University Press, 2008.

[89] Cosimo Bambi, Douglas Spolyar, Alexander D. Dolgov, Katherine Freese, and Marta Volonteri. Implications of primordial black holes on the first stars and the origin of the super–massive black holes. *Mon.Not.Roy.Astron.Soc.*, 399:1347–1356, 2009.

[90] P.C. Peters and J. Mathews. Gravitational radiation from point masses in a Keplerian orbit. *Phys.Rev.*, 131:435–439, 1963.

[91] E.S. Phinney. A Practical theorem on gravitational wave backgrounds. 2001.

[92] Richard Anantua, Richard Easther, and John T. Giblin. GUT-Scale Primordial Black Holes: Consequences and Constraints. *Phys.Rev.Lett.*, 103:111303, 2009.

[93] (ed.) Frolov, V.P. and (ed.) Novikov, I.D. Black hole physics: Basic concepts and new developments. 1998.

[94] A. D. Dolgov. Neutrinos in cosmology. *physrep*, 370:333–535, November 2002.

[95] M. E. Gertsenshtein. Wave resonance of light and gravitational waves . *Sov. Phys. JETP*, 14:84, 1961.

[96] N. V. Mitskevich. *Fizicheskie polya v obschej teorii otnositelnosti (Physical fields in general relativity)*. Nauka, Moscow Russia, 1970.

[97] D. Boccaletti, V. Sabbata, P. Fortini, and C. Gualdi. Conversion of photons into gravitons and vice versa in a static electromagnetic field. *Il Nuovo Cimento B Series 10*, 70:129–146, 1970.

[98] V. K. Dubrovich. Generation of an electromagnetic wave by a plane gravitational wave in a constant magnetic field . *Izv. Spet. Astro. Obs.*, 6:27, 1972.

[99] Ya. B. Zel'dovich. Electromagnetic and gravitational waves in a stationary magnetic field . *Sov. Phys. JETP*, 38:652, 1974.

[100] Daniele Fargion. Prompt and delayed radio bangs at kilohertz by SN1987A: A Test for gravitation - photon conversion. *Grav.Cosmol.*, 1:301–310, 1995.

[101] Georg Raffelt and Leo Stodolsky. Mixing of the Photon with Low Mass Particles. *Phys.Rev.*, D37:1237, 1988.

[102] W. Heisenberg and H. Euler. Consequences of Dirac's theory of positrons. *Z.Phys.*, 98:714–732, 1936.

[103] Julian S. Schwinger. On gauge invariance and vacuum polarization. *Phys.Rev.*, 82:664–679, 1951.

[104] E. Brezin and C. Itzykson. Polarization phenomena in vacuum nonlinear electrodynamics. *Phys.Rev.*, D3:618–621, 1971.

[105] Stephen L. Adler. Photon splitting and photon dispersion in a strong magnetic field. *Annals Phys.*, 67:599–647, 1971.

[106] Carlo Giunti and Chung W. Kim. Fundamentals of Neutrino Physics and Astrophysics. 2007.

[107] R. Durrer, P.G. Ferreira, and T. Kahniashvili. Tensor microwave anisotropies from a stochastic magnetic field. *Phys.Rev.*, D61:043001, 2000.

[108] John D. Barrow, Pedro G. Ferreira, and Joseph Silk. Constraints on a primordial magnetic field. *Phys.Rev.Lett.*, 78:3610–3613, 1997.

[109] Daniela Paoletti and Fabio Finelli. Constraints on a Stochastic Background of Primordial Magnetic Fields with WMAP and South Pole Telescope data. 2012.

[110] Daniela Paoletti and Fabio Finelli. CMB Constraints on a Stochastic Background of Primordial Magnetic Fields. *Phys.Rev.*, D83:123533, 2011.

[111] Daniela Paoletti, Fabio Finelli, and Francesco Paci. The full contribution of a stochastic background of magnetic fields to CMB anisotropies. *Mon.Not.Roy.Astron.Soc.*, 396:523–534, 2009.

[112] Tina Kahniashvili, Yurii Maravin, and Arthur Kosowsky. Faraday rotation limits on a primordial magnetic field from Wilkinson Microwave Anisotropy Probe five-year data. *Phys.Rev.*, D80:023009, 2009.

[113] Chiara Caprini and Ruth Durrer. Gravitational wave production: A Strong constraint on primordial magnetic fields. *Phys.Rev.*, D65:023517, 2001.

[114] Chiara Caprini and Ruth Durrer. Limits on stochastic magnetic fields: A Defense of our paper [1]. *Phys.Rev.*, D72:088301, 2005.

[115] Arthur Kosowsky, Tina Kahniashvili, George Lavrelashvili, and Bharat Ratra. Faraday rotation of the Cosmic Microwave Background polarization by a stochastic magnetic field. *Phys.Rev.*, D71:043006, 2005.

[116] Massimo Giovannini. The Magnetized universe. *Int.J.Mod.Phys.*, D13:391–502, 2004.

[117] Dario Grasso and Hector R. Rubinstein. Magnetic fields in the early universe. *Phys.Rept.*, 348:163–266, 2001.

[118] J.J. Matese and R.F. O'Connell. Neutron Beta Decay in a Uniform Constant Magnetic Field. *Phys.Rev.*, 180:1289–1292, 1969.

[119] R. F. O'CONNELL and J. J. MATESE. Effect of a constant magnetic field on the neutron beta decay rate and its astrophysical implications. *Nature*, 222(5194):649–650, 05 1969.

[120] GEORGE GREENSTEIN. Primordial helium production in [ldquo]magnetic[rdquo] cosmologies. *Nature*, 223(5209):938–939, 08 1969.

[121] Peter J. Kernan, Glenn D. Starkman, and Tanmay Vachaspati. Comment on 'Constraints on the strength of primordial B fields from big bang nucleosynthesis reexamined'. *Phys.Rev.*, D56:3766–3767, 1997.

[122] Bao-lian Cheng, Angela V. Olinto, David N. Schramm, and James W. Truran. Constraints on the strength of primordial magnetic fields from big bang nucleosynthesis revisited. *Phys.Rev.*, D54:4714–4718, 1996.

[123] Peter J. Kernan, Glenn D. Starkman, and Tammay Vachaspati. Big bang nucleosynthesis constraints on primordial magnetic fields. *Phys.Rev.*, D54:7207–7214, 1996.

[124] Dario Grasso and H.R. Rubinstein. Limits on possible magnetic fields at nucleosynthesis time. *Astropart.Phys.*, 3:95–102, 1995.

[125] N. A. Zabotin and P. D. Naselskii. The Neutrino Background in the Early Universe and Temperature Fluctuations in the Cosmic Microwave Radiation. *sovast*, 26:272, June 1982.

[126] B. J. T. Jones and R. F. G. Wyse. The ionisation of the primeval plasma at the time of recombination. *aap*, 149:144–150, August 1985.

[127] M.S. Pshirkov and D. Baskaran. Limits on High-Frequency Gravitational Wave Background from its interplay with Large Scale Magnetic Fields. *Phys.Rev.*, D80:042002, 2009.

[128] A.D. Dolgov. Neutrinos in the Early Universe. *Sov.J.Nucl.Phys.*, 33:700–706, 1981.

[129] G. Sigl and G. Raffelt. General kinetic description of relativistic mixed neutrinos. *Nucl.Phys.*, B406:423–451, 1993.

[130] A.D. Dolgov. Neutrinos in cosmology. *Phys.Rept.*, 370:333–535, 2002.

[131] D. G. Hummer. Total Recombination and Energy Loss Coefficients for Hydrogenic Ions at Low Density for 10 T/E/Z/2 10/7K. *mnras*, 268:109, May 1994.

[132] D. Pequignot, P. Petitjean, and C. Boisson. Total and effective radiative recombination coefficients. *aap*, 251:680–688, November 1991.

[133] J. Dunkley et al. Five-Year Wilkinson Microwave Anisotropy Probe (WMAP) Observations: Likelihoods and Parameters from the WMAP data. *Astrophys.J.Suppl.*, 180:306–329, 2009.

[134] Alain Coc. Primordial Nucleosynthesis. 2012.

[135] I. Lehmann, Gunther Hasinger, M. Schmidt, R. Giacconi, J. Truemper, et al. The rosat deep survey: vi. x-ray sources and optical identifications of the ultra deep survey. *Astron.Astrophys.*, 371:833–857, 2001.

[136] M. Akiyama, K. Ohta, T. Yamada, N. Kashikawa, M. Yagi, W. Kawasaki, M. Sakano, T. Tsuru, Y. Ueda, T. Takahashi, I. Lehmann, G. Hasinger, and W. Voges. Optical Identification of the ASCA Large Sky Survey. *apj*, 532:700–727, April 2000.

[137] Wu-yang Tsai and Thomas Erber. Photon Pair Creation in Intense Magnetic Fields. *Phys.Rev.*, D10:492, 1974.

[138] Wu-yang Tsai and Thomas Erber. The Propagation of Photons in Homogeneous Magnetic Fields: Index of Refraction. *Phys.Rev.*, D12:1132, 1975.

[139] W. Dittrich and H. Gies. Probing the quantum vacuum. Perturbative effective action approach in quantum electrodynamics and its application. *Springer Tracts Mod.Phys.*, 166:1–241, 2000.

[140] W. Heitler. *Quantum theory of radiation*. 1954.

[141] R. Cruddace, F. Paresce, S. Bowyer, and M. Lampton. On the opacity of the interstellar medium to ultrasoft X-rays and extreme-ultraviolet radiation. *APJ*, 187:497–504, February 1974.

[142] O. Klein and T. Nishina. Über die Streuung von Strahlung durch freie Elektronen nach der neuen relativistischen Quantendynamik von Dirac. *Zeitschrift fur Physik*, 52:853–868, November 1929.

[143] Roberto Gilli. The x-ray background and the deep x-ray surveys. 2003.

[144] M. Ajello, J. Greiner, G. Sato, D.R. Willis, G. Kanbach, et al. Cosmic X-ray background and Earth albedo Spectra with Swift/BAT. 2008.

[145] Guenther Hasinger. Formation and evolution of supermassive black holes in galactic centers: Observational constraints. *AIP Conf.Proc.*, 666:227–236, 2003.

[146] Gunther Hasinger, Richard Burg, Riccardo Giacconi, Maarten Schmidt, Joachim Truemper, et al. The ROSAT Deep Survey. 1. X-ray sources in the Lockman Field. *Astron.Astrophys.*, 329:482–494, 1998.

Appendices

Appendix A

Basics of cosmology

A.1 Cosmological Principle and FLRW metric

Today we know very well that the earth is not the center of our Universe. Moreover, our solar system, our galaxy or our local group of galaxies does not occupy a special position in the Universe. This would suggest that all positions in the Universe are equivalent, independently where the observer is located. In fact, a large portion of modern cosmology is built on the *Cosmological Principle*, which states that on large scales our universe is homogeneous and isotropic. Homogeneity here applies only to large scales of the order of kpc where we consider a portion of universe averaged on large scales and doesn't apply to the universe in detail because on galactic scales our universe is inhomogeneous rather than homogeneous. However, homogeneity on large scales doesn't guarantees that the entire Universe is smooth, but we can safely assume as a work hypotheses that a region at least as large as our Hubble volume is smooth.

The Cosmological Principle should be putted in a mathematical framework in order to describe the evolution of the Universe. The first step to be done in this direction, is to choose a coordinate system equivalent for all observers and this can be achieved by choosing a spatial coordinate x^i with origin $x^i = 0$ at earth or on our Milky Way. Having fixed the origin of our coordinate system, we can choose the axes directions in such a way that the coordinate direction is fixed by the line of sight from the earth to some typical object or galaxy and with a scale distance defined by the apparent luminosities of distant galaxies. The time coordinate can be defined by using the Universe evolution as a standard clock. From CMB observations we know that its temperature has been monotonically decreasing since the last scattering time, so we can choose for example the CMB temperature T_γ and define the time event as a function of the temperature $t(T_\gamma)$. The chosen coordinate system (x,t) so defined is called the cosmic standard coordinate system.

The metric for a space which obeys to the Cosmological Principle is the maximally-

symmetric Friedemann-Robertson-Walker (FRW) metric which reads

$$ds^2 = -dt^2 + a^2(t)\left(\frac{dr^2}{1-Kr^2} + r^2 d\theta^2 + r^2 \sin^2\theta d\phi^2\right), \tag{A.1}$$

where $a(t)$ is the scale factor which is defined as $x(t) = a(t)r$ with $x(t)$ being the proper distance, (t, r, θ, ϕ) are called comoving coordinates, K is the spatial curvature which can have the values $+1, 0, -1$ respectively for spaces of constant positive, negative, or zero curvature. Here we will considerer only an Euclidean space with flat spatial geometry, namely $K = 0$ and Equation A.1 becomes

$$ds^2 = -dt^2 + a^2(t)\left(dr^2 + r^2 d\Omega^2\right), \tag{A.2}$$

where $d\Omega$ is the differential solid angle.

It is interesting to consider the geometrical properties of the metric given by Equation A.1 which has the following metric components

$$g_{00} = -1, \quad g_{rr} = \frac{a^2(t)}{1-Kr^2}, \quad g_{\theta\theta} = a^2(t)r^2, \quad g_{\phi\phi} = a^2(t)r^2\sin^2\theta. \tag{A.3}$$

Maximally-symmetric spaces have the property that the Riemann tensor can be simply written as

$$R_{\mu\nu\alpha\beta} = K(g_{\alpha\nu}g_{\mu\beta} - g_{\beta\nu}g_{\mu\alpha}), \tag{A.4}$$

and with the help of metric components given by Equation A.3 the non zero spatial components of the Riemann tensor, Ricci tensor and Ricci scalar are given by

$${}^3R_{ijkl} = \frac{K}{a^2(t)}(g_{ik}g_{lj} - g_{il}g_{jk}), \quad {}^3R_{ij} = \frac{2K}{a^2(t)}g_{ij}, \quad {}^3R = \frac{6K}{a^2(t)}. \tag{A.5}$$

A.2 Cosmological redshift

The Friedmann metric Equation A.1 is non static because of the time dependence of the scale factor $a(t)$. Since $a(t)$ multiplies the spatial coordinates, any proper distance $d(t)$ will change with time in proportion to $a(t)$

$$d(r,t) = a(t)\int_0^r \frac{dr}{\sqrt{1-Kr^2}}. \tag{A.6}$$

In the case of an Euclidean space, we have a flat geometry with $K = 0$ and the proper distance is simply given by $d(t) = a(t)r$.

In order to establish if the scale factor $a(t)$ is a decreasing, increasing or constant function, is important to see how the electromagnetic radiation propagates in the FLRW metric. Since electromagnetic radiation (photons) propagates on null geodesics, their line element in any space is $ds^2 = 0$. If we consider the electromagnetic radiation coming toward the origin (us) in the radial direction, the condition $ds^2 = 0$ gives

$$dt = \pm a(t)\frac{dr}{\sqrt{1-Kr^2}}. \tag{A.7}$$

Thus, if the light ray leaves the souce located at the co-moving coordinate r_1 at the proper time t_1 it will reach the origin $r = 0$ at the time t_0 given by

$$\int_{t_1}^{t_0} \frac{dt}{a(t)} = \int_0^{r_1} \frac{dr}{\sqrt{1 - Kr^2}}. \tag{A.8}$$

Differentiating Equation A.8, we get the following relation between the interval δt_1 of two departure signals and δt_0 of their arrival intervals

$$\frac{\delta t_1}{a(t_1)} = \frac{\delta t_0}{a(t_0)}. \tag{A.9}$$

Since δt_1 and δt_0 are respectively the times between two successive wave crests of the emitted and detected light, the corresponding wavelength of the emitted and detected light ($\lambda = 1/\delta t$) is related to the scale factor $a(t_1)$ and $a(t_0)$ as follows

$$\frac{\lambda_1}{\lambda_0} = \frac{a(t_1)}{a(t_0)}. \tag{A.10}$$

If $a(t)$ is increasing (decreasing) this led to a redshift (blueshift) of the light from the source. Thus, the change in the scale factor in cosmology is defined through the term $1 + z$ which is defined as

$$1 + z = \frac{f_1}{f_0} = \frac{\lambda_0}{\lambda_1}, \tag{A.11}$$

where f is the light frequency. In the case of *redshift* z is positive and in the case of *blueshift* z is negative. If a source is located near to us we can expand the scale factor $a(t)$ in power series and get

$$a(t) = a(t_0) + \dot{a}(t_0)(t - t_0) + ... = a(t_0)[1 + H_0(t - t_0) + ...], \tag{A.12}$$

where the coefficient H_0 is called the *Hubble constant*

$$H_0 = H(t_0) = \frac{\dot{a}(t_0)}{a(t_0)}. \tag{A.13}$$

A.3 Friedmann equations

With the metric components given by Equation A.3 let us now derive the Friedemann equations and see how the Universe evolve with time. The dynamics of the Universe is governed by Einstein field equations which we can write in a convenient form

$$R_{\mu\nu} = 8\pi G\,(T_{\mu\nu} - \frac{1}{2} g_{\mu\nu} T). \tag{A.14}$$

First of all we need to calculate the Ricci tensor which is given by

$$R_{\mu\nu} = \partial_\rho \Gamma^\rho_{\nu\mu} - \partial_\nu \Gamma^\rho_{\rho\mu} + \Gamma^\rho_{\rho\sigma}\Gamma^\sigma_{\nu\mu} - \Gamma^\rho_{\nu\sigma}\Gamma^\sigma_{\rho\mu}, \tag{A.15}$$

where the Christoffel symbols are given by Equation 1.3. We need to calculate only R_{00} and R_{ij}. We don't need to calculate R_{i0} because its a three vector and must vanish in the FRW metric. Before calculating the components of $R_{\mu\nu}$ let us see which components of the affine connection are different from zero. Thus we have

$$\Gamma^0_{ij} = a\dot{a}\,h_{ij}, \tag{A.16}$$

$$\Gamma^i_{0j} = \frac{a}{\dot{a}}\delta_{ij}, \tag{A.17}$$

$$\Gamma^i_{jk} = \frac{1}{2}g^{il}(\partial_k g_{lj} + \partial_j g_{lk} - \partial_l g_{jk}), \tag{A.18}$$

where $g_{ij} = a^2(t)h_{ij}$ and δ_{ij} being the Kronecker symbol. The non zero components of the Ricci tensor now read

$$R_{00} = -\partial_0\Gamma^i_{0i} - \Gamma^j_{0k}\Gamma^k_{0i} = -3\frac{d}{dt}\left(\frac{\dot{a}}{a}\right) - 3\left(\frac{\dot{a}}{a}\right)^2 = -3\frac{\ddot{a}}{a} \tag{A.19}$$

$$R_{ij} = 2\dot{a}^2 h_{ij} + a\ddot{a}h_{ij} + {}^3R_{ij} = (2\dot{a}^2 + a\ddot{a} + 2k)h_{ij} \tag{A.20}$$

$$R_{0i} = 0. \tag{A.21}$$

Next step is to have an expression for the energy-momentum tensor which satisfies the requirements of isotropy and homogeneity. This means that the components $T_{0i} = 0$ and the most general form of the energy momentum tensor is that of a perfect fluid characterized by a time dependent energy density $\rho(t)$ and pressure $p(t)$. The expression for the energy- momentum tensor of a perfect fluid is given by

$$T^{\mu\nu} = pg^{\mu\nu} + (p+\rho)u^\mu u^\nu, \qquad g_{\mu\nu}u^\mu u^\nu = -1, \tag{A.22}$$

where the fluid four-velocity is normalized in such a way that $u^\mu = (1,0,0,0)$. The components of $T_{\mu\nu}$ are given by

$$T_{00} = \rho(t), \quad T_{0i} = 0, \quad T_{ij} = a^2(t)p(t)h_{ij}. \tag{A.23}$$

Let us define $S_{\mu\nu} = T_{\mu\nu} - g_{\mu\nu}T/2$, then the S_{00} and S_{ij} components read

$$S_{ij} = T_{ij} - \frac{1}{2}h_{ij}a^2(T^k_k + T^0_0) = \frac{a^2}{2}(\rho - p)h_{ij} \tag{A.24}$$

$$S_{00} = T_{00} + \frac{1}{2}(T^k_k + T^0_0) = \frac{1}{2}(\rho + 3p) \tag{A.25}$$

$$S_{0i} = 0. \tag{A.26}$$

Now we have all needed quantities in order to solve the Einstein field equations, Equation A.14, which gives the following equations for R_{00} and R_{ij}

$$\frac{\ddot{a}}{a} + 2\frac{\dot{a}^2}{a^2} + 2\frac{K}{a^2} = 4\pi G(\rho - p) \tag{A.27}$$

$$-\frac{3\ddot{a}}{a} = 4\pi G(3p + \rho). \tag{A.28}$$

We can sum together Equation A.27 and Equation A.28 by multiplying first Equation A.27 by a factor three. As a result we get the following Friedmann equation

$$H^2 = \frac{8\pi G\rho}{3} - \frac{K}{a^2}. \tag{A.29}$$

In order to have a complete set of equations for the dynamics of the Universe we miss an equation describing the conservation of energy in the FLRW metric. We can get such an equation by simply writing down the conservation of the energy-momentum tensor in the FLRW metric. Since the space-time is curved, the conservation of energy-momentum tensor in general relativity reads

$$\nabla_\mu T^{\mu\nu} = 0. \tag{A.30}$$

Since we are interested in the energy conservation, Equation A.30 for the components $T^{0\mu}$ gives

$$\nabla_\mu T^{0\mu} = \partial_t T^{00} + \Gamma^0_{ij} T^{ij} + \Gamma^i_{i0} T^{00} = 0. \tag{A.31}$$

Taking into account both Equation A.16 and Equation A.17 and introducing into Equation A.31 we get the following equation

$$\dot{\rho} + 3H(p + \rho) = 0 \tag{A.32}$$

The energy conservation, Equation A.32 and Equation A.29 are the two fundamental equations in cosmology which can completely describe the dynamics of the Universe once we know how the pressure p is related with the energy density ρ. The most simplest relation between the two is the equation of state $p = w\rho$, where w is a constant. In this case the solution of Equation A.32 for a flat geometry, $K = 0$, is simply given by

$$\rho \propto a^{-3(1+w)}. \tag{A.33}$$

The most important cases in cosmology are respectively for matter, radiation and vacuum domination energy density which correspond to $(w = 0, \rho/3, -1)$ respectively. For matter dominated Universe the energy density scales as

$$\rho(t) = \rho(t_0) \left(\frac{a(t_0)}{a(t)} \right)^3. \tag{A.34}$$

Introducing Equation A.34 into Equation A.33 we get the following solution for the scale factor

$$a(t) \propto t^{-2/3}, \tag{A.35}$$

which gives the following relation of the Hubble parameter with cosmological time,

$$H = 2/3t. \tag{A.36}$$

Combining Equation A.36 with Equation A.29 we get the following relation of energy density with time for the Einstein-de Sitter model

$$\rho(t) = 1/6\pi G t^2. \tag{A.37}$$

For an Universe dominated by radiation (RD) the energy density scales with the scale factor as

$$\rho(t) = \rho(t_0)\left(\frac{a(t_0)}{a(t)}\right)^4, \tag{A.38}$$

and the scale factor scales with the cosmological time as

$$a(t) \propto t^{1/2}. \tag{A.39}$$

In this case the relation of the Hubble parameter with time is $H = 1/2t$ which gives the following relation of the energy density with time

$$\rho(t) = 3/32\pi G t^2. \tag{A.40}$$

In the FLRW metric the connection between the curvature and the energy density is given by Equation A.29. This equation can be written in a more convenient form such as

$$\frac{K}{H^2 a^2} \equiv \Omega - 1, \tag{A.41}$$

where Ω is called the density parameter which is defined as

$$\Omega = \frac{\rho}{\rho_c}, \qquad \rho_c = \frac{3H^2}{8\pi G}, \tag{A.42}$$

where ρ_c is called critical energy density. From Equation A.41 we can easily see that if $K = 1, \rho > \rho_c$ then $\Omega > 1$ which implies that the geometry of the Universe is closed and it will contract up to a singularity at $a = 0$. For $K = 0$ the geometry of the Universe is flat (Euclidean) and $\Omega = 1$. In this model the Universe will expand forever since $a(t) > 0$. In the case of hyperbolic geometry (open Universe) $K = -1$ and $\Omega < 1$ and the Universe will eventually expands forever.

In general the energy content in the Universe is a mixture of non-relativistic matter, relativistic matter and vacuum energy, namely $\rho = \sum_i \rho_i$, where ρ_i is the contribution from the i-th mixture. One can obtain very useful relations by expressing the total energy density ρ as a function of the density parameter of the i-th mixture. In general by an arbitrary constant curvature K and using Equation A.42 we obtain the following important expression for the total energy density as a function of time

$$\rho(t) = \rho_c(t_0)\left[\Omega_M\left(\frac{a_0}{a}\right)^3 + \Omega_R\left(\frac{a_0}{a}\right)^4 + \Omega_\Lambda\right], \tag{A.43}$$

where Ω_M is the present epoch density parameter of matter, Ω_R is the present epoch density parameter of radiation and Ω_Λ is the present epoch density parameter associated to the vacuum energy. Still using Equation A.42 we can define a density parameter associated the curvature of the Universe, which at present is $\Omega_K = -K/a_0^2 H_0^2$ where the total density parameter satisfies the relation

$$\Omega_M + \Omega_R + \Omega_\Lambda + \Omega_K = 1. \tag{A.44}$$

By introducing Equation A.43 into Equation A.29 and after some algebraical manipulations we get the following equations for the differential time

$$dt = -\frac{dx}{H_0 x\sqrt{\Omega_\Lambda + \Omega_K x^{-2} + \Omega_M x^{-3} + \Omega_R x^{-4}}}, \tag{A.45}$$

where $x = a/a_0 = 1/(1+z)$. Integration over time gives an important relation of the cosmological time as a function of redshift

$$t(z) = \frac{1}{H_0}\int_0^{1/(1+z)} \frac{dx}{x\sqrt{\Omega_\Lambda + \Omega_K x^{-2} + \Omega_M x^{-3} + \Omega_R x^{-4}}}. \tag{A.46}$$

A.4 Thermodynamics in the FLRW metric

As we saw in the previous section, the universe has been expanding since its formation and passed different stages of cosmological evolution. Despite, the fact that thermodynamic equilibrium is not maintained in an expanding universe, CMB observations suggest that during its early stages, the particles composing the early plasma can be considered to a good approximation in *local* thermodynamic equilibrium with each other. For a particle in local thermodynamic equilibrium the number density, energy density and pressure are given by

$$n = \frac{g}{(2\pi)^3}\int d^3p f(|\mathbf{p}|), \tag{A.47}$$

$$\rho = \frac{g}{(2\pi)^3}\int d^3p E(|\mathbf{p}|) f(|\mathbf{p}|), \tag{A.48}$$

$$p = \frac{g}{(2\pi)^3}\int d^3p \frac{|\mathbf{p}|}{3E} f(|\mathbf{p}|), \tag{A.49}$$

where g is the is the number of degrees of freedom, $\mathbf{p}$ is the particle momentum and $f(|\mathbf{p}|)$ is the equilibrium distribution function which in the FLRW metric depend only on the scalar momentum, $p = |\mathbf{p}|$. If the considered particles are in kinetic and chemical equilibrium, their distribution function can be written as

$$f(E) = \frac{1}{e^{(E-\mu)/T} \pm 1}, \tag{A.50}$$

where $E = \sqrt{p^2 + m^2}$, μ is the chemical potential which satisfies $\sum_i \mu_i = 0$, T is the plasma temperature and the sign $\pm$ takes into account for the different statistics satisfied by bosons (-1) and fermions (+1). Inserting Equation A.50 into Equation A.47 we get the following expressions for the particle number density, energy density and pressure

$$n = \frac{g}{2\pi^2}\int_m^\infty dE \frac{E(E^2-m^2)^{1/2}}{\exp[(E-\mu)/T] \pm 1}, \tag{A.51}$$

$$\rho = \frac{g}{2\pi^2}\int_m^\infty dE \frac{E^2(E^2-m^2)^{1/2}}{\exp[(E-\mu)/T] \pm 1}, \tag{A.52}$$

$$p = \frac{g}{6\pi^2}\int_m^\infty dE \frac{(E^2-m^2)^{3/2}}{\exp[(E-\mu)/T] \pm 1}. \tag{A.53}$$

Let us assume that the i species under consideration have mass, m_i and temperature T_i not necessarily in thermal equilibrium with the other particles. Let also $T = T_\gamma$ be the temperature of photons in the plasma, then the total energy density and pressure of all particles in equilibrium with the i species would be

$$\rho = T^4 \sum_i \left(\frac{T_i}{T}\right)^4 \frac{g_i}{2\pi^2} \int_{x_i}^{\infty} du \frac{u^2(u^2 - x_i^2)^{1/2}}{\exp[(u - y_i] \pm 1}, \tag{A.54}$$

$$p = T^4 \sum_i \left(\frac{T_i}{T}\right)^4 \frac{g_i}{6\pi^2} \int_{x_i}^{\infty} du \frac{(u^2 - x_i^2)^{3/2}}{\exp[(u - y_i] \pm 1}, \tag{A.55}$$

where we have defined $u = E/T, x_i = m_i/T$ and $y_i = \mu_i/T$. If the species in consideration are relativistic $T \gg m$, then from Equation A.51 we get the following expressions for the energy density for bosons and fermions

$$\rho = \frac{\pi^2}{30} g T^4 \quad \text{(bosons)}, \qquad \rho = \left(\frac{7}{8}\right) \frac{\pi^2}{30} g T^4 \quad \text{(fermions)}. \tag{A.56}$$

In the primordial plasma most of the particles were relativistic, $T \gg m$ and since the energy density and pressure of non relativistic particles scale with energy as $\propto (mT)^{3/2} \exp[-(m-\mu)/T]$, their contribution to the energy density of the plasma can be safely neglected. In this case to the energy density and pressure would contribute only the relativistic particles and the expressions for the energy density and pressure read

$$\rho_r = \frac{\pi^2}{30} g_*(T) T^4 \tag{A.57}$$

$$p_r = \rho_r/3 = \frac{\pi^2}{90} g_*(T) T^4, \tag{A.58}$$

where $g_*(T)$ is the total number of effectively massless ($m_i \ll T$) degrees of freedom and is a function of the temperature

$$g_*(T) = \sum_{i=bosons} g_i \left(\frac{T_i}{T}\right)^4 + \frac{7}{8} \sum_{i=fermions} g_i \left(\frac{T_i}{T}\right)^4. \tag{A.59}$$

During the evolution of the universe g_* changes with temperature and as a results its value at different epochs is important since it tells us the number of effectively massless species contributing to the plasma. In fact, for $T > 300$ GeV according to the standard model of particle physics the number of relativistic particles is made of 3 generations of quarks (u, d, t) and leptons (e, μ, ν), 8 gluons, 3 vectorial bosons and 1 complex Higgs doublet. In this case the effective numbers of degrees of freedom accounts for $g_* = 106.75$. For 1 MeV $< T <$ 100 MeV would contribute to the plasma the photon, 3 species of neutrinos and $e^{\pm}$ and $g_* = 10.75$. For temperature $T \ll$ MeV the only species contributing to the plasma would be 3 neutrino species and the photon which account for $g_* = 3.36$.

As as far as local thermal equilibrium is concerned, a quantity which remains constant during the universe expansion is the entropy per co-moving volume. It can be derived by starting from the second law of thermodynamics in an expanding universe $dE = TdS - pdV$ where S is the entropy and $V \propto a^3(t)$ is the co-moving volume. By writing $E = \rho V$ and $S = sV$ where s is the entropy density, the second law of thermodynamics reads

$$d\rho = (Ts - \rho - p)\frac{dV}{V} + Tds. \tag{A.60}$$

Using the fact that the energy density depends only on the temperature $\rho = \rho(T)$, the first term on the right hand side of Equation A.60 must vanish. Thus we get the following expression for the entropy density s,

$$s = \frac{p+\rho}{T}. \tag{A.61}$$

Both the energy density and the pressure are dominated by the relativistic particles, so intreating both Equation A.57 into Equation A.61 we get

$$s = \frac{2\pi^2}{45} g_{*S} T^3, \tag{A.62}$$

where g_{*S} is the effective number of relativistic particles for conserved entropy

$$g_*(T) = \sum_{i=bosons} g_i \left(\frac{T_i}{T}\right)^3 + \frac{7}{8} \sum_{i=fermions} g_i \left(\frac{T_i}{T}\right)^3. \tag{A.63}$$

Comparison between Equation A.59 and shows that as far as the temperature of relativistic species is the same there is no difference between $g_*(T)$ and g_{*S}. Conservation of the entropy in a co-moving volume, $S = a^3 s = constant$ implies that

$$g_{*S} a^3 T^3 = constant, \tag{A.64}$$

and therefore $T \propto g_{*S}^{-1/3} a^{-1}$. If g_{*S} is constant we get the familiar result $T \propto 1/a$ but whenever the factor g_{*S} enters Equation A.64 the temperature of the universe evolve differently in comparison with the familiar result $T \propto 1/a$. Physically this means that whenever a particle disappears or does annihilate its entropy is transferred to the other particles in the plasma and therefore its conserved. This does happen for $T \ll$ MeV where the electron and positron do annihilate and transfer their entropy to the photons and neutrinos. Equation A.64 is an important result and is widely used throughout this thesis.

List of Figures

List of Tables